GENETIC AND MOLECULAR CHARACTERIZATION OF MAIZE RESPONSE TO SHADE SIGNALS

by Patrice Gilbert Dubois

GENETIC AND MOLECULAR CHARACTERIZATION OF MAIZE RESPONSE TO SHADE SIGNALS

A Dissertation

Presented to the Faculty of the Graduate School

of Cornell University

In Partial Fulfillment of the Requirements for the Degree of

Doctor of Philosophy

by

Patrice Gilbert Dubois

August 2010

GENETIC AND MOLECULAR CHARACTERIZATION OF MAIZE RESPONSE TO SHADE SIGNALS

Patrice Gilbert Dubois, Ph. D.

Cornell University 2010

In the dense stand of a typical maize field, chlorophyll and carotenoids pigments efficiently absorb blue and red (R) light but the longer far-red (FR) wavelengths are transmitted through the canopy or reflected by the vegetation. This selective absorption causes a reduction both in the R to FR ratio and in the photosynthetically active radiation. Together, they indicate the proximity of neighboring vegetation and induce a series of adaptive responses collectively known as shade avoidance syndrome. To characterize R/FR signaling in maize, an end-of-day FR (EOD-FR) assay was developed. A survey of genetically diverse inbreds, plus teosinte and a modern hybrid, revealed distinct elongation responses in seedling tissues. A quantitative trait loci (QTL) analysis of EOD-FR elongation responses identified several QTL for the mesocotyl and 1st leaf sheath tissues. The *phyB1 phyB2* mutant series, introgressed in B73 and W22 inbred backgrounds, confirmed the central role played by the phytochromes in mediating EOD-FR responses. The contribution of gibberellic acid and abscisic acid to EOD-FR responses was investigated both at constant temperature and when a chilling treatment was applied during dark breaks. To examine the role played by the two *PhyB* paralogs on plant architecture and flowering time variation, a series of traits were measured at maturity in B73 and W22 introgressions carrying the *phyB1 phyB2* mutant series. This analysis revealed that the

subfunctionalization of *PhyB* paralogs was dependent on the genetic background. Results from a pilot experiment with densely planted rows suggest that both *PhyB1* and *PhyB2* are involved in regulating azimuthal leaf orientation. Variation in plant architecture relative to cardinal position was examined using more than 5000 lines grown in a single field plot. Results suggest that sunset twilight operates similarly to EOD-FR in regulating plant height. That is, plants in the western section of the field, exposed to a higher intensity of FR during twilight sunset, are taller than in the eastern section. Finally, a reverse genetic approach to identify several *phyA* and *phyC* mutant alleles is described. Together, these studies provide the most detailed characterization to date of phytochrome response in both seedling and mature maize plants.

BIOGRAPHICAL SKETCH

The son of Jacqueline Deshaies and Clément Dubois, Patrice Gilbert Dubois is native of Trois-Rivières, located in the province of Québec, Canada. He holds a Bachelor's degree in agronomy from Laval University and a Master's degree in plant biology from the same institution. The subject of his Master's thesis was the investigation of the efficacy of an *Activator* transposon mutagenesis system in the model plant species *Arabidopsis thaliana* using a mutant background increasing transposon activity (Dubois *et al*., Plant Journal, 1998). After completing his Master's thesis, he joined Monsanto Company, working five years as a molecular biologist at their St. Louis headquarters. While there, he helped develop transgenic expression systems for different crop species, more specifically the engineering and validation of tissue-specific promoters. During his stay with the company, he co-authored seven patents related to gene expression in plants.

To broaden his understanding of plant physiology and crop improvement, and with the support of a "Fonds Quebecois de la Recherche sur la Nature et les Technologies" (FQRNT) fellowship, he joined the Plant Breeding and Genetics PhD program of Cornell University in 2006. With Dr. Thomas Brutnell of the Boyce Thompson Institute as his thesis advisor, his research focused on the genetic and molecular characterization of maize developmental responses associated with shade signals. During the course of his PhD, he first-authored a book chapter on light signal transduction in the Handbook of Maize: Its Biology and contributed illustration figures to the 5th edition of Taiz & Zeiger's Plant Physiology textbook. At the time of this writing, a manuscript based on chapter two this PhD's dissertation has been accepted for publication in Plant Physiology.

One of the most remarkable features in our domesticated races is that we see in them adaptation, not indeed to the animal's or plant's own good, but to man's use or fancy.

— Charles Darwin

Un peu plus à l'ouest.

— Tryphon Tournesol

ACKNOWLEDGMENTS

First and foremost, I would like to thank my family of all their support they provided me through my life, especially my mother Jacqueline Deshaies and my father Clément Dubois. I would also like to thank Clémence Dubé and Gilles Deshaies for their constant encouragement for pursuing graduate studies.

I am heartily thankful to Dr. Thomas Brutnell for welcoming me in his laboratory and for his thoughtful guidance through my PhD research. For their sound advise and support, I am also grateful to the members of my advisory committee: Drs. Edward Buckler, Owen Hoekenga, Wojciech Pawlowski, and Haiyang Wang.

I would like to acknowledge my colleagues of the Brutnell laboratory and of the Boyce Thompson Institute. I would like to also acknowledge my fellow colleagues and professors of the Plant Breeding and Genetics Department of Cornell University. I thank Dr. Sherry Flint-Garcia (University of Missouri) for the sharing of unpublished genetics stocks, Dr. Tim Setter for the abscisic acid analysis, and Gregory Olsefski and Karl Kremling for their technical assistance. I am also grateful to the Boyce Thompson Institute greenhouse and mechanical shop staff, especially Don Slocum and Dave McDonald. I acknowledge Fonds Québécois de la Recherche sur la Nature et les Technologies (FQRNT) for their financial support and Dr. Roger C. Levesque for his gracious help with the fellowship proposal.

TABLE OF CONTENTS

LIST OF FIGURES

LIST OF TABLES

LIST OF ABBREVIATIONS

μM	micromolarity
μmol	micromole
A	adenine
ABA	abscisic acid
B	blue light
bHLH	basic helix-loop-helix
bp	base pair
BS	bundle sheath
C°	Celsius degree
cDNA	complementary DNA
cm	centimeter
cM	centiMorgan
Cry	cryptochrome
D	darkness
d	days
DEPC	diethylpyrocarbonate
DF	degree of freedom
DMSO	dimethyl sulfoxide
DNA	deoxyribonucleic acid
dNTPs	deoxyribinucleoside triphosphates
DTT	dithiothreitol
E	east
ELISA	enzyme-linked immunosorbent assay

EOD-FR	end-of-day far-red
EMS	ethylmethane sulfonate
Fig	figure
FR	far-red light
G	green light, or guanine (Chapter Six)
GA	gibberellic acid
h	hour
ha	hectare
HIR	high irradiance response
IBM	intermated B73 x Mo17
K	potassium
kDa	kilo Dalton
kg	kilogram
L	Linnaeus
LD	long day
LED	light emitting diode
LFR	low fluence response
M	mesophyll
m	meter
Mb	megabase
mg	milligram
min	minute
mL	milliliter
mm	millimeter
mM	millimolarity
Mu	*Mutator*

mRNA	messenger ribonucleic acid
n	number
N	north (Chapter Four only)
N	nitrogen
NAM	nested association mapping
NIL	near isogenic line
nm	nanometer
NSS	non-stiff stalk
P	phosphate
P	probability value
PAR	photosynthetically active radiation
PBZ	paclobutrazol
PCR	polymerase chain reaction
Phot	phototropin
Phy	phytochrome
PIF	phytochrome interacting factor
Prob	probability
PVC	polyvinyl chloride
QTL	quantitative trait loci
R	red light
Rbcs	rubisco small subunit
RNA	ribonucleic acid
rpm	rotation per minute
S	south
SAS	shade avoidance syndrome
SD	short day

SE	standard error
sec	second
SS	stiff stalk
ssp	subspecies
SUS	sucrose synthase
t	Student's statistical test
TS	tropical/semi-tropical
U	unit
U.S.	United States
UTR	untranslated region
UV	ultraviolet radiation
v / v	volume per volume
VLFR	very low fluence response
W	west (Chapter Four only)
W	white light
WT	wild-type

LIST OF SYMBOLS

%	percentage
χ^2	chi square
H^2	broad-sense heritability
PΦB	tetrapyrrole chromophore
r^2	Pearson's correlation coefficient

CHAPTER ONE

LIGHT SIGNAL TRANSDUCTION NETWORKS IN MAIZE *

Abstract

Light signal transduction networks integrate environmental signals with endogenous developmental programs. Several photoreceptors, including phytochromes, cryptochromes, and phototropins as well as some of their signaling partners have been characterized in higher plants. Recent studies in maize have revealed the importance of phytochromes in the regulation of several agronomically important traits. However, much less is known of blue light responses. Several studies have suggested that light signaling response has been the target of plant breeding programs in the past and we discuss strategies for enhancing the agronomic performance of maize through the manipulation of light signal transduction pathways.

* Dubois PG, Brutnell TP (2009) *In* S Hake, JL Bennetzen, eds, Handbook of Maize. Its Biology, Vol 1. Springer, New York, pp 205-228.

1.1 Introduction

In the absence of light, a germinating seedling undergoes a period of skotomorphogenic development fueled by its starch reserves with shoot and root growth guided by gravitropism. The shoot apex, enclosed in the protective coleoptile, is pushed toward the soil surface by the elongation of the mesocotyl. Nearing the soil surface, the seedling perceives light and the transition from skotomorphogenesis to photomorphogenesis begins (Smith, 1982). This developmental transition is associated with global transcriptional change (Parks et al., 2001; Tepperman et al., 2001; Jiao et al., 2005) that is mediated through the relocalization (Sakamoto and Nagatani, 1996; Kircher et al., 1999; Jiao et al., 2007), phosphorylation (Ryu et al., 2005; Al-Sady et al., 2006) and degradation (Vierstra, 2003) of light response regulators. The morphological alterations include a reduction of elongation growth, an enhancement of root growth and the activation of photosynthetic development (Fig. 1.1). Throughout its life cycle, the integration of exogenous light cues with endogenous genetic programs allows the maize plant to constantly optimize its developmental program in response to environmental change (Quail et al., 1995; Smith, 1995).

Figure 1.1 Eight day-old maize seedlings grown in darkness (D) or under greenhouse conditions (W). In the D (left), seedling tissues including the coleoptile and mesocotyl elongate and photosynthetic development is retarded (skotomorphogenesis). Under W (right side), mesocotyl elongation in inhibited, leaves expand, and photosynthetic differentiation is initiated (photomorphogenesis). Significant variations in both skotomorphogenic and photomorphogenic development are often observed among inbred lines of maize. (A) B73 and (B) W22 inbred seedlings.

Plants have multiple mechanisms to sense and respond to their light environment. The fluence (measured in μmol of photon m^{-2}), fluence rate (also called irradiance, measured in μmol m^{-2} sec^{-1}), spectral quality (measured in wavelength, nm), and direction of radiation are monitored (Bjorn and Vogelmann, 1994). Wavelengths perceived by plants are typically classified into UV-B (280-320 nm), UV-A (320-380 nm), blue (B, 380-495 nm), green (G, 495-570 nm), yellow/orange (570-620 nm), red (R, 620-690 nm), and far-red (FR, 690-800 nm). The

photosynthetically active radiation (PAR) encompasses a spectrum that can be used for photosynthesis and is generally defined as wavelengths between 400 and 700 nm (white light, W). Chlorophylls have absorption maxima in the B (430-455 nm) and in the R (640-660 nm) and carotenoids absorb light primarily in the B (400-500 nm). Most of the G and FR are either transmitted through green tissues or reflected by the plant, and thus have the potential to serve as cues in sensing the vegetative environment (Fig. 1.2; Halliday and Fankhauser, 2003; Folta and Maruhnich, 2007).

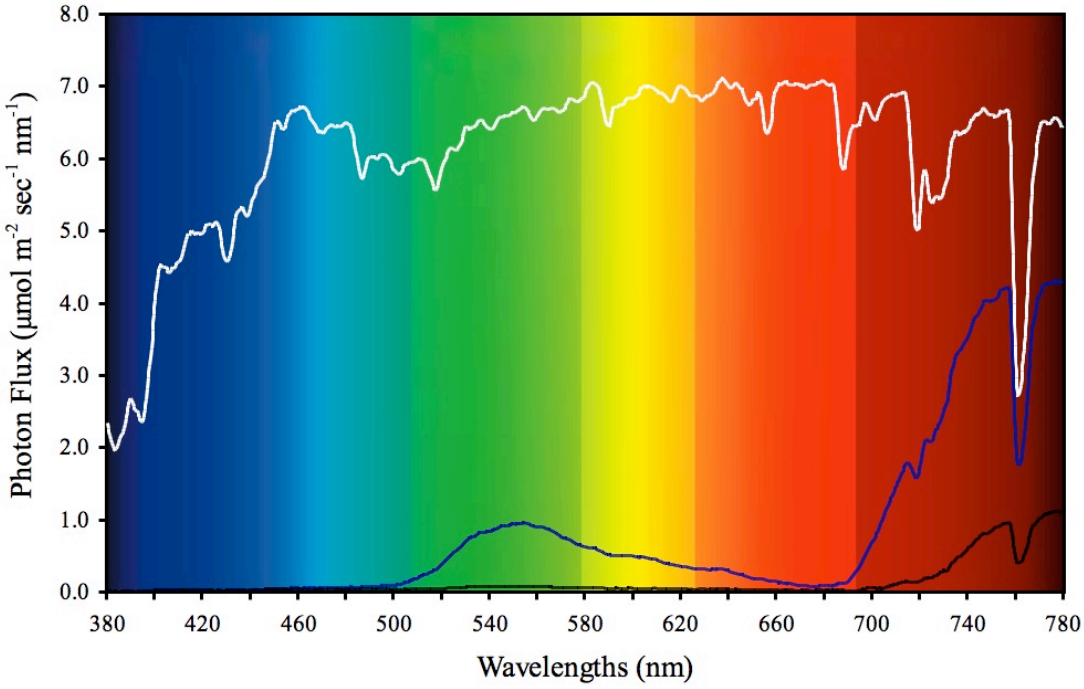

Figure 1.2 Three spectroradiometer readings taken in a maize plot (Emerson Garden, Cornell University, 09/08/2006). The white trace shows the light spectrum recorded above the canopy on a sunny day where R:FR was approximately 1.15. The light transmitted through a leaf blade (blue trace) is enriched in G and FR regions of the spectrum. The black trace is the light spectrum at ground level under the maize canopy (row spacing of 18 inches). The R:FR is reduced to approximately 0.06. The drop in irradiance around 760 nm is due to the absorption of these wavelengths by atmospheric water vapor.

Although early studies of photomorphogenesis, most notably by Charles Darwin, focused on monocot grass seedlings such as maize and oat (Whippo and

Hangarter, 2006), the vast majority of our current molecular understanding of light responses has come from studies of the dicot model Arabidopsis (Jiao et al., 2007). Through detailed molecular and genetic characterizations, several photoreceptors and downstream components of light response networks have been defined (Mathews, 2006; Christie, 2007; Jiao et al., 2007). These studies have also begun to reveal the complex interplay between light, hormonal signaling pathways (Vandenbussche et al., 2003) and the circadian clock (Salter et al., 2003). Despite our detailed understanding of the process in Arabidopsis, there are many reasons to revisit species such as maize and related grasses. Comparisons of light signal transduction networks between evolutionarily distant monocot and dicot species has provided insight into the function of the photoreceptor gene family members (Childs et al., 1997; Izawa et al., 2000; Takano et al., 2001; Sawers et al., 2002; Takano et al., 2005; Sheehan et al., 2007). In addition, a detailed characterization of these networks in crop species will provide potential targets for agronomic improvement (Sawers et al., 2005; Kebrom and Brutnell, 2007). The goal of this chapter is to summarize our current understanding of light signaling in maize and related monocots and to discuss how the manipulation of these pathways can be integrated into yield-enhancing breeding strategies.

1.2 Red/Far-red Signaling in Maize

Phytochromes are R/FR photoreversible chromoproteins composed of two apoprotein monomers, each bound to a tetrapyrrole chromophore synthesized from heme in the plastid (Mathews and Sharrock, 1997; Terry, 1997). Phylogenic analysis indicates that three major phytochrome lineages (*PHYA*, *PHYB*, and *PHYC*) are present in all angiosperms (Mathews and Donoghue, 1999). In Arabidopsis, the family has expanded to five members: *PHYA*, *PHYB*, *PHYC*, *PHYD*, and *PHYE* (Clack et al.,

1994). In monocot grasses such as rice and sorghum, only three members are present: *PHYA*, *PHYB*, and *PHYC* (Mathews and Sharrock, 1996, 1997; Goff et al., 2002). The absence of *PHYE* and *PHYD* from the monocots (Mathews, 2006), suggests that the expansion of the phytochrome gene family has been limited to the dicots or that *PHYE* was lost soon after divergence of monocots and dicot lineages. This divergence in phytochrome gene family structure has likely been accompanied by variation in downstream components. Indeed, studies of phytochrome signaling in maize, rice and sorghum have revealed significant divergence in both photoreceptor function and downstream response (Childs et al., 1997; Takano et al., 2001; Takano et al., 2005; Sheehan et al., 2007).

The apoprotein is composed of two separable domains joined by a protease-sensitive hinge region: a 60-70 kDa N-terminal photosensory region and 55 kDa C-terminal regulatory region (Fig. 1.3; Rockwell et al., 2006). The N-terminus contains a chromophore binding GAF domain (Fischer et al., 2005; Wagner et al., 2005) and a Pfr-stabilizing PHY domain. The C-terminus contains PAS repeats that are necessary for nuclear import (Chen et al., 2004) and a histidine kinase-related domain required for autophosphorylation of the holoenzyme following light activation (Yeh and Lagarias, 1998). The N-terminal domain is sufficient for activity in Arabidopsis when dimerized and translocated to the nucleus, suggesting that the C-terminus largely functions to attenuate phytochrome responses (Matsushita et al., 2003).

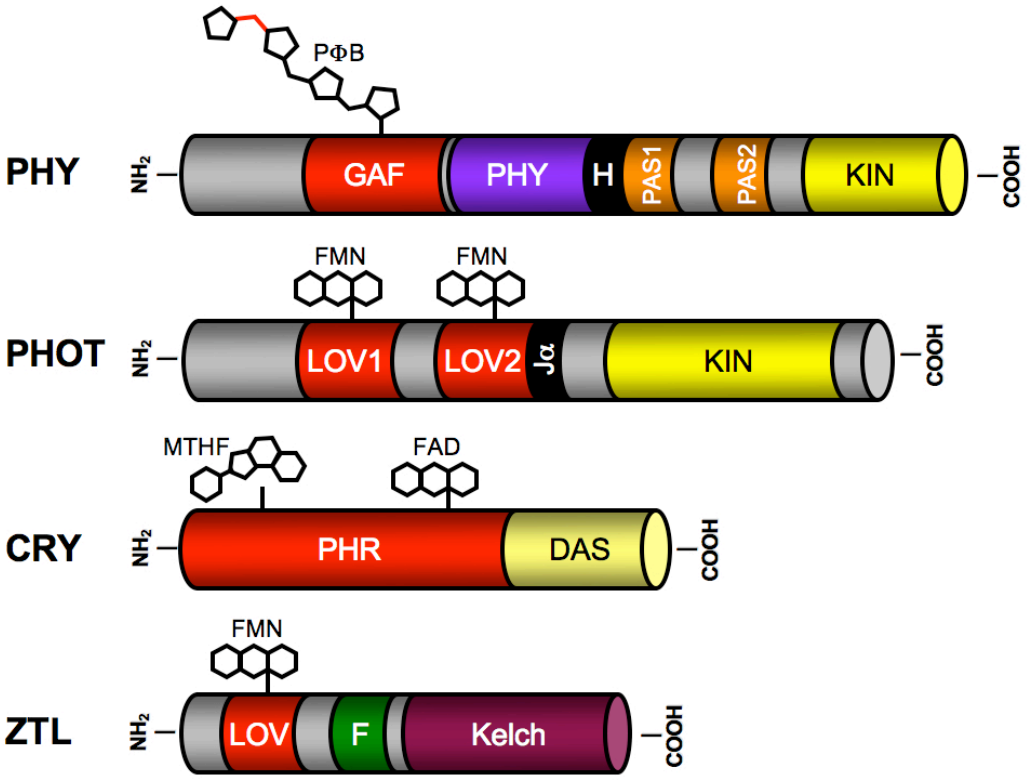

Figure 1.3. Schematic representation of characterized photoreceptors. PHY: The holoprotein is composed of a chromophore-attachment region (GAF) where an isomerization of PΦB at C15 (in red) allows the conversion between Pr and Pfr forms, a PHY domain (Montgomery and Lagarias, 2002), a hinge region (H), a nuclear localization region comprised of two PAS domains involved in the phytochrome dimerization and protein interaction, and a kinase domain involved in autophosphorylation (KIN) (Sheehan et al., 2004; Rockwell et al., 2006). PHOT: Phototropin apoprotein domains includes: LOV1 and LOV2 (Light, Oxygen, or Voltage) sensing domains and their FMN chromophore attachment regions, a conserved α-helix domain (Jα), and a kinase domain (KIN) required for autophosphorylation in response to B (Christie, 2007). CRY: The cryptochrome apoprotein domains include: a photolyase homology region (PHR) where both MTHF (methenyltetrahydrofolate) and FAD (flavin adenine dinucleotide) cofactors are bound, and a DQXVP-acidic-STAES conserved motif (DAS) (Lin, 2002; Klar et al., 2007). ZTL: The recently discovered ZTL/ADO family have three major domains: a B/UV-A sensing LOV domain, an F-box for the degradation of protein targets, and a C-terminal Kelch domain involved in protein-protein interaction (Banerjee and Batschauer, 2005).

Phytochrome apoproteins are synthesized in the inactive Pr form and autocatalytically assemble with a linear tetrapyrrole chromophore (PΦB) in the cytosol (Lagarias and Lagarias, 1989; Terry et al., 1993; Terry, 1997). The chromophore prosthetic group is covalently bound to a conserved cysteine residue found in the N-terminal region via a thioester linkage. The photoconversion from Pr to Pfr results in photo-isomerization of the C15 double bond followed by a series of light-independent chromophore-protein relaxation steps (Rudiger et al., 1983; Andel et al., 1996). The conformational changes induced by the conversion to the Pfr form allow its translocation into the nucleus where it interacts with downstream components of the pathway (Jiao et al., 2007).

Phytochromes mediate responses to the intensity and duration of light through three distinct modes of action (Mancinelli, 1994). These include very low fluence responses (VLFR) where physiological effects can be achieved with fluences as low as 0.0001 μmol m^2, low fluence responses (LFR) requiring fluences ranging from 1 up to 1000 μmol m^2 and high irradiance responses (HIR) requiring prolonged or continuous exposure at high fluence rates. Both VLFRs and LFRs obey the law of reciprocity where the magnitude of the response is function of both the fluence rate and the time of exposure, however, only LFR display photoreversibility. HIRs are proportional to both the fluence rate and the duration of irradiation. It is important to note that the same physiological response may be mediated by phytochromes acting in more than one response mode. For instance, seed germination in Arabidopsis is mediated both by PhyA acting in the VLFR mode and by PhyB acting in the LFR mode (Shinomura et al., 1996).

1.2.1 Maize Phytochrome Apoprotein Family

In maize, an ancient allopolyploidization event expanded the phytochrome family number to six: *PhyA1, PhyA2, PhyB1, PhyB2, PhyC1,* and *PhyC2* (Sheehan et al., 2004). *PhyA1*, *PhyB1*, and *PhyC1* are located on chromosome 1 and likely derived from one ancestral genome whereas *PhyA2*, *PhyC2* (chromosome 5) and *PhyB2* (chromosome 9) are located in syntenic regions on homeologous chromosomes and thus likely derived from the other ancestral genome. All six maize genes are predicted to encode functional apoproteins and are actively transcribed (Sheehan et al., 2004). Transcripts for *PhyA*, *PhyB* and *PhyC* accumulate to higher levels in many seedling tissues of plants grown in the D relative to W. In the D, transcripts of *PhyA* predominate, suggesting that PHYA may mediate the transition from D- to W-growth whereas all three phytochromes may contribute to light responses. Highly similar expression patterns for *PhyA* homeologs indicate that the encoded products are largely redundant in function, whereas transcripts from *PhyB1* and *PhyC1* prevail over their respective homeologs in all seedling tissues examined (Sheehan et al., 2004).

1.2.2 **elm1,** *A Chromophore Deficient Mutant*

A series of elegant phenotypic screens using EMS-mutagenized Arabidopsis populations allowed the identification of the first phytochrome mutants based on their etiolated development under W (Koornneef et al., 1980). A similar approach using transposon-mutagenized populations was used to identify the first light-signaling mutant of maize. The *elm1* (*elongated mesocotyl 1*) mutant was initially identified in a sand bench screen as a pale green plant with an elongated mesocotyl (Sawers et al., 2002). The mutants fail to accumulate spectrophotometrically detectable pools of

phytochrome due to a block in chromophore biosynthesis. Cloning of *Elm1* revealed that it encodes an enzyme with phytochromobilin synthase activity, the last enzymatic step in the chromophore biosynthetic pathway. The lesion in *elm1* was mapped to a single base pair substitution at the 3' splice junction of intron III (Sawers et al., 2004). This lesion results in a greatly reduced pool of in-frame transcripts capable of directing the synthesis of a full-length phytochromobilin synthase protein.

As all phytochrome apoproteins likely bind the same chromophore (Terry, 1997), characterization of the *elm1* mutant has provided an opportunity to examine the role of phytochromes in seedling and mature plant development (Sawers et al., 2002). Mesocotyl lengths of R- and FR-grown *elm1* plants were not significantly different from D-grown plants, indicating that phytochromes are essential for the suppression of mesocotyl elongation under R and FR. Chlorophyll and carotenoid content are also reduced in *elm1* mutants relative to wild-type (WT) seedlings. Characterization of photosynthetic gene expression in *elm1* mutants further defined a role for phytochromes in regulating both nuclear (*Cab* and *RbcS*) and plastid (*psbA* and *rbcL*) gene expression under R. However, under W *rbcL* and *psbA* expression was similar in WT and *elm1*, suggesting that B photoreceptors can largely compensate for a loss in phytochrome function in directing plastid transcript accumulation. At maturity, *elm1* plants are taller than their isogenic WT siblings, slightly pale green, often lodge and flower early (Sawers et al., 2002; Markelz et al., 2003). These phenotypes are consistent with reduced light responses that persist throughout development.

Unfortunately, the interpretation of *elm1* mutant phenotypes is problematic due to the residual accumulation of some full-length *Elm1* transcripts. It is likely that low levels of phytochromobilin accumulate in mutant tissues that are below the limits of detection for spectrophotometric assays (Sawers et al., 2004). Thus, some active phytochrome pools may allow for a limited response to R and FR. For instance, *Cab*

and *RbcS* gene expression increases slightly when *elm1* mutants are exposed to R, suggesting that phytochromes are functional (Sawers et al., 2002). When the light-dependent accumulation of sucrose synthase (SUS) was examined in wild-type tissues, high levels of SUS were present in the D but decreased dramatically under R (Qiu et al., 2007). The degradation of SUS in light also occurred in the *elm1* mutant (Steve Huber, personal communication), suggesting that phytochromes do not mediate the light-dependent degradation of SUS. Alternatively, the low levels of phytochrome that accumulate in *elm1* tissues may be sufficient to mediate degradation of SUS. Such caveats illustrate the challenges associated with the interpretation of any phenotype associated with a weak mutant allele.

1.2.3 Phytochrome Apoprotein Mutants

The first phytochrome mutant described in monocots was a *phyB* mutant of sorghum (ma_3^R; Childs et al. 1997). Reverse genetic screens have been successfully utilized in rice to identify mutants in each of the three genes encoding the phytochrome apoproteins (Takano et al., 2001; Takano et al., 2005; Jeong et al., 2007). To date, only *phyB1* and *phyB2* single and double mutants have been characterized in maize revealing both overlapping and non-redundant roles for the two PHYB homeologs (Sheehan et al., 2007). In seedling tissues, both *PhyB1* and *PhyB2* contribute to the degradation of *PhyA2* and the accumulation of *PhyC1* transcripts under W. In mature plants, both *PhyB1* and *PhyB2* contribute to the control of plant height, ear node height, stem diameter, and leaf sheath-internode ratio. However, mesocotyl elongation is regulated by *PhyB1* whereas *PhyB2* predominates in the regulation of flowering time. Thus, it appears that *PhyB* homeologs of maize have undergone some subfunctionalization but maintain many overlapping functions as

well. Characterizations of the phytochrome mutants in monocots have revealed diverse roles for phytochromes in both seedling and mature plant growth and are summarized in Table 1.1.

Table 1.1 Characterized Phytochromes of Maize, Rice, and Sorghum

PHY	Roles / Traits	References
Maize PHYB1	Plant and ear node height, culm diameter, leaf sheath and internode lengths in mature plants. Constant W (Wc), Rc, and Bc: mesocotyl elongation. *PhyA* and *Cab* transcript levels. Delays flowering under short day (SD) and long day (LD).	Sheehan et al., 2007
Maize PHYB2	Plant height, ear node height, culm diameter, leaf sheath and internode lengths in mature plants. *PhyA* and *Cab* transcript levels. Delays flowering under LD conditions.	Sheehan et al., 2007
Rice PHYA	FR-HIR: mesocotyl and internode elongation, crown root growth orientation. FR-VLFR and FR-HIR: coleoptile elongation. Rc control of leaf and internode length. Bc control of leaf angle. R-LFR- and FR-mediated *Lhcb* and *RbcS* transcript levels. Flowering time regulation under SD and LD conditions.	Takano et al., 2001 and 2005 Xie et al., 2007
Rice PHYB	R-HIR: coleoptile and first leaf elongation. Brassinosteroid regulation of leaf angle and coleoptile elongation in seedlings. R-mediated *Lhcb* and *RbcS* transcript levels. Perception of night break. Mediates *Os*CRY2 degradation. R-LFR and B/FR reversible coleoptile growth inhibition. Flowering time regulation under SD and LD conditions.	Hirose et al., 2006 Ishikawa et al., 2005 Jeong et al., 2007 Takano et al., 2005 Xie et al., 2007
Rice PHYC	FR-HIR: coleoptile, 1st leaf and 2nd internode elongation. R- and FR-mediated *Lhcb* and *RbcS* transcript levels. Flowering time regulation under SD and LD conditions.	Takano et al., 2005
Sorghum PHYB	Seedling elongation. Plant height, height to the ligule, leaf sheath, and sheath/blade ratio in mature plants. Repress *SbTB1* (suppressor of axillary bud outgrowth). Regulation of circadian ethylene production. Delays flowering under SD and LD conditions.	Finlayson et al., 1998, 1999, and 2007 Kebrom et al., 2006 Pao and Morgan, 1986

1.3 Blue Light Signaling in Maize

One of the best-characterized B responses in plants is phototropic curvature (Fig. 1.4). Studies by Charles and Francis Darwin first showed that light is sensed by the tip of the coleoptile while the bending occurs further down (Darwin, 1880). Further characterizations, including detailed kinetic measurements in maize, revealed that B was most effective in mediating this response and required the lateral transport of auxin (Iino, 1990). Although these studies have clearly shown a relationship between auxin synthesis and transport to phototropic curvature in maize, the molecular mechanisms have remained elusive. Recently, an auxin-induced K^+ channel has been implicated in mediating the differential growth of coleoptiles in response to B (Philippar et al., 1999; Fuchs et al., 2003). K^+ channels have also been implicated in the function of maize guard cells to regulate stomatal movement (Buchsenschutz et al., 2005), another phototropin-mediated response (Christie, 2007). A role for auxin in controlling elongation of stem tissues was revealed by the characterization of the semi-dwarf *brachytic2* (*br2*) mutant. The *Br2* gene of maize encodes a P-glycoprotein required for light-dependent polar auxin transport (Multani et al., 2003). Interestingly, the sorghum ortholog of this gene appears to have been a target of selection (plant height) in breeding programs. In Arabidopsis, mutations in closely related *br2* homologs result in the mislocalization of the auxin efflux carrier PIN1, increased lateral auxin transport and hypertropic bending (Noh et al., 2003). A characterization of phototropic-insensitive mutants of maize (Fig. 1.4), may help to further define components of this pathway (Baskin et al., 1999; T. Baskin, personal communication).

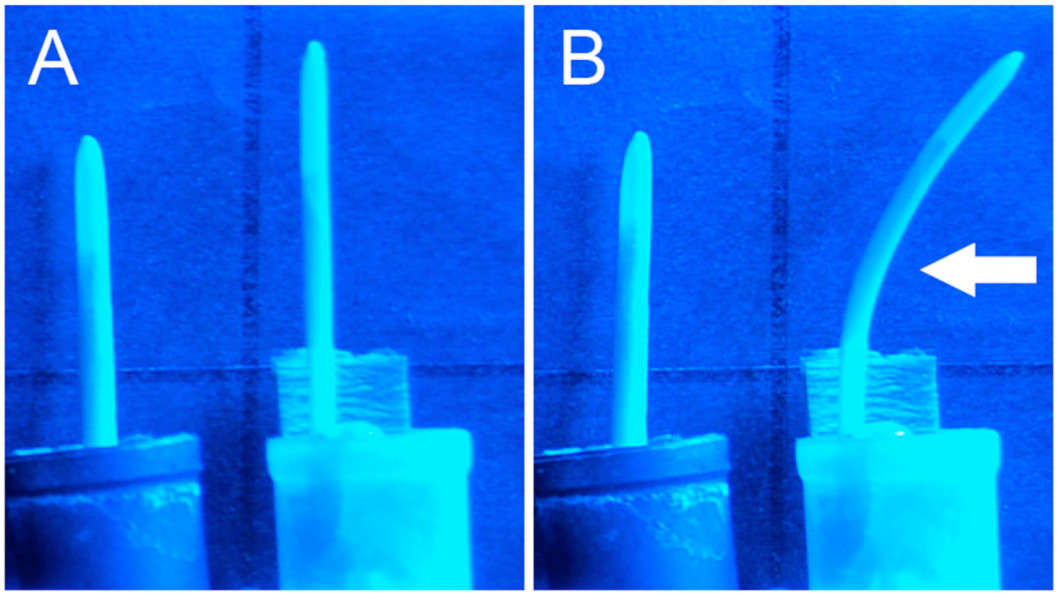

Figure 1.4 The phototropic curvature of maize seedlings in response to unidirectional B. A non-responsive *blueless* mutant (left) and WT B73 inbred on the right (A) prior to and (B) after a 4h B exposure.

Progress on identifying additional components of B-mediated growth has been limited in maize. As shown in Fig. 1.3, a number of B photoreceptors have been identified in Arabidopsis. Although a putative phototropin has been identified in maize (GenBank accession: AF033263), no mutations have been reported in this or other potential B photoreceptors.

1.4 Light Regulation of C4 Photosynthetic Development

Maize, like many semi-tropical and tropical grass species, utilizes C4 photosynthesis (Edwards and Walker, 1983) to efficiently capture CO_2 under warm, dry conditions (Sage and Monson, 1999). This specialized form of photosynthesis is achieved through the partitioning of photosynthetic activities between two morphologically and biochemically distinct cell types. Maize leaf blades display

Kranz anatomy where files of photosynthetic bundle sheath (BS) cells surround the vasculature and are themselves surrounded by a layer of mesophyll (M) cells. As CO_2 diffuses into the leaf through the stomata, it first fixed into a C4 sugar in M cells that diffuses to the BS. Once inside the BS plastid, the sugar is decarboxylated and the CO_2 fixed by Rubisco in the Calvin cycle. By sequestering Rubisco in the CO_2-rich environment of the BS, photorespiration is greatly reduced (Hatch, 1971; von Caemmerer and Furbank, 2003). Despite the increased energy required for generating this CO_2 gradient, C4 photosynthesis is still more efficient than C3 photosynthesis at high temperatures due to the enhanced oxygenase activity of Rubisco in C3 plants (Jordan and Ogren, 1984; Sage, 2004).

Decades of research have provided us with a detailed understanding of the biochemistry underlying C4 photosynthesis (Sage and Monson, 1999). However, our understanding of the networks mediating the differential expression of suites of genes and proteins is much less complete (Sawers et al., 2007). Light is one factor that regulates the abundance of many of photosynthetic enzymes and initiates the cell-specific accumulation of transcripts (Sheen and Bogorad, 1986, 1987; Langdale et al., 1988; Sheen and Bogorad, 1988). Cis-acting elements have been defined for a number of genes that appear to control the differential accumulation of photosynthetic transcripts in response to light (Sheen, 1999). For instance, the *Rbcs* gene contains both constitutive and light-responsive promoter elements, and sequences within the 5' and 3' UTRs that drive cell-specific expression (Schaffner and Sheen, 1991; Bansal et al., 1992). The induction of *Rbcs* in BS is dependent on a R signal, whereas repression of *RbcS* transcript accumulation in the mesophyll cells is dependent on B (Purcell et al., 1995). Both 5' and 3' non-coding sequences appear to be required for light induction and repression of *Rbcs* transcript accumulation (Viret et al., 1994). Some trans-acting factors have also been identified that regulate cell-specific accumulation

of photosynthetic enzymes, including a YY1-like suppressor of *Rbcs* accumulation (Xu et al., 2001) and a *Dof1* transcription factor that may regulate light-induced expression of PEPCase (Yanagisawa, 2000). UV-B also plays a role in the regulation of malic enzyme transcript (*Me1*) and protein accumulation, suggesting a role for C4 enzymes in the repair of UV-induced damage (Drincovich et al., 1998; Casati et al., 1999). Several mutants have been identified in genetic screens that disrupt the cell-specific accumulation of photosynthetic enzymes (Roth et al., 1996; Hall et al., 1998; Hall et al., 1998; Brutnell et al., 1999). However, these mutations do not appear to alter cell fates, but rather alter a subset of photosynthetic enzyme or transcript accumulation patterns. Together, these studies suggest a complex interplay between light and developmental regulators during C4 differentiation.

To examine the contributions of phytochrome to C4 differentiation, transcripts encoding *Ppc*, *RbcS2* and *Me1* were examined in the *elm1* mutant (Markelz et al., 2003). In W the transcript levels of each of these three genes accumulates to similar levels in the mutant tissues as in WT and the cell-specific patterns of expression are maintained. When plants are shifted from W to D, levels of *Ppc* and *RbcS2* decline more rapidly in the *elm1* background than in the WT. *Me1* transcript levels declined slowly over a 72h time course with a similar profile in both the *elm1* mutant and WT. When W-grown plants were shifted to monochromatic B, R, or FR, the cell-specific patterns of gene expression were maintained in the *elm1* mutant. These results suggest a limited role for phytochromes in maintaining C4 photosynthetic gene expression under W, but imply a role for phytochromes in regulating the levels of some photosynthetic genes in the D (Markelz et al., 2003). As previously mentioned, low levels of chromophore likely accumulate in the *elm1* mutant, thus it is possible that small active pools of phytochrome are sufficient to induce a C4 photosynthetic state. With the recent identification of complete loss-of-function alleles of *phyB1* and *phyB2*

(Sheehan et al., 2007), it should now be possible to directly address the role of *PhyB* in regulating C4 differentiation.

1.5 Light Regulation of Anthocyanin Biosynthesis

Flavonoid biosynthesis (including anthocyanins) is arguably one of the most well-characterized pathways in maize (Dooner et al., 1991). The structural genes encoding the biosynthetic enzymes and regulatory genes encoding transcription factors were some of the first genes cloned in plants (Kreuzaler et al., 1983; Cone et al., 1986; Paz-Ares et al., 1986). Thus, it is perhaps surprising how little is known of the molecular networks underlying light regulation of this pathway in maize. This is, in part, due to the lack of well-characterized light signaling mutants of maize until recently (Sawers et al., 2004; Sheehan et al., 2007). In addition, many of the early studies of anthocyanin accumulation were likely confounded by the segregation of regulatory elements that mediated both light-dependent and -independent accumulation of anthocyanins (Beggs and Wellman, 1985). Nevertheless, several studies have shown that light is necessary for the expression of both regulatory and structural genes in the pathway (Gavazzi et al., 1990; Cone et al., 1993; Procissi et al., 1997; Petroni et al., 2000; Pilu et al., 2003) as well as the subcellular localization of the anthocyanins (Grotewold et al., 1998).

The accumulation of anthocyanins upon UV-B exposure has been suggested to serve a photoprotective function (Stapleton and Walbot, 1994; Casati and Walbot, 2003). However, the photoreceptor(s) that mediate this response in maize have remained elusive. A detailed analysis of the specific wavelengths necessary for the induction of regulatory and enzyme-encoding genes indicates that B and UV-B are

most effective in mediating anthocyanin accumulation in young seedling tissues (Piazza et al., 2002). However, R and UV-A also contribute to the response. In endosperm tissues, both B and R contributed equally to accumulation of anthocyanins, though neither treatment on its own conditions as high a level of anthocyanins as W, suggesting a synergism between B and R signal transduction pathways (Piazza et al., 2002). These findings are consistent with observations that anthocyanin accumulation is greatly reduced in the aleurone of the *elm1* mutant (T. Brutnell, unpublished data), suggesting that both R- and B-induced accumulation of anthocyanins in the aleurone may require active phytochrome pools.

1.6 The Shade Avoidance Syndrome

Historical data on U.S. maize production shows an uninterrupted growth in average yields (see chapters by J. Holland and F. Troyer). In the 1930's grain yields averaged approximately 1,500 kg/ha whereas current grain yields are now greater than 10,000 kg/ha (Tollenaar and Wu, 1999; Troyer, 2006). One key factor that has contributed to these gains have been a steady increase in planting densities (Troyer, 1996; O'Bryan et al., 2006) while maintaining relatively constant per plant yields (Duvick, 1997).

The selective absorption of R and B by the chlorophyll results in a decrease in the ratio of R to FR (R:FR) of both transmitted and reflected light. This spectral shift is perceived by the plant as an indication of the presence of neighboring vegetation (Smith, 2000; Franklin and Whitelam, 2005). This proximity detection occurs before canopy closure, thus allowing the plant to anticipate a competitive threat and adjust its growth accordingly (Ballare et al., 1990; Ballare, 1999; Ballare and Casal, 2000). In response to both neighbor proximity (low R:FR) and vegetative shade (low R:FR and

reduced PAR), many plants display a series of morphological changes referred to as shade avoidance responses or the shade avoidance syndrome (SAS) (Smith, 1995).

In maize, the SAS is characterized by a decrease in chlorophyll content, an increase in plant height, a reduction in the number of tillers, thinner, longer and more erect leaf blades, an elongation of internodes and leaf sheaths and a reduction in root development (Kasperbauer and Karlen, 1994; Maddonni et al., 2001; Andrieu et al., 2006). Prolonged exposure to low R:FR also impairs reproductive development, causing an acceleration of flowering, a decrease in kernel number per plant and grain yield per plant (Borras et al., 2003; Hashemi et al., 2005; Maddonni and Otegui, 2006). The most striking example of the SAS in a modern field setting can be seen at borders where higher R:FR and PAR dramatically affect plant growth (Fig. 1.5). This also demonstrates that a significant SAS is still operational in modern hybrids, despite breeding efforts that have likely attenuated many shade avoidance responses (Ballare and Casal, 2000; Maddonni et al., 2001; Maddonni et al., 2002).

Figure 1.5 A classic shade avoidance response can be observed at the border of this maize field. Plants at the edge of the field are shorter and experience higher R:FR and PAR relative to shaded individuals. (Upstate NY, 08/17/2007).

The molecular mechanisms underlying the SAS have been most intensively investigated in Arabidopsis (Franklin and Whitelam, 2005; Vandenbussche et al., 2005). Through the use of genetic screens (Cerdan and Chory, 2003), expression profiling (Devlin et al., 2003; Salter et al., 2003; Roig-Villanova et al., 2006) and physiological studies (Steindler et al., 1999), components of the SAS pathway are being defined. The low R:FR associated with canopy shade is transduced by the phytochromes through a modulation of the amount of active Pfr. In Arabidopsis, phyB predominates in mediating many of these responses but additional phytochromes are also involved (Smith and Whitelam, 1997; Devlin et al., 2003; Franklin et al., 2003).

In maize, much less is known of the molecular components of the SAS. The *elm1, phyB1* and *phyB2* single and double mutants each display several traits associated with shade response at maturity, including increased plant height and early flowering (Sawers et al., 2002; Sheehan et al., 2007), suggesting that PHYB may modulate many of the shade avoidance responses in maize. However, *PhyA* has also been implicated in mediating the SAS in sorghum (Finlayson et al., 2007). In Arabidopsis, a family of bHLH (basic helix-loop-helix) transcription factors family have been defined that interact with phytochromes (Duek and Fankhauser, 2005; Monte et al., 2007). These phytochrome-interacting factors (PIF) and PIF-like factors (PIL) act as both positive and negative regulators to mediate changes in gene transcription; (Martinez-Garcia et al., 2000; Huq and Quail, 2002; Kim et al., 2003; Huq et al., 2004; Oh et al., 2004; Oh et al., 2007; Shin et al., 2007), including responses to vegetative shade (Salter et al., 2003; Sessa et al., 2005). Recent studies in rice (Nakamura et al., 2007) and maize (Matthew Hudson, personal communication) suggest that a related class of proteins may also be functional in the monocots to mediate phytochrome responses. Other proteins that may mediate responses to vegetative shade belong to the homeodomain-leucine zipper (HD-zip) class and include ATHB-2 and ATHB-4 in Arabidopsis. These genes are regulated by R:FR and overexpression of ATHB-2 results in a phenotype that mimics the SAS (Carabelli et al., 1996; Steindler et al., 1999). Several plant hormones including auxins, gibberellins, brassinosteroids, and ethylene as well as some herbivore-induced phenolics have been defined as components of the SAS (Reed et al., 1996; Finlayson et al., 1999; Morelli and Ruberti, 2000; Pierik et al., 2004; Vandenbussche et al., 2005; Izaguirre et al., 2006).

1.7 Dissecting the Light Signal Transduction Networks

How do we further define the components of the light signal transduction pathways in maize? Several reverse genetic programs have recently been developed for maize (see chapters by D. McCarty and C. Weil). These programs will greatly facilitate targeting approaches that are based on our current understanding of light signal transduction in model plants. Another means to define components of light signaling networks is through exploitation of genetic diversity. Quantitative trait loci (QTL) analysis and genome-wide association mapping techniques both afford advantages to mapping quantitative variation (see chapters by R. Tuberosa and A. Rafalski). Mapping populations where elements of both bi-parental populations and association analysis are combined can overcome some of the limitations of both techniques, such as population structure (association mapping) and low resolution (QTL analysis) (Ersoz et al., 2007). A survey of light response in maize conducted with a panel of diverse maize germplasm revealed that North American temperate inbreds are less responsive than tropical and semi-tropical inbreds lines. This result suggests that light response may have been a target of selection (Markelz et al., 2003) and that QTL and genome wide association mapping techniques may prove fruitful in defining novel variation.

1.8 Manipulation of Light Signaling Pathways

Overexpression of photoreceptors has been widely used as a method to alter plant stature and yield (Hudson, 2007). However, these experiments have met with mixed success. In tobacco, overexpression of an oat *PhyA* using the CaMV-35 promoter resulted in a reallocation of resources to the leaf rather than the stem, thus

increasing harvest index (Robson et al., 1996). It is likely that increased pool of active *PHYA* beyond the seedling stage enhanced FR-HIR and attenuated the *PhyB*-mediated SAS. A similar approach was taken to engineer wheat through overexpression of an oat *phyA* using the maize ubiquitin promoter (Shlumukov et al., 2001). Although the seedlings displayed some enhanced response to FR, the effects on field grown plants have yet to be determined. In rice, two similar studies were conducted using the same transgenic construct. The light-regulated and tissue-specific *rbcS* promoter was used to express the Arabidopsis *PhyA* gene. Overexpression of *PhyA* in an *Indica* variety increased grain yield from 6-20% in greenhouse-grown plants (Garg et al., 2006), but in a *Japonica* variety it reduced tiller number and overall grain yield (Kong et al., 2004). These studies suggest that perturbation of light signaling networks may have quite varied consequences depending on the genotype of the plant and its intrinsic light transduction networks. Thus, a large number of transgenic events across a broad germplasm collection may be necessary to fully explore the consequences of manipulating light signal transduction pathways.

An alternate approach for manipulating the SAS in maize can be the utilization of photo-insensitive phytochrome mutants. A single amino acid substitution in Arabidopsis *PHYB* (Y276H) results in constitutive photomorphogenic development in the dark, a light-independent activation of gene expression and a R/FR insensitivity (Su and Lagarias, 2007). As suggested by the authors, such constitutive activation of phytochrome response may have applications in engineering plant architecture in crop plants. However, as mentioned above, modern maize hybrids have retained some response to vegetative shade that are likely beneficial under high density. For instance, in addition to increase hyponasty, relatively higher R:FR present between rows causes an azimuthal leaf orientation of leaves that limits physical interactions between adjacent plants and maximizes leaf area index (Maddonni et al., 2001; Maddonni et

al., 2002). These results suggest that some plasticity in the SAS may be beneficial for plants to achieve optimal yields under high density plantings (Pagano and Maddonni, 2007). Thus, the engineering of shade response may require a more fine-tuned approach, perhaps through the manipulation of downstream components.

1.9 Conclusion

Despite a detailed understanding in Arabidopsis, our knowledge of light signal transduction networks in maize remains limited. Through the isolation and characterization of photoreceptor mutants, roles for phytochrome in several agronomically important traits have been defined. With the availability of maize genomic sequence, the development of reverse genetic tools and sophisticated mapping populations, it will soon be possible to functionally define many components of light signaling networks. The potential for engineering plant architecture through the manipulation of photoreceptors and downstream components suggests that a more detailed understanding of these pathways in maize could lead to the improvement of this important food, feed and fuel crop.

1.10 Acknowledgements

The authors would like to thank Matthew Hudson, Tesfamichael Kebrom, and Michael Gore for comments on the manuscript, Keith Williams for the coleoptile curvature photographs, and Tobias Baskin for sharing the blueless maize mutant. Support for this work was provided by grants from the National Science Foundation to T.P.B. and by a FQRNT fellowship to P.G.D.

REFERENCES

Al-Sady B, Ni W, Kircher S, Schafer E, Quail PH (2006) Photoactivated phytochrome induces rapid PIF3 phosphorylation prior to proteasome-mediated degradation. Mol Cell **23:** 439-446

Andel F, 3rd, Lagarias JC, Mathies RA (1996) Resonance raman analysis of chromophore structure in the lumi-R photoproduct of phytochrome. Biochemistry **35:** 15997-16008

Andrieu B, Hillier J, Birch C (2006) Onset of sheath extension and duration of lamina extension are major determinants of the response of maize lamina length to plant density. Ann Bot (Lond) **98:** 1005-1016

Ballare CL (1999) Keeping up with the neighbours: phytochrome sensing and other signalling mechanisms. Trends Plant Sci **4:** 97-102

Ballare CL, Casal JJ (2000) Light signals perceived by crop and weed plants. Field Crops Res **67:** 149-160

Ballare CL, Scopel AL, Sanchez RA (1990) Far-red radiation reflected from adjacent leaves: An early signal of competition in plant canopies. Science **247:** 329-332

Banerjee R, Batschauer A (2005) Plant blue-light receptors. Planta **220:** 498-502

Bansal KC, Viret JF, Haley J, Khan BM, Schantz R, Bogorad L (1992) Transient expression from *cab*-m1 and *rbcS*-m3 promoter sequences is different in mesophyll and bundle sheath cells in maize leaves. Proc Natl Acad Sci U S A **89:** 3654-3658

Baskin TI, McGuffin J, Sonderman BS (1999) On the weak phototropic response of the maize variety, strawberry popcorn. Maydica **44:** 119-125

Beggs CJ, Wellman E (1985) Analysis of light-controlled anthocyanin formation in coleoptiles of *Zea mays* L.: The role of UV-B, blue, red and far-red light. Photochem Photobiol **41:** 481-486

Bjorn LO, Vogelmann (1994) Quantification of light. *In* RE Kendrick, GHM Kronenberg, eds, Photomorphogenesis in plants, Ed 2nd. Kluwer Academics, pp 17-25

Borras L, Maddonni GA, Otegui Me (2003) Leaf senescence in maize hybrids: plant population, row spacing and kernel set effects. Field Crops Res **82:** 13-26

Brutnell TP, Sawers RJ, Mant A, Langdale JA (1999) BUNDLE SHEATH DEFECTIVE2, a novel protein required for post-translational regulation of the rbcL gene of maize. Plant Cell **11:** 849-864

Buchsenschutz K, Marten I, Becker D, Philippar K, Ache P, Hedrich R (2005) Differential expression of K^+ channels between guard cells and subsidiary cells within the maize stomatal complex. Planta **222:** 968-976

Carabelli M, Morelli G, Whitelam G, Ruberti I (1996) Twilight-zone and canopy shade induction of the Athb-2 homeobox gene in green plants. Proc Natl Acad Sci U S A **93:** 3530-3535

Casati P, Drincovich MF, Edwards GE, Andreo CS (1999) Regulation of the expression of NADP-malic enzyme by UV-B, red and far-red light in maize seedlings. Braz J Med Biol Res **32:** 1187-1193

Casati P, Walbot V (2003) Gene expression profiling in response to ultraviolet radiation in maize genotypes with varying flavonoid content. Plant Physiol **132:** 1739-1754

Cerdan PD, Chory J (2003) Regulation of flowering time by light quality. Nature **423:** 881-885

Chen M, Chory J, Fankhauser C (2004) Light signal transduction in higher plants. Annu Rev Genet **38:** 87-117

Childs KL, Miller FR, Cordonnier-Pratt MM, Pratt LH, Morgan PW, Mullet JE (1997) The sorghum photoperiod sensitivity gene, Ma_3, encodes a phytochrome B. Plant Physiol **113:** 611-619

Christie JM (2007) Phototropin blue-light receptors. Annu Rev Plant Biol **58:** 21-45

Clack T, Mathews S, Sharrock RA (1994) The phytochrome apoprotein family in Arabidopsis is encoded by five genes: the sequences and expression of PHYD and PHYE. Plant Mol Biol **25:** 413-427

Cone KC, Burr FA, Burr B (1986) Molecular analysis of the maize anthocyanin regulatory locus *C1*. Proc Natl Acad Sci U S A **83:** 9631-9635

Cone KC, Cocciolone SM, Moehlenkamp CA, Weber T, Drummond BJ, Tagliani LA, Bowen BA, Perrot GH (1993) Role of the regulatory gene *pl* in the photocontrol of maize anthocyanin pigmentation. Plant Cell **5:** 1807-1816

Darwin C (1880) The power of movement in plants. John Murray, London

Devlin PF, Yanovsky MJ, Kay SA (2003) A genomic analysis of the shade avoidance response in Arabidopsis. Plant Physiol **133:** 1617-1629

Dooner HK, Robbins TP, Jorgensen RA (1991) Genetic and developmental control of anthocyanin biosynthesis. Annu Rev Genet **25:** 173-199

Drincovich MF, Casati P, Andreo CS, Donahue R, Edwards GE (1998) UV-B induction of NADP-malic enzyme in etiolated and green maize seedlings. Plant Cell Environ **21:** 63-70

Duek PD, Fankhauser C (2005) bHLH class transcription factors take centre stage in phytochrome signalling. Trends Plant Sci **10:** 51-54

Duvick DN (1997) What is yield? *In* GO Edmeades, ed, Developing drought and low N-tolerant maize. CIMMYT, El Batan, Mexico, pp 332-335

Edwards GE, Walker DA (1983) C3, C4: Mechanisms of cellular and environmental regulation of photosynthesis. Blackwell scientific publications, Oxford

Ersoz E, Yu J, Buckler ES (2007) Applications of linkage disequilibrium and association mapping in crop plants. *In* R Varshney, R Tuberosa, eds, Genomics-assisted Crop Improvement. Springer.

Finlayson SA, Hays DB, Morgan PW (2007) *phyB-1* sorghum maintains responsiveness to simulated shade, irradiance and red light: far-red light. Plant Cell Environ **30:** 952-962

Finlayson SA, Lee IJ, Mullet JE, Morgan PW (1999) The mechanism of rhythmic ethylene production in sorghum. The role of phytochrome B and simulated shading. Plant Physiol **119:** 1083-1089

Fischer AJ, Rockwell NC, Jang AY, Ernst LA, Waggoner AS, Duan Y, Lei H, Lagarias JC (2005) Multiple roles of a conserved GAF domain tyrosine residue in cyanobacterial and plant phytochromes. Biochemistry **44:** 15203-15215

Folta KM, Maruhnich SA (2007) Green light: a signal to slow down or stop. J Exp Bot

Franklin KA, Praekelt U, Stoddart WM, Billingham OE, Halliday KJ, Whitelam GC (2003) Phytochromes B, D, and E act redundantly to control multiple physiological responses in Arabidopsis. Plant Physiol **131:** 1340-1346

Franklin KA, Whitelam GC (2005) Phytochromes and shade-avoidance responses in plants. Ann Bot (Lond) **96:** 169-175

Fuchs I, Philippar K, Ljung K, Sandberg G, Hedrich R (2003) Blue light regulates an auxin-induced K^+-channel gene in the maize coleoptile. Proc Natl Acad Sci U S A **100:** 11795-11800

Garg AK, Sawers RJ, Wang H, Kim JK, Walker JM, Brutnell TP, Parthasarathy MV, Vierstra RD, Wu RJ (2006) Light-regulated overexpression of an Arabidopsis phytochrome A gene in rice alters plant architecture and increases grain yield. Planta **223:** 627-636

Gavazzi G, Mereghetti M, Consonni G, Tonelli C (1990) *Sn*, a light-dependent and tissue-specific gene of maize: the genetic basis of its instability. Genetics **125:** 193-199

Goff SA, Ricke D, Lan TH, Presting G, Wang R, Dunn M, Glazebrook J, Sessions A, Oeller P, Varma H, Hadley D, Hutchison D, Martin C, Katagiri F, Lange BM, Moughamer T, Xia Y, Budworth P, Zhong J, Miguel T, Paszkowski U, Zhang S, Colbert M, Sun WL, Chen L, Cooper B, Park S, Wood TC, Mao L, Quail P, Wing R, Dean R, Yu Y, Zharkikh A, Shen R, Sahasrabudhe S, Thomas A, Cannings R, Gutin A, Pruss D, Reid J, Tavtigian S, Mitchell J, Eldredge G, Scholl T, Miller RM, Bhatnagar S, Adey N, Rubano T, Tusneem N, Robinson R, Feldhaus J, Macalma T, Oliphant A, Briggs S (2002) A draft sequence of the rice genome (*Oryza sativa* L. ssp. *japonica*). Science **296:** 92-100

Grotewold E, Chamberlin M, Snook M, Siame B, Butler L, Swenson J, Maddock S, St Clair G, Bowen B (1998) Engineering secondary metabolism in maize cells by ectopic expression of transcription factors. Plant Cell **10:** 721-740

Hall LN, Rossini L, Cribb L, Langdale JA (1998) GOLDEN 2: a novel transcriptional regulator of cellular differentiation in the maize leaf. Plant Cell **10:** 925-936

Hall LN, Roth R, Brutnell TP, Langdale JA (1998) Cellular differentiation in the maize leaf is disrupted by bundle sheath defective mutations. Symp Soc Exp Biol **51:** 27-31

Halliday K, Fankhauser C (2003) Phytochrome-hormonal signalling networks. New Phytologist **157:** 449-463

Hashemi AM, Herbert SJ, Putnam DH (2005) Yield response of corn to crowding stress. Agron J **97:** 839-846

Hatch MD (1971) The C4-pathway of photosynthesis: evidence for an intermediate pool of carbon dioxide and the identity of the donor C4 acid. Biochem J **125:** 425-432

Hudson M (2007) Photoreceptor biotechnology. *In* GC Whitelam, KJ Halliday, eds, Light and plant development, Vol 30. Blackwell, Oxford

Huq E, Al-Sady B, Hudson M, Kim C, Apel K, Quail PH (2004) Phytochrome-interacting factor 1 is a critical bHLH regulator of chlorophyll biosynthesis. Science **305:** 1937-1941

Huq E, Quail PH (2002) PIF4, a phytochrome-interacting bHLH factor, functions as a negative regulator of phytochrome B signaling in Arabidopsis. Embo J **21:** 2441-2450

Iino M (1990) Phototropism: mechanism and ecological implications. Plant Cell Environ **13:** 633-650

Izaguirre MM, Mazza CA, Biondini M, Baldwin IT, Ballare CL (2006) Remote sensing of future competitors: impacts on plant defenses. Proc Natl Acad Sci U S A **103:** 7170-7174

Izawa T, Oikawa T, Tokutomi S, Okuno K, Shimamoto K (2000) Phytochromes confer the photoperiodic control of flowering in rice (a short-day plant). Plant J **22:** 391-399

Jeong DH, Lee S, Kim SL, Hwang I, An G (2007) Regulation of brassinosteroid responses by phytochrome B in rice. Plant Cell Environ **30:** 590-599

Jiao Y, Lau OS, Deng XW (2007) Light-regulated transcriptional networks in higher plants. Nat Rev Genet **8:** 217-230

Jiao Y, Ma L, Strickland E, Deng XW (2005) Conservation and divergence of light-regulated genome expression patterns during seedling development in rice and Arabidopsis. Plant Cell **17:** 3239-3256

Jordan DB, Ogren WL (1984) The CO_2/O_2 specificity of ribulose 1,5-bisphoshate carboxylase/oxygenase. Planta **161:** 308-313

Kasperbauer MJ, Karlen DL (1994) Plant spacing and reflected far-red light effects on phytochrome-regulated photosynthate allocation in corn seedlings. Crop Sci **34:** 1564-1569

Kebrom T, Brutnell TP (2007) The molecular analysis of the shade avoidance syndrome in the grasses has begun. J Ex Bot **58:** 3079-3089

Kim J, Yi H, Choi G, Shin B, Song PS (2003) Functional characterization of phytochrome interacting factor 3 in phytochrome-mediated light signal transduction. Plant Cell **15:** 2399-2407

Kircher S, Kozma-Bognar L, Kim L, Adam E, Harter K, Schafer E, Nagy F (1999) Light quality-dependent nuclear import of the plant photoreceptors phytochrome A and B. Plant Cell **11:** 1445-1456

Klar T, Pokorny R, Moldt J, Batschauer A, Essen LO (2007) Cryptochrome 3 from *Arabidopsis thaliana*: structural and functional analysis of its complex with a folate light antenna. J Mol Biol **366:** 954-964

Kong S-G, Lee D-S, Kwak S-N, Kim J-K, Sohn J-K, Kim I-S (2004) Characterization of sunlight-grown transgenic rice plants expressing Arabidopsis phytochrome A. Mol Breeding **14:** 35-45

Koornneef M, Rolff E, Spruitt CJP (1980) Genetic control of light-induced hypocotyl elongation in *Arabidopsis thaliana* L. Zeitschrift fur Pflanzenphysiologie **100:** 147-160

Kreuzaler F, Ragg H, Fautz E, Kuhn DN, Hahlbrock K (1983) UV-induction of chalcone synthase mRNA in cell suspension cultures of *Petroselinum hortense*. Proc Natl Acad Sci U S A **80:** 2591-2593

Lagarias JC, Lagarias DM (1989) Self-assembly of synthetic phytochrome holoprotein *in vitro*. Proc Natl Acad Sci U S A **86:** 5778-5780

Langdale JA, Zelitch I, Miller E, Nelson T (1988) Cell position and light influence C4 versus C3 patterns of photosynthetic gene expression in maize. EMBO J **7:** 3643-3651

Lin C (2002) Blue light receptors and signal transduction. Plant Cell **14 Suppl:** S207-225

Maddonni GA, Chelle M, Drouet J-L, Andrieu B (2001) Light interception of contrasting azimuth canopies under square and rectangular plant spatial distributions: simulations and crop measurements. Field Crops Res **70:** 1-13

Maddonni GA, Otegui ME (2006) Intra-specific competition in maize: Contribution of extreme plant hierarchies to grain yield, grain yield component and kernel composition. Field Crops Res **97:** 155-166

Maddonni GA, Otegui ME, Andrieu B, Chelle M, Casal JJ (2002) Maize leaves turn away from neighbors. Plant Physiol **130:** 1181-1189

Maddonni GA, Otegui ME, Cirilo AG (2001) Plant population density, row spacing and hybrid effects on maize canopy architecture and light attenuation. Field Crops Res **71:** 181-193

Mancinelli A (1994) The physiology of phytochrome action. *In* RE Kendrick, GHM Kronenberg, eds, Photomorphogenesis in Plants, Ed 2. Kluwer, Dordrecht, pp 211-269

Markelz NH, Costich DE, Brutnell TP (2003) Photomorphogenic responses in maize seedling development. Plant Physiol **133:** 1578-1591

Martinez-Garcia JF, Huq E, Quail PH (2000) Direct targeting of light signals to a promoter element-bound transcription factor. Science **288:** 859-863

Mathews S (2006) Phytochrome-mediated development in land plants: red light sensing evolves to meet the challenges of changing light environments. Mol Ecol **15:** 3483-3503

Mathews S, Donoghue MJ (1999) The root of angiosperm phylogeny inferred from duplicate phytochrome genes. Science **286:** 947-950

Mathews S, Sharrock RA (1996) The phytochrome gene family in grasses (Poaceae): a phylogeny and evidence that grasses have a subset of the loci found in dicot angiosperms. Mol Biol Evol **13:** 1141-1150

Mathews S, Sharrock RA (1997) Phytochrome gene diversity. Plant Cell Environ **20:** 666-671

Matsushita T, Mochizuki N, Nagatani A (2003) Dimers of the N-terminal domain of phytochrome B are functional in the nucleus. Nature **424:** 571-574

Monte E, Al-Sady B, Leivar P, Quail PH (2007) Out of the dark: how the PIFs are unmasking a dual temporal mechanism of phytochrome signalling. J Exp Bot **58:** 3125-3133

Montgomery BL, Lagarias JC (2002) Phytochrome ancestry: sensors of bilins and light. Trends Plant Sci **7:** 357-366

Morelli G, Ruberti I (2000) Shade avoidance responses. Driving auxin along lateral routes. Plant Physiol **122:** 621-626

Multani DS, Briggs SP, Chamberlin MA, Blakeslee JJ, Murphy AS, Johal GS (2003) Loss of an MDR transporter in compact stalks of maize *br2* and sorghum *dw3* mutants. Science **302:** 81-84

Nakamura Y, Kato T, Yamashino T, Murakami M, Mizuno T (2007) Characterization of a set ofphytochrome-interacting factor-like bHLH proteins in *Oryza sativa*. Biosci Biotechnol Biochem **71:** 1183-1191

Noh B, Bandyopadhyay A, Peer WA, Spalding EP, Murphy AS (2003) Enhanced gravi- and phototropism in plant *mdr* mutants mislocalizing the auxin efflux protein PIN1. Nature **423:** 999-1002

O'Bryan K, Paszkiewicz S, Butzen S (2006) Corn hybrid response to plant population. Crop Insights, Pioneer Hi-bred International, Inc., Johnston, Iowa. **16**

Oh E, Kim J, Park E, Kim JI, Kang C, Choi G (2004) PIL5, a phytochrome-interacting basic helix-loop-helix protein, is a key negative regulator of seed germination in *Arabidopsis thaliana*. Plant Cell **16:** 3045-3058

Oh E, Yamaguchi S, Hu J, Yusuke J, Jung B, Paik I, Lee HS, Sun TP, Kamiya Y, Choi G (2007) PIL5, a phytochrome-interacting bHLH protein, regulates gibberellin responsiveness by binding directly to the GAI and RGA promoters in Arabidopsis seeds. Plant Cell **19:** 1192-1208

Pagano E, Maddonni GA (2007) Intra-specific competition in maize: Early established hierarchies differ in plant growth and biomass partitioning to the ear around silking. Field Crops Res **101:** 306-320

Parks BM, Folta KM, Spalding EP (2001) Photocontrol of stem growth. Curr Opin Plant Biol **4:** 436-440

Paz-Ares J, Wienand U, Peterson PA, Saedler H (1986) Molecular cloning of the *c* locus of *Zea mays*: a locus regulating the anthocyanin pathway. Embo J **5:** 829-833

Petroni K, Cominelli E, Consonni G, Gusmaroli G, Gavazzi G, Tonelli C (2000) The developmental expression of the maize regulatory gene *Hopi* determines germination-dependent anthocyanin accumulation. Genetics **155:** 323-336

Philippar K, Fuchs I, Luthen H, Hoth S, Bauer CS, Haga K, Thiel G, Ljung K, Sandberg G, Bottger M, Becker D, Hedrich R (1999) Auxin-induced K^+ channel expression represents an essential step in coleoptile growth and gravitropism. Proc Natl Acad Sci U S A **96:** 12186-12191

Piazza P, Procissi A, Jenkins GI, Tonelli C (2002) Members of the *c1/pl1* regulatory gene family mediate the response of maize aleurone and mesocotyl to different light qualities and cytokinins. Plant Physiol **128:** 1077-1086

Pierik R, Cuppens ML, Voesenek LA, Visser EJ (2004) Interactions between ethylene and gibberellins in phytochrome-mediated shade avoidance responses in tobacco. Plant Physiol **136:** 2928-2936

Pilu R, Piazza P, Petroni K, Ronchi A, Martin C, Tonelli C (2003) *pl-bol3*, a complex allele of the anthocyanin regulatory *pl1* locus that arose in a naturally occurring maize population. Plant J **36:** 510-521

Procissi A, Dolfini S, Ronchi A, Tonelli C (1997) Light-dependent spatial and temporal expression of pigment regulatory genes in developing maize seeds. Plant Cell **9:** 1547-1557

Purcell M, Mabrouk YM, Bogorad L (1995) Red/far-red and blue light-responsive regions of maize *rbcS*-m3 are active in bundle sheath and mesophyll cells, respectively. Proc Natl Acad Sci U S A **92:** 11504-11508

Qiu QS, Hardin SC, Mace J, Brutnell TP, Huber SC (2007) Light and metabolic signals control the selective degradation of sucrose synthase in maize leaves during deetiolation. Plant Physiol **144:** 468-478

Quail PH, Boylan MT, Parks BM, Short TW, Xu Y, Wagner D (1995) Phytochromes: photosensory perception and signal transduction. Science **268:** 675-680

Reed JW, Foster KR, Morgan PW, Chory J (1996) Phytochrome B affects responsiveness to gibberellins in Arabidopsis. Plant Physiol **112:** 337-342

Robson PR, McCormac AC, Irvine AS, Smith H (1996) Genetic engineering of harvest index in tobacco through overexpression of a phytochrome gene. Nat Biotechnol **14:** 995-998

Rockwell NC, Su YS, Lagarias JC (2006) Phytochrome structure and signaling mechanisms. Annu Rev Plant Biol **57:** 837-858

Roig-Villanova I, Bou J, Sorin C, Devlin PF, Martinez-Garcia JF (2006) Identification of primary target genes of phytochrome signaling. Early transcriptional control during shade avoidance responses in Arabidopsis. Plant Physiol **141:** 85-96

Roth R, Hall LN, Brutnell TP, Langdale JA (1996) *bundle sheath defective2*, a mutation that disrupts the coordinated development of bundle sheath and mesophyll cells in the maize leaf. Plant Cell **8:** 915-927

Rudiger W, Thummler F, Cmiel E, Schneider S (1983) Chromophore structure of the physiologically active form (P(fr)) of phytochrome. Proc Natl Acad Sci U S A **80:** 6244-6248

Ryu JS, Kim JI, Kunkel T, Kim BC, Cho DS, Hong SH, Kim SH, Fernandez AP, Kim Y, Alonso JM, Ecker JR, Nagy F, Lim PO, Song PS, Schafer E, Nam HG (2005) Phytochrome-specific type 5 phosphatase controls light signal flux by enhancing phytochrome stability and affinity for a signal transducer. Cell **120:** 395-406

Sage RF (2004) The evolution of C4 photosynthesis. New Phytol **161:** 341-370

Sage RF, Monson RK (1999) C4 plant biology. Academic press, San Diego

Sakamoto K, Nagatani A (1996) Nuclear localization activity of phytochrome B. Plant J **10:** 859-868

Salter MG, Franklin KA, Whitelam GC (2003) Gating of the rapid shade-avoidance response by the circadian clock in plants. Nature **426:** 680-683

Sawers RJ, Linley PJ, Farmer PR, Hanley NP, Costich DE, Terry MJ, Brutnell TP (2002) *elongated mesocotyl1*, a phytochrome-deficient mutant of maize. Plant Physiol **130:** 155-163

Sawers RJ, Linley PJ, Gutierrez-Marcos JF, Delli-Bovi T, Farmer PR, Kohchi T, Terry MJ, Brutnell TP (2004) The *Elm1* (*ZmHy2*) gene of maize encodes a phytochromobilin synthase. Plant Physiol **136:** 2771-2781

Sawers RJ, Liu P, Anufrikova K, Hwang JT, Brutnell TP (2007) A multi-treatment experimental system to examine photosynthetic differentiation in the maize leaf. BMC Genomics **8:** 12

Sawers RJ, Sheehan MJ, Brutnell TP (2005) Cereal phytochromes: targets of selection, targets for manipulation? Trends Plant Sci **10:** 138-143

Schaffner AR, Sheen J (1991) Maize *rbcS* promoter activity depends on sequence elements not found in dicot *rbcS* promoters. Plant Cell **3:** 997-1012

Sessa G, Carabelli M, Sassi M, Ciolfi A, Possenti M, Mittempergher F, Becker J, Morelli G, Ruberti I (2005) A dynamic balance between gene activation and repression regulates the shade avoidance response in Arabidopsis. Genes Dev **19:** 2811-2815

Sheehan MJ, Farmer PR, Brutnell TP (2004) Structure and expression of maize phytochrome family homeologs. Genetics **167:** 1395-1405

Sheehan MJ, Kennedy LM, Costich DE, Brutnell TP (2007) Subfunctionalization of *PhyB1* and *PhyB2* in the control of seedling and mature plant traits in maize. Plant J **49:** 338-353

Sheen J (1999) C4 Gene Expression. Annu Rev Plant Physiol Plant Mol Biol **50:** 187-217

Sheen J, Bogorad L (1988) Differential expression in bundle sheath and mesophyll cells of maize of genes for photosystem II components encoded by the plastid genome. Plant Physiol **86:** 1020-1026

Sheen JY, Bogorad L (1986) Differential expression of six light-harvesting chlorophyll a/b binding protein genes in maize leaf cell types. Proc Natl Acad Sci U S A **83:** 7811-7815

Sheen JY, Bogorad L (1987) Differential expression of C4 pathway genes in mesophyll and bundle sheath cells of greening maize leaves. J Biol Chem **262:** 11726-11730

Shin J, Park E, Choi G (2007) PIF3 regulates anthocyanin biosynthesis in an HY5-dependent manner with both factors directly binding anthocyanin biosynthetic gene promoters in Arabidopsis. Plant J **49:** 981-994

Shinomura T, Nagatani A, Hanzawa H, Kubota M, Watanabe M, Furuya M (1996) Action spectra for phytochrome A- and B-specific photoinduction of seed germination in *Arabidopsis thaliana*. Proc Natl Acad Sci U S A **93:** 8129-8133

Shlumukov LR, Barro F, Barcelo P, Lazzeri P, Smith H (2001) Establishment of far-red high irradiance responses in wheat through transgenic expression of an oat phytochrome A gene. Plant Cell and Environ **24:** 703-712

Smith H (1982) Light quality, photoperception and plant strategy. Annu Rev Plant Physiol **33:** 481-518

Smith H (1995) Physiological and ecological function within the phytochrome family. Annu Rev Plant Physiol Plant Mol Biol **46:** 289-315

Smith H (2000) Phytochromes and light signal perception by plants-an emerging synthesis. Nature **407:** 585-591

Smith H, Whitelam GC (1997) The shade avoidance syndrome: Multiple responses mediated by multiple phytochromes. Plant Cell Environ **20:** 840-844

Stapleton AE, Walbot V (1994) Flavonoids can protect maize DNA from the induction of ultraviolet radiation damage. Plant Physiol **105:** 881-889

Steindler C, Matteucci A, Sessa G, Weimar T, Ohgishi M, Aoyama T, Morelli G, Ruberti I (1999) Shade avoidance responses are mediated by the ATHB-2 HD-zip protein, a negative regulator of gene expression. Development **126:** 4235-4245

Su YS, Lagarias JC (2007) Light-independent phytochrome signaling mediated by dominant GAF domain tyrosine mutants of Arabidopsis phytochromes in transgenic plants. Plant Cell **19:** 2124-2139

Takano M, Inagaki N, Xie X, Yuzurihara N, Hihara F, Ishizuka T, Yano M, Nishimura M, Miyao A, Hirochika H, Shinomura T (2005) Distinct and cooperative functions of phytochromes A, B, and C in the control of deetiolation and flowering in rice. Plant Cell **17:** 3311-3325

Takano M, Kanegae H, Shinomura T, Miyao A, Hirochika H, Furuya M (2001) Isolation and characterization of rice phytochrome A mutants. Plant Cell **13:** 521-534

Tepperman JM, Zhu T, Chang HS, Wang X, Quail PH (2001) Multiple transcription-factor genes are early targets of phytochrome A signaling. Proc Natl Acad Sci U S A **98:** 9437-9442

Terry MJ (1997) Phytochrome chromophore-deficient mutants. Plant Cell Environ **20:** 740-745

Terry MJ, Wahleithner JA, Lagarias JC (1993) Biosynthesis of the plant photoreceptor phytochrome. Archives of Biochemistry and Biophysics **306:** 1-15

Tollenaar M, Wu J (1999) Yield improvement in temperate maize is attributable to greater stress tolerance. Crop Sci **39:** 1597-1604

Troyer AF (1996) Breeding widely adapted, popular maize hybrids. Crop Sci **46:** 528-543

Troyer FA (2006) Adaptedness and heterosis in corn and mule hybrids. Crop Sci **46:** 528-543

Vandenbussche F, Pierik R, Millenaar FF, Voesenek LA, Van Der Straeten D (2005) Reaching out of the shade. Curr Opin Plant Biol **8:** 462-468

Vandenbussche F, Vriezen WH, Smalle J, Laarhoven LJ, Harren FJ, Van Der Straeten D (2003) Ethylene and auxin control the Arabidopsis response to decreased light intensity. Plant Physiol **133:** 517-527

Vierstra RD (2003) The ubiquitin/26S proteasome pathway, the complex last chapter in the life of many plant proteins. Trends Plant Sci **8:** 135-142

Viret JF, Mabrouk Y, Bogorad L (1994) Transcriptional photoregulation of cell-type-preferred expression of maize *rbcS*-m3: 3' and 5' sequences are involved. Proc Natl Acad Sci U S A **91:** 8577-8581

von Caemmerer S, Furbank RT (2003) The C4 pathway: an efficient CO_2 pump. Photosynth Res **77:** 191-207

Wagner JR, Brunzelle JS, Forest KT, Vierstra RD (2005) A light-sensing knot revealed by the structure of the chromophore-binding domain of phytochrome. Nature **438:** 325-331

Whippo CW, Hangarter RP (2006) Phototropism: bending towards enlightenment. Plant Cell **18:** 1110-1119

Xu T, Purcell M, Zucchi P, Helentjaris T, Bogorad L (2001) TRM1, a YY1-like suppressor of *rbcS*-m3 expression in maize mesophyll cells. Proc Natl Acad Sci U S A **98:** 2295-2300

Yanagisawa S (2000) Dof1 and Dof2 transcription factors are associated with expression of multiple genes involved in carbon metabolism in maize. Plant J **21:** 281-288

Yeh KC, Lagarias JC (1998) Eukaryotic phytochromes: light-regulated serine/threonine protein kinases with histidine kinase ancestry. Proc Natl Acad Sci U S A **95:** 13976-13981

CHAPTER TWO

PHYSIOLOGICAL AND GENETIC CHARACTERIZATION OF END-OF-DAY FAR-RED LIGHT RESPONSE IN MAIZE SEEDLINGS *

Abstract

Developmental responses associated with end-of-day far-red light (EOD-FR) signaling were investigated in maize (*Zea mays* ssp. *mays*) seedlings. A survey of genetically diverse inbreds of temperate and tropical/semi-tropical origins, together with teosinte (*Zea mays* ssp. *parviglumis*) and a modern hybrid revealed distinct elongation responses. A mesocotyl elongation response to the EOD-FR treatment was largely absent in the tropical/semi-tropical lines, but both hybrid and temperate inbred responses were of the same magnitude as teosinte, suggesting that EOD-FR-mediated mesocotyl responses were not lost during the domestication or breeding processes. The genetic architecture underlying seedling responses to EOD-FR was investigated using the Intermated B73 x Mo17 mapping population. Among the different quantitative trait loci identified, two were consistently detected for elongation and responsiveness under EOD-FR, but none were associated with known light signaling loci. The central role of phytochromes in mediating EOD-FR responses was shown using a *phyB1 phyB2* mutant series. Unlike the coleoptile and 1st leaf sheath, EOD-FR-mediated elongation of the mesocotyl appears predominantly controlled by GA. EOD-FR also reduced ABA levels in the mesocotyl for both wild-type and *phyB1 phyB2* double mutants, suggesting a FR-mediated but PHYB-independent control of ABA accumulation. EOD-FR elongation responses were attenuated in both wild-type and

phyB1 phyB2 double mutants when a chilling stress was applied during the dark period, concomitant with an increase in ABA levels. We present a model for EOD-FR response that integrates light and hormonal control of seedling elongation.

* Dubois PG, Olsefski GT, Flint-Garcia S, Setter TL, Hoekenga OA, Brutnell TP. (Accepted for publication) Plant Physiol.

2.1 Introduction

Plants utilize a complex network of photoreceptors to monitor the spectral quality, fluence, direction, and duration of light (Smith, 1995). These photosensory pigments include phytochromes that sense red (R, 580-690 nm) and FR (690-800 nm), and the cryptochromes, phototropins, and zeitlupes for blue (380-495 nm) and UV-A (320-380 nm). The light reflected and transmitted by the vegetation creates a canopy characterized by reductions in both the R to FR ratio (R:FR) and the photosynthetically active radiation (400-700 nm). This light environment induces adaptive biochemical and morphological responses known as the shade avoidance syndrome (Smith and Whitelam, 1997). These responses can be induced early in development, before canopy closure, through FR reflected from adjacent neighbor plants (Ballare et al., 1990) or from low-lying weeds (Rajcan and Swanton, 2001) which can negatively impact yields in maize (Rajcan et al., 2004), even if only present early in the growing season (Liu et al., 2009).

R:FR signals are transduced by the phytochrome family of photoreceptors (Franklin and Whitelam, 2007). In rice (*Oryza sativa*) and sorghum (*Sorghum bicolor*), three genes constitute the phytochrome family: PHYA, PHYB, and PHYC. In maize, an ancient alloploidization has doubled the family size to six: *PhyA1*,

PhyA2, *PhyB1*, *PhyB2*, *PhyC1*, and *PhyC2* (Sheehan et al., 2004). Although many similarities are apparent between maize and Arabidopsis (*A. thaliana*) light response, there are significant differences between members of the phytochrome gene family in copy number and selection pressures that have resulted in the divergence of phytochrome signaling networks (Sawers et al., 2005; Sheehan et al., 2007). Thus far, only three phytochrome mutants have been characterized in maize: *elm1*, *phyB1*, and *phyB2*. The *elm1* mutant carries a mutation in phytochromobilin synthase, necessary for the biosynthesis of the chromophore common to all phytochromes (Sawers et al., 2004). The mutation severely reduces the total phytochrome pool but the weak nature of the allele enables a partial responsiveness to R and FR (Markelz et al., 2003). At maturity, *elm1* mutants have elongated internodes, pale green leaves, and flower early (Sawers et al., 2002). Mutations at *phyB1* and *phyB2* also impair light signal transduction. At maturity, both PHYB1 and PHYB2 contribute to plant height, stem diameter, and sheath:internode length, but PHYB2 predominates in the control of flowering (Sheehan et al., 2007). Like the sorghum and rice *phyB* mutants (Childs et al., 1997; Takano et al., 2005; Kebrom et al., 2010), both *elm1* and *phyB1 phyB2* double mutants constitutively display several traits associated with low R:FR response (Sawers et al., 2002; Markelz et al., 2003; Sheehan et al., 2007).

In Arabidopsis, R/FR-mediated responses are developmentally complex and involve the PIF proteins (Duek and Fankhauser, 2005) and many hormones including auxins (Tao et al., 2008), ethylene (Khanna et al., 2007), jasmonate (Moreno et al., 2009) and GA (Djakovic-Petrovic et al., 2007). In particular, there is a direct interaction between PIF and DELLA proteins that govern phytochrome-mediated elongation (de Lucas et al., 2008; Feng et al., 2008; Lorrain et al., 2008). DELLA proteins also regulate FR-inhibition of germination by ABA (Piskurewicz et al., 2009), suggesting an interaction between the PIFs and ABA signaling. Complex crosstalk

between light and temperature has also been reported (Franklin, 2009). In Arabidopsis, colder temperatures can repress the early flowering phenotype of the *phyB* mutant (Halliday et al., 2003). These studies suggest a complex interplay between light, hormone and temperature to fine-tune elongation response.

The end-of-day FR (EOD-FR) treatment consists of a pulse of FR given at subjective dusk (Kasperbauer, 1971) and triggers a circadian clock-gated response (Salter et al., 2003). EOD-FR treatments result in a minimal pool of active Pfr during dark period (Fankhauser and Casal, 2004) and plants submitted to daily treatments display similar developmental responses to those elicited by a continuous photoperiod with low R:FR (Smith, 1994). One of the key features that contributed to the discovery of the phytochromes is the photoreversibility of the response (Borthwick et al., 1952). These low-fluence responses (LFR) are induced or repressed by alternating R or FR treatments (Mancinelli, 1994). The LFR nature of EOD-FR in maize was previously demonstrated in 5 d old mesocotyl and coleoptile tissues (Gorton and Briggs, 1980). The EOD-FR treatment offers several advantages over growing plants in continuous low R:FR, including exposing plants to relatively brief treatment periods thus potentially reducing genotype x environment effects. It also facilitates kinetic assays of phytochrome response as treatments are limited to a single point in the diurnal cycle and can be delivered at any stage in plant development. Finally, as relatively low fluences of light are needed to saturate EOD-FR responses, large populations of seedlings can be screened without the need for large numbers of FR light emitting diodes (LED) or sophisticated light chambers.

Here, we have examined EOD-FR-mediated responses in maize and its closest relative teosinte (*Zea mays* ssp. *parviglumis*). A survey of genetically diverse maize and teosinte accessions revealed extensive tissue-specific variations in mesocotyl, coleoptile, and 1st leaf sheath elongation. EOD-FR responses were greatly attenuated

in tropical/semi-tropical (TS) accessions, but present in teosinte, temperate inbreds and a modern commercial hybrid suggesting that the EOD-FR response is plastic in *Zea mays*. To investigate the genetic regulation underlying seedling responses to EOD-FR, we performed a quantitative trait loci (QTL) analysis using the Intermated B73 x Mo17 (IBM) recombinant inbred population. We identified several QTL that regulate mesocotyl and 1st leaf sheath response to EOD-FR and show that these QTL mediate tissue-specific responses. The *phyB1 phyB2* mutant series was also evaluated, indicating that the two *PhyB* paralogs are largely redundant in mediating EOD-FR response. Pharmacological assays revealed a major role for GA in promoting mesocotyl, but not coleoptile or 1st leaf sheath elongation in response to EOD-FR treatments. In contrast, EOD-FR reduced mesocotyl ABA levels. A chill treatment (10°C) applied during dark breaks attenuated EOD-FR elongation responses. Based on these observations, we discuss a model that integrates temperature, light and hormonal inputs in the regulation of mesocotyl elongation.

2.2 Results

2.2.1 An EOD-FR Treatment Induces a Phytochrome-Mediated Low Fluence Response in Seedlings

We developed an EOD-FR assay to screen large numbers of maize seedlings in a conventional growth chamber (see Materials and Methods). One section was equipped with white (W) fluorescent lights, plus lateral R and FR LED modules, while a similar section was used for the W control treatments. Spectral irradiances were measured for all light treatments (Fig. 2.1). Seedlings grown under W only in both sections showed no significant differences in elongation responses between the two

chamber sections, confirming equivalent growth conditions (data not shown). The robustness of a daily 15 min EOD-FR treatment was initially confirmed using two maize inbreds belonging to two heterotic groups: B73 (stiff stalk, SS) and W22 (non-stiff stalk, NSS). After a 10 d growth period, mesocotyl, coleoptile, and 1st leaf sheath lengths were measured (Fig. 2.2A). For both inbred lines, the EOD-FR treatment caused a significant increase in the length of all three seedling tissues measured. Proportionally, the emerged mesocotyl was the most responsive tissue followed by the coleoptile and the 1st leaf sheath (Fig. 2.2B). EOD-FR-treated plants were also significantly thinner and paler than controls, both features of *elm1* and *phyB1 phyB2* double mutant plants (Sawers et al., 2002; Sheehan et al., 2007) and reminiscent of seedling phenotypes observed at high planting densities (Dubois and Brutnell, 2009).

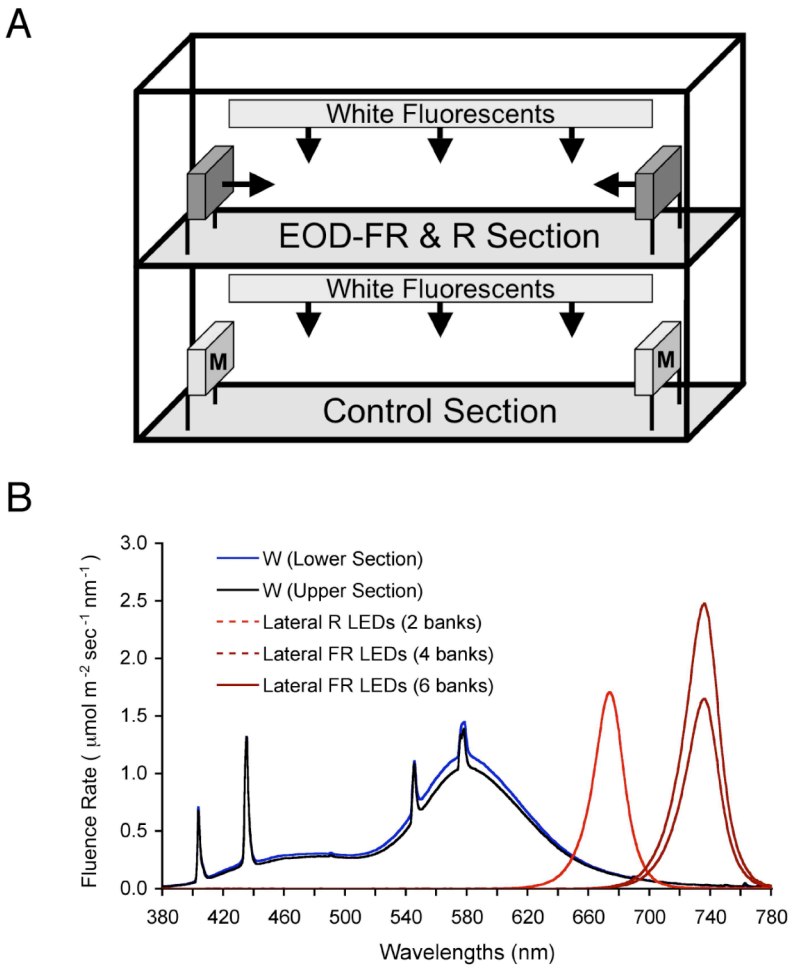

Figure 2.1 Growth chamber design and spectral measurements of the different light treatments. A, Schematic of the lighting system in each section of the growth chamber. The lower section was used for W control treatments and also contains mock equipment to generate a similar distribution of reflected W scatter as upper chamber. The upper section contained R and FR LED banks at the sides of chamber. B, Spectral fluence rate measurements of the different light treatments. Fluorescent lighting was provided by overhead lamps. Lateral R and FR treatments were provided using either 4 FR LED banks and 2 R LED banks (FR-R reversal) or 6 FR LED banks (EOD-FR only). M, mock equipment.

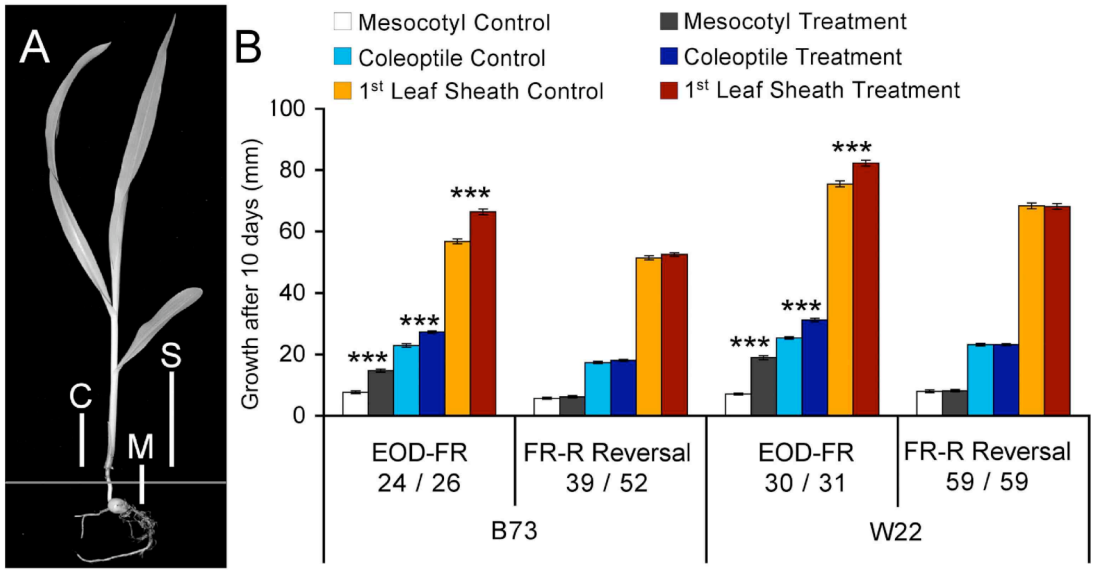

Figure 2.2 Seedling responses to EOD-FR and FR-R reversal treatments. A, Seedling traits measured 10 days after planting. The horizontal grey line represents the soil surface. M., mesocotyl; C., coleoptile; S., 1st leaf sheath. B, Responses to daily EOD-FR treatments on maize seedlings and photoreversibility by subsequent R treatments. Seedlings of B73 and W22 inbreds were subjected to either a daily pulse of 15 min of FR at the end of a 10 h photoperiod (EOD-FR) or the EOD-FR treatment immediately followed by an additional 15 min. pulse of R. For both EOD-FR and FR-R treatments, control seedlings received 10 h W only. The values are representative of the mean ± SE of seedlings used for each light treatment. The number of seedlings measured for W control /EOD-FR (left side) or W control /FR-R (right side) are shown below each graph. Asterisks indicate significance between the two light treatments using Student's *t* test for each line (*** $P < 0.001$).

To examine the photoreversibility of the EOD-FR treatment on mesocotyl, coleoptile, and 1st leaf sheath elongation, a pulse of 15 min of R (47.4 μmol m^{-2} sec^{-1}) was applied immediately after FR (51.1 μmol m^{-2} sec^{-1}). Seedlings of both inbreds were not significantly different than W control for all three traits measured (Fig. 2.2B). *In vitro* measurements on Pr/Pfr reversibility (Kelly and Lagarias, 1985) indicated that 15 min of FR is sufficient to photoconvert ~ 97% of Pfr to Pr. The subsequent R treatment converts ~ 85% the phytochrome pools to Pfr before

developmental responses are irreversibly transduced. Thus, the EOD-FR response induced by this treatment regime is likely mediated by phytochromes acting in the LFR mode.

The impact of EOD-FR on aboveground biomass was examined using the B73 inbred and a commercial hybrid (34P88, Pioneer Hi-Bred). Dry weights were measured after 10 d growth. As in all the experiments, identical planting densities were used for both light treatments to reduce confounding effect of crowding on seedling development. For both inbred and hybrid seedlings, no significant differences in dry weights (B73 Student's $t = 0.58$, $P = 0.59$; 34P88 Student's $t = 1.4$, $P = 0.21$) were observed between the two light treatments. These results suggest that at this developmental stage, the EOD-FR treatment causes a repartitioning of photosynthate between tissues rather than a change in biomass.

2.2.2 Responsiveness to EOD-FR Varies Among a Genetically Diverse Germplasm Panel

To examine the range of variation in the EOD-FR response in maize, a panel of genetically diverse maize lines was screened. The panel consisted of the 26 founders of the Nested Association Mapping (NAM) population (McMullen et al., 2009), Mo17 and W22. These 28 lines were screened for their response to EOD-FR (Table 2.1) and include SS, NSS, popcorn, sweet corn, TS and mixed (likely TS admixtures) inbred accessions (Liu et al., 2003). Seedlings displayed significant variation for tissue elongation under control and EOD-FR treatments (Fig. 2.3). As a group, TS accessions were generally significantly shorter than non-TS (mainly temperates) for all three seeding traits and under both light treatments (Student's t test, all P values < 0.001 except for 1st leaf sheath under EOD-FR where $P = 0.03$; Fig. 2.3). When

comparing the three most common inbred lines used in genetic research (B73, Mo17, and W22), B73 and W22 had the two longest mesocotyl lengths under both light treatments among the panel while Mo17 was much shorter but displayed the strongest EOD-FR elongation response of the three. This developmental pattern was also observed for coleoptile and 1st leaf sheath. Thus, significant variation was observed both between TS and non-TS lines and also within non-TS lines.

Table 2.1. *Seedling responses to EOD-FR treatments in a panel of genetically diverse maize inbreds.*

			Mesocotyl		Coleoptile		1st Leaf Sheath	
Inbreds	Group	Individuals C / EOD-FR	EOD-FR Response Ratio	(%)	EOD-FR Response Ratio	(%)	EOD-FR Response Ratio	(%)
B73	SS	57 / 58	INC***	56.6	INC***	13.3	INC***	11.5
B97	NSS	29 / 30	INC***	55.9	INC**	14.5	NS	--
Ky21	NSS	16 / 23	INC**	63.9	NS	--	NS	--
M162W	NSS	20 / 19	NS	--	INC***	19.0	INC**	14.3
Mo17	NSS	29 / 25	INC***	134.2	INC***	22.2	INC***	23.0
MS71	NSS	31 / 31	INC*	41.8	INC***	9.0	INC***	11.0
Oh43	NSS	30 / 30	INC***	105.0	INC***	18.5	INC***	20.9
W22	NSS	32 / 31	INC***	77.3	INC***	16.4	INC**	5.6
HP301	Popcorn	18 / 26	INC***	87.8	NS	--	INC*	11.6
Il14H	Sweet	28 / 28	INC***	43.2	NS	--	INC***	15.8
P39	Sweet	24 / 30	NS	--	INC*	17.4	INC**	17.0
M37W	Mixed	27 / 30	INC*	47.7	INC*	5.6	NS	--
Mo18W	Mixed	17 / 17	INC***	109.8	NS	--	NS	--
Oh7B	Mixed	31 / 31	INC***	117.8	INC***	15.7	INC***	25.7
Tx303	Mixed	29 / 31	INC**	68.1	NS	--	INC**	8.8
CML103	TS	24 / 28	INC*	162.3	INC**	13.1	NS	--
CML228	TS	30 / 32	INC*	160.9	INC***	14.1	INC***	20.2
CML247	TS	31 / 28	NS	--	INC***	21.7	INC***	19.5
CML277	TS	30 / 26	NS	--	INC***	14.8	INC***	18.3
CML322	TS	26 / 19	NS	--	INC*	17.4	INC***	20.2
CML333	TS	30 / 27	NS	--	INC***	18.1	NS	--
CML52	TS	32 / 32	NS	--	INC***	19.1	INC***	18.3
CML69	TS	23 / 20	NS	--	INC***	15.8	INC**	15.6
Ki11	TS	31 / 32	NS	--	NS	--	INC***	11.1
Ki3	TS	27 / 23	NS	--	INC***	33.3	INC***	21.7
NC350	TS	31 / 32	INC*	87.1	INC***	18.3	INC***	22.4
NC358	TS	32 / 28	INC***	64.4	INC***	18.3	INC*	7.2
Tzi8	TS	12 / 17	NS	--	NS	--	NS	--

Maize inbreds are grouped based on population structure. Limited seed availability for Tzi8, combined with poor germination contributed to reduced statistical power in analyzing this line. C, control; SS, temperate stiff stalk; NSS, temperate non-stiff stalk; TS, tropical/subtropical; Ind., number of individual measured for W control and EOD-FR treatments respectively; INC, significant elongation increase over control treatment; NS, non-significant difference between the two treatments; based on Student's *t* test (* $P < 0.05$, ** $P < 0.01$, *** $P < 0.001$).

Figure 2.3 Growth responses in a genetically diverse maize inbred panel. A, Mesocotyl length. B, Coleoptile length. C, 1st leaf sheath length. The values represent the mean ± SE. Student's *t* tests between the W control and EOD-FR treatments for each line and the numbers of individuals used for each line and treatments are presented in Table 2.1. D, Comparison between non-TS and TS inbreds for mesocotyl, coleoptile, and 1st leaf sheath length under EOD-FR and control treatments (* $P < 0.05$, *** $P < 0.001$). NSS, non-stiff stalk; SS, stiff stalk; TS, tropical/subtropical; non-TS, inbreds from the diversity panel (Table 2.1) that are not of tropical/subtropical origin. White bars, W control; grey bars, EOD-FR treatment.

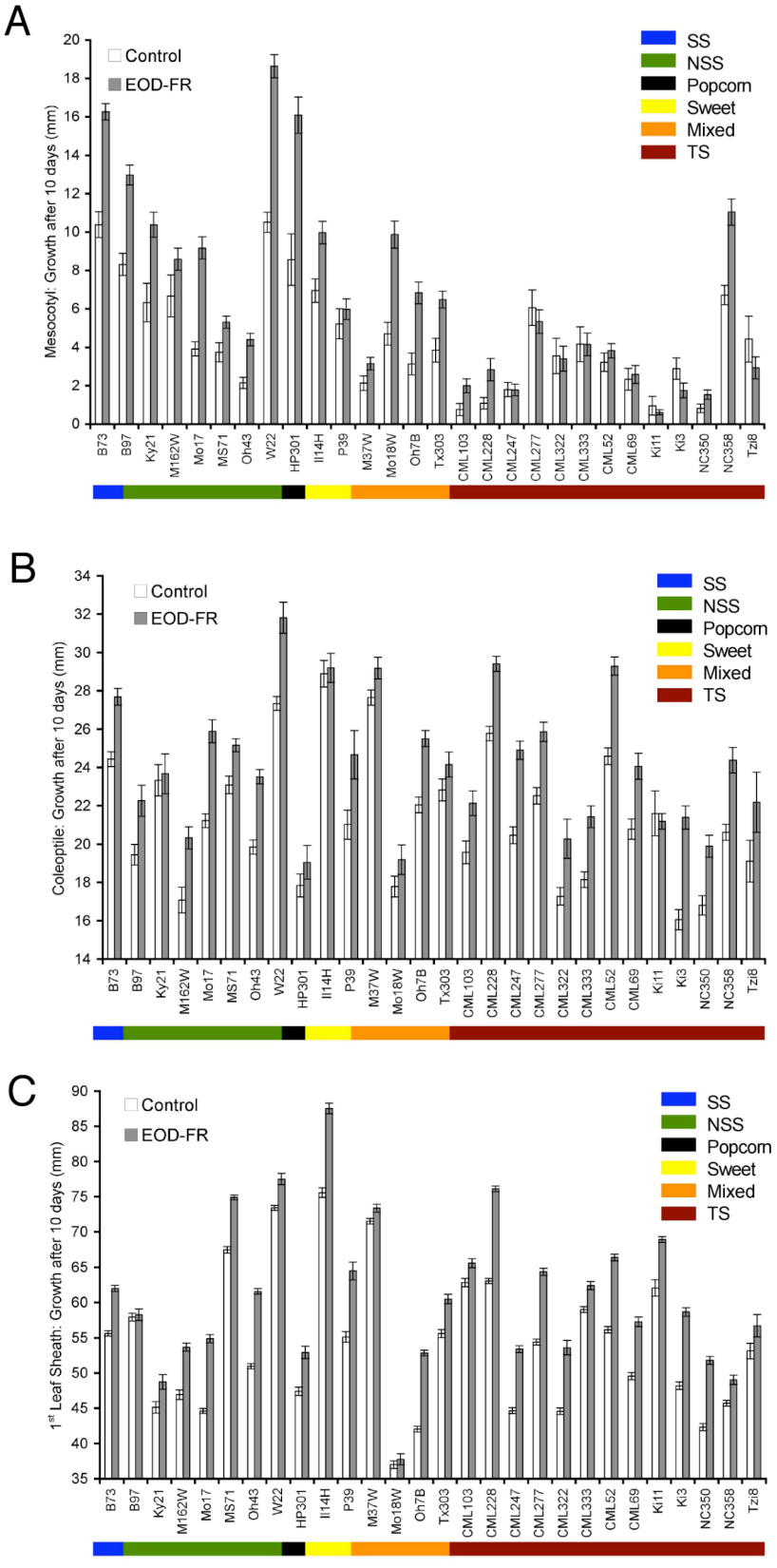
A
Control
EOD-FR
SS
NSS
Popcorn
Sweet
Mixed
TS
Mesocotyl: Growth after 10 days (mm)
B
Coleoptile: Growth after 10 days (mm)
C
1st Leaf Sheath: Growth after 10 days (mm)
B73
B97
Ky21
M162W
Mo17
MS71
Oh43
W22
HP301
Il14H
P39
M37W
Mo18W
Oh7B
Tx303
CML103
CML228
CML247
CML277
CML322
CML333
CML52
CML69
Ki11
Ki3
NC350
NC358
Tzi8

Figure 2.3 (Continued)

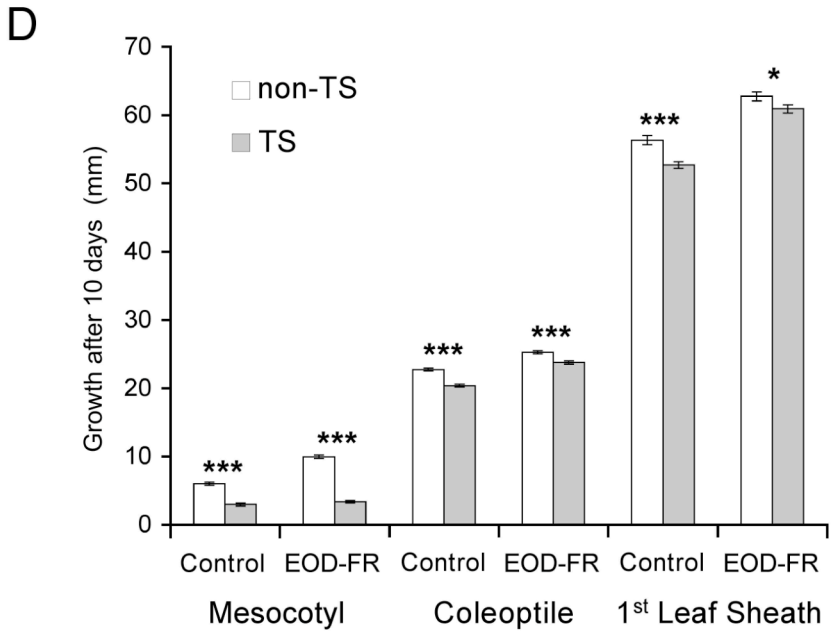

To compare seedling responsiveness to EOD-FR, a response ratio was defined as the percentage increase in tissue length induced by the EOD-FR treatment relative to the W control (EOD-FR response ratio; Table 2.1). Most of the TS lines did not display a significant response for mesocotyl elongation, such that the TS lines as a group were significantly different from all others in mesocotyl behavior ($\chi^2 = 9.69$, $P = 0.002$). The non-TS lines have on average 29% and 30% Southern Dent and Northern Flint landrace backgrounds respectively, versus 13% and 6% for TS lines (Liu et al., 2003). Contrary to the general tendency, mesocotyl tissues of only four TS lines (CML103, CML228, NC350 and NC358) responded significantly ($P < 0.05$) to EOD-FR. Interestingly, these four inbreds have a higher proportion of Southern Dent (averaging 23%) relative to the other TS lines of the panel (averaging 0.9%) (Student's $t = 3.48$, $P = 0.02$). No such distinction within the TS lines exists for the contribution of the three other historic landrace groupings considered: Tropical

Lowland, Tropical Highland, and Northern Flint (Liu et al., 2003). It is worth noting that the photoperiodic regulation of flowering associated with several tropical accessions was attenuated by introgression with temperate germplasm to facilitate their study under long-day seasons (Holland and Goodman, 1995). Thus, selection for early flowering may have accompanied selection for mesocotyl sensitivity to low R:FR. However, no such distinction based on origin could be made for coleoptile or 1st leaf sheath EOD-FR response ratios, suggesting that only the mesocotyl tissues of TS accessions are less sensitive to low R:FR signals while coleoptile and 1st leaf sheath tissues respond in TS as well as non-TS lines. Among the three seedling traits, only coleoptile and 1st leaf sheath EOD-FR response ratios were weakly correlated (r = 0.53), indicating that a tissue-specific control of EOD-FR-mediated responses occurs in the seedling.

To further assess the consequences of domestication and breeding selection on FR-mediated responses, the maize ancestor teosinte (Doebley et al., 2006), and a commercial hybrid (34P88) were also grown under EOD-FR. In both cases, the mesocotyl, coleoptile, and 1st leaf sheath were all significantly responsive to EOD-FR (Fig. 2.4). Teosinte EOD-FR elongation ratios were 65%, 17%, and 14% for the mesocotyl, coleoptile and 1st leaf sheath, respectively, while the hybrid ratios were 128%, 16%, and 16%, respectively. In both cases, these results are within the range observed in the inbred diversity panel. Interestingly, teosinte and 34P88 mesocotyl responsiveness is similar to temperate, but not TS inbred lines.

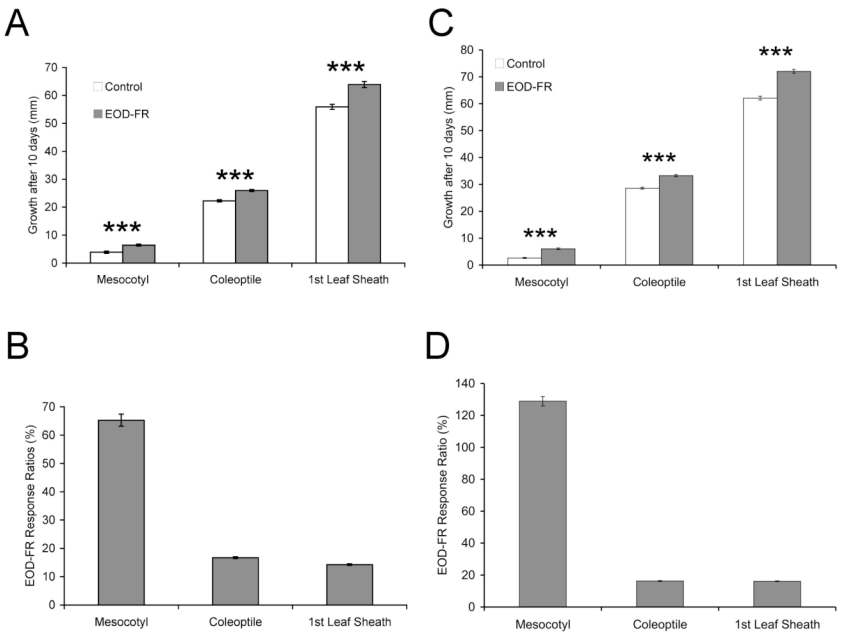

Figure 2.4 Seedling responses to EOD-FR treatments in teosinte and maize hybrid 34P88. Mesocotyl, coleoptile and 1st leaf sheath lengths 10 days after planting (A, teosinte; C, maize hybrid). The values are representative of the mean ± SE. EOD-FR response ratios ± SE for each of the three traits derived from the measurements presented in A and C (B, teosinte; D, maize hybrid). Number of teosinte seedlings measured for W control and EOD-FR treatments (A) were 85 and 81, respectively. Number of maize hybrid seedlings measured for W control and EOD-FR treatments (C) were 55 and 52, respectively. Asterisks indicate Student's *t* test significance between the two light treatments (*** $P < 0.001$).

2.2.3 The Genetic Control of EOD-FR-Mediated Elongation Responses

The survey of a diverse panel of inbred accessions identified a range of EOD-FR-mediated elongation responses. It also revealed significant variation between B73 and Mo17, the two parents of the IBM mapping population (Lee et al., 2002). In order to map the genetic components regulating EOD-FR responses, the IBM population was screened under W control and EOD-FR treatments. Seedling traits analyzed were:

mesocotyl and 1st leaf sheath length under W control and EOD-FR treatments, and EOD-FR response ratios. The distribution of mesocotyl and 1st leaf sheath lengths and corresponding EOD-FR response ratios were all symmetrical and unimodal (Fig. 2.5), thus no transformation of the data was made prior to QTL analysis. Transgressive segregation in the IBM population was observed for all traits measured (Fig. 2.5). Broad-sense heritability (H^2) of the mesocotyl length was 0.80 for W control and 0.87 for EOD-FR while 1st leaf sheath length heritability was 0.89 for W control and 0.90 for EOD-FR. EOD-FR response ratios H^2 were lower, 0.52 for the mesocotyl and 0.63 for the 1st leaf sheath.

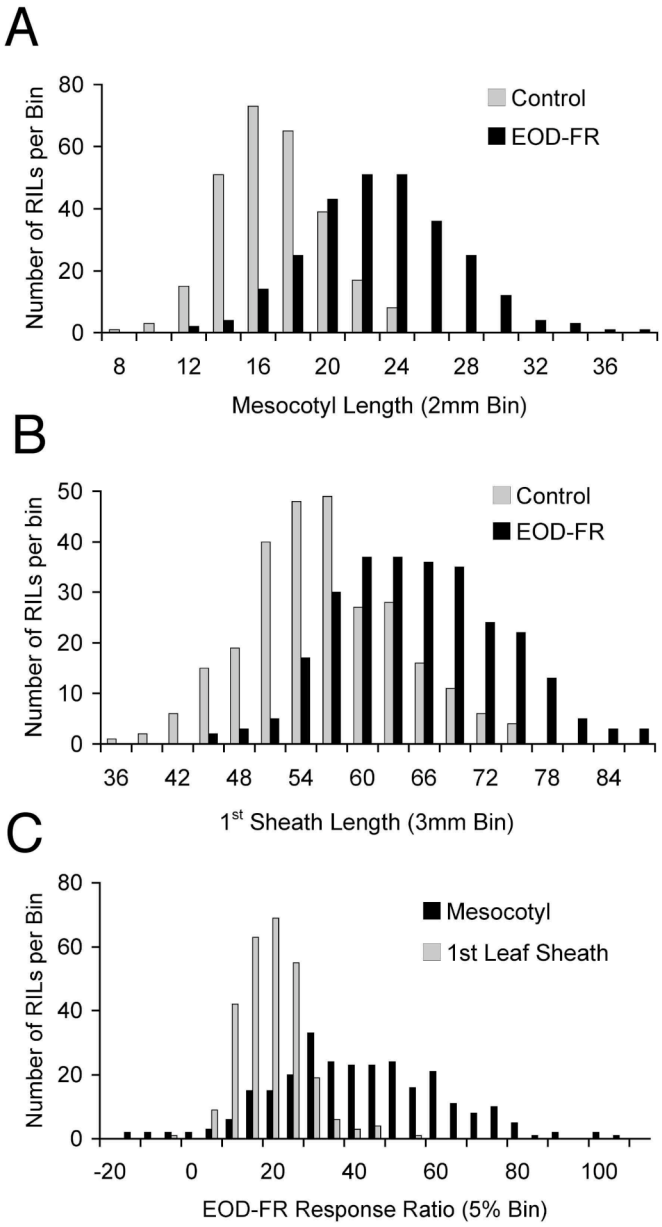

Figure 2.5 Distribution of seedling lengths and EOD-FR response ratios for the IBM mapping population. A, Mesocotyl lengths. B, 1st leaf sheath lengths. C, EOD-FR response ratios for mesocotyl and 1st leaf sheath. Median lengths of mesocotyl for W and EOD-FR were 17.14 and 23.97 mm (B73) and 12.94 mm and 18.35 mm (Mo17), respectively. Median values for 1st leaf sheath lengths for W control and EOD-FR were 49.76 and 58.72 mm (B73 inbred) and 49.31 mm and 62.09 mm (Mo17 inbred), respectively. EOD-FR response ratios for the mesocotyl were 39.8% (B73 inbred) and 41.8% (Mo17 inbred), respectively and for the 1st leaf sheath were 18.0% (B73 inbred) and 25.9% (Mo17 inbred), respectively.

A total of 16 QTL were identified among all traits analyzed. Plots of the composite interval mapping are presented in Fig. 2.6 and summarized in Table 2.2. Only two independent QTL were identified for mesocotyl and 1st leaf sheath EOD-FR response ratios. Interestingly, these two QTL were also detected as EOD-FR elongation QTL for the corresponding seedling trait (Fig. 2.6). The mesocotyl QTL specific to both EOD-FR elongation and EOD-FR response ratio is located on chromosome 9 (bin 9.03), while the 1st leaf sheath QTL is located on chromosome 4 (bin 4.09). For both QTL, the Mo17 allele is responsible for the enhanced response to EOD-FR. These results are consistent with the diversity inbred panel survey (Table 2.1), which also identified Mo17 as having a greater responsiveness to EOD-FR than B73. Furthermore, when all QTL were considered together, a majority of the alleles conferring enhanced EOD-FR responsiveness were from Mo17 (11 out of 16, Table 2.2).

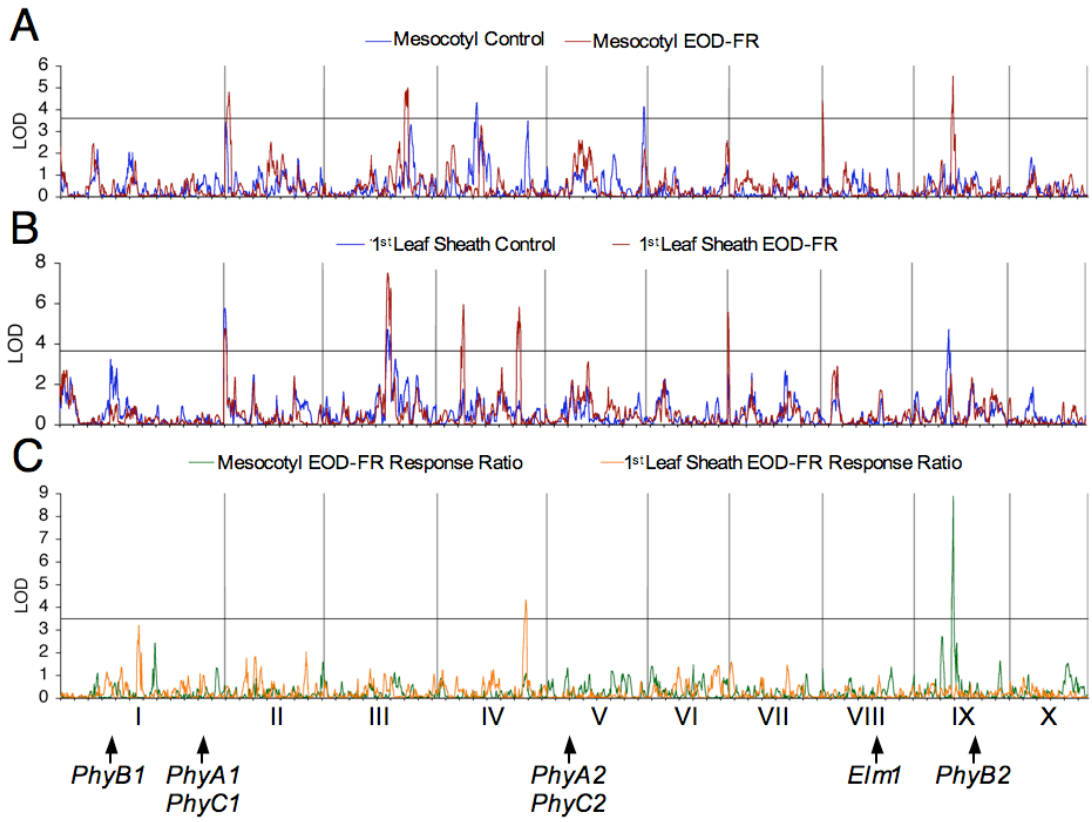

Figure 2.6 QTL analysis of EOD-FR-mediated seedling elongation in the IBM mapping population. LOD plots for seedling lengths and EOD-FR response ratios are shown. A, Mesocotyl length for W control and EOD-FR treatments. B, 1st leaf sheath length for W control and EOD-FR treatments. C, EOD-FR response ratios of mesocotyl and 1st leaf sheath. The horizontal line across each plot indicates the 95% confidence threshold (mesocotyl, 3.58; 1st leaf sheath 3.63; EOD-FR response ratios, 3.48). Vertical lines across each plot delimit each maize chromosome and are numbered along the chromosomal position in C. Arrows indicate the positions of the phytochrome gene family members and *Elm1*. Increments on the X axis represents ~ 80 cM.

Table 2.2. *Significant QTL identified by composite interval analysis for each trait.*

Trait		LOD	Donor Allele	Interval (cM)	Peak (cM)	Marker at Peak	Bin	r^2 at Peak	Model Summary r^2 Adj.	Model Summary *F* Score
Meso-cotyl	Control	4.29	B73	244-253	250.8	umc191	4.04	8.0	13.0	19.38
		4.12	Mo17	582-589	584.3	mmp175	5.08	7.8		
	EOD-FR	4.78	B73	12-34	28.0	php20568b	2.01	7.2	26.7	16.09
		4.84	Mo17	473-496	485.4	umc1404	3.07	6.0		
		4.39	Mo17	0-5	0.0	npi220a	8.01	6.1		
		5.52	Mo17	226-236	233.5	umc1921	9.03	6.8		
	EOD-FR Resp. Ratio	8.87	Mo17	222-236	233.1	umc20	9.03	14.0	5.1	12.94
1st Leaf Sheath	Control	5.74	B73	0-23	6.0	isu53a	2.01	15.9	23.9	20.99
		4.68	Mo17	369-402	381.4	umc60	3.06	7.5		
		4.69	Mo17	214-222	219.8	mmp2	9.03	6.4		
	EOD-FR	4.70	B73	0-19	12.0	isu144a	2.01	15.2	30.2	16.94
		7.47	Mo17	367-402	379.4	umc60	3.06	13.2		
		5.92	Mo17	161-185	179.4	umc1902	4.03	8.7		
		5.80	Mo17	498-523	511.6	umc2135	4.09	6.9		
		5.55	B73	0-7	2.7	csu582	7.00	6.7		
	EOD-FR Resp. Ratio	4.31	Mo17	534-552	545.3	umc1999	4.09	11.0	4.9	13.30

For each QTL detected, the following are listed: the LOD (logarithm of the odds), the parent donor allele, the IBM version 1 (cM) interval distance at threshold $\alpha = 0.05$, the location of the maximum LOD score ("peak"), the marker closest to the peak location, the chromosomal bin location, the r^2 value at the peak (%), and an analysis of variance model summary including the adjusted r^2 for each trait (%), the *F* test score and its associated *P* value. r^2 represents the proportion of phenotypic variation explained by a QTL and adjusted r^2 represents the percentage of the phenotypic variation explained by the all the significant QTL detected for each trait. All *F* scores in the model summary have *P*-values < 0.001.

To examine in more detail the contribution of QTL in bins 4.09 and 9.03, a series of teosinte-maize NILs was used to evaluate their EOD-FR responsiveness. These lines carry small introgressed regions of the teosinte genome in the B73 inbred background. A NIL containing a teosinte introgression corresponding to bin 4.09 did not show enhanced EOD-FR responsiveness relative to the B73 parent and was not characterized further (data not shown). Two additional NILs were also characterized.

The NIL Z033E0026 carries a teosinte introgression of ~100 Mb of chromosome 9 (18.6 to 118.5 Mb, between markers PZA00860 to PZA01819), which spans the QTL interval within bin 9.03 (between 86 and 96 Mb). This NIL also carries two small introgressions at the end of chromosomes 1 (2 Mb, PHM9807 to PZA00243) and 4 (6 Mb, PHM5599 to PZA00282). The NIL Z31E0512 contains a single teosinte introgression on the short arm of chromosome 9 (12.2 Mb, PHM3925 to PZA00466), and this interval does not overlap with the bin 9.03 QTL interval. Thus Z31E0512 was selected as a control for the evaluation of Z033E0026. Neither of the introgressions found in the NILs used contain the candidate gene PhyB2, which is found at 130.6 Mb on chromosome 9 (Fig. 2.6). These two lines and the B73 parent were grown under EOD-FR and EOD-FR response ratios were measured (Fig. 2.7). Line Z033E0026 displayed significantly higher EOD-FR response ratios than the control line for all three of the measured traits. This was surprising as the maize QTL at 9.03 regulated mesocotyl and not in 1st leaf sheath elongation. The mesocotyl and coleoptile lengths of Z033E0026 were also longer than B73 in both W control and EOD-FR treatments. These results suggest that the QTL that displays a tissue-specific response in the IBM population may be broader in its effect on seedling development. The line Z033E0026 has been crossed with B73 to dissociate the two non-target introgressions on chromosome 1 and 4, and to initiate fine mapping of the 9.03 EOD-FR responsive QTL.

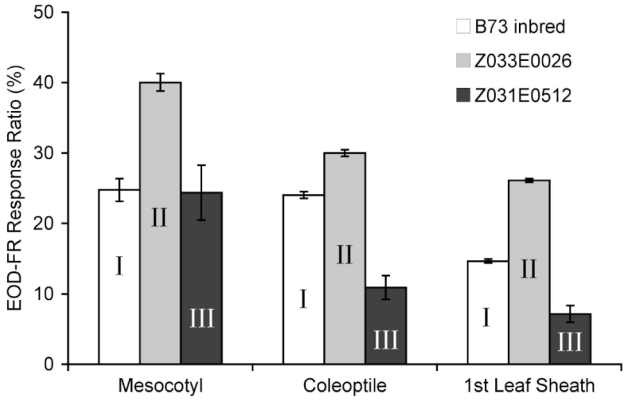

Figure 2.7 EOD-FR response ratios of B73 NILs containing a teosinte introgression. Response ratios for seedling tissues are shown for B73 and introgression lines Z033E0026 (carries chromosome 9 QTL interval) and Z031E0512 (carries a different chromosome 9 segment). Number of measurements for W control and EOD-FR treatments, respectively were: B73 (33 and 27 for mesocotyl, 64 and 57 for coleoptile and 1st leaf sheath), Z033E0026 (32 and 33 for mesocotyl, 59 and 61 for coleoptile and 1st leaf sheath), Z031E0512 (18 and 19 for mesocotyl, coleoptile and 1st leaf sheath). Both NILs were compared to B73 wild-type using Student's t test. A different roman number indicates a P value smaller than 0.05 for each trait.

2.2.4 PhyB1 *and* PhyB2 *are Largely Redundant in Mediating EOD-FR Responses*

In maize, only three light signaling mutants have been described: *elm1* is a weak allele encoding phytochromobilin synthase (Sawers et al., 2004), *phyB1* is a *Mutator* (*Mu*) insertion loss-of-function allele and *phyB2* is the naturally-occurring deletion allele found in the Northern Flint inbred France 2 (Sheehan et al., 2007). A second loss-of-function allele of *phyB2*, carrying a *Mu* insertion (May et al., 2003), was identified during the course of these studies. The *elm1*, *phyB1-Mu* and *phyB2-Mu* alleles were backcrossed multiple generations into the B73 and W22 inbreds to generate a single and double mutant series. Introgressions into an inbred line facilitate detailed phenotypic comparisons between near-isogenic lines. The use of more than one background allows the evaluation of trans-acting genetic modifiers on a mutant

phenotype (Neuffer et al., 1997). Seedling phenotypes of the *phyB* series along with its recurrent parent are presented for both B73 and W22 (Fig. 2.8). Ten days after sowing, the 3rd leaf blade had fully emerged in the B73 seedlings. However, in the W22 background, this leaf blade was only visible in the wild-type under both light treatments and for the two single *phyB* mutants under W control treatments. The development of the *phyB1 phyB2* double mutant in W22 also was delayed relative to B73.

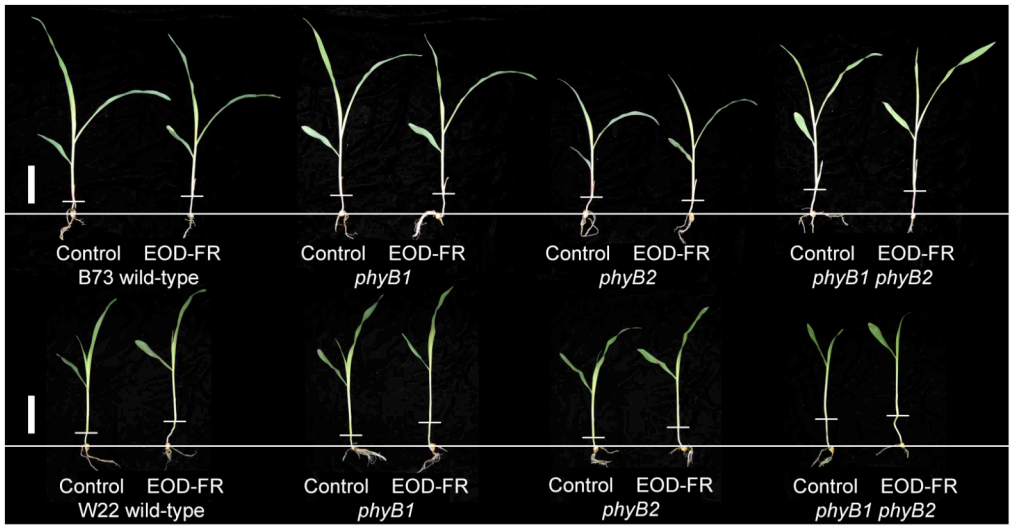

Figure 2.8 Phenotypes of phytochrome *phyB* single and double mutants in B73 and W22 inbreds. Photographs were taken 10 days after planting. The upper panel shows introgressions into the B73 inbred and the lower panel W22 inbreds. Bar = 50 mm. Kernels were aligned along the long horizontal line and the mesocotyl-1st leaf sheath junction is shown by the short horizontal bar.

EOD-FR response ratios for mesocotyl, coleoptile and 1st leaf sheath are presented for B73 (Fig. 2.9A) and W22 (Fig. 2.9B) introgressions. These data show that the responsiveness to EOD-FR is almost completely attenuated in the *phyB1 phyB2* double mutant. However, a small response can still be detected in the mesocotyl (Fig. 2.10). Each of the single mutants and wild-type lines were responsive to EOD-FR. However, significant differences in EOD-FR response ratios exist

between *phyB1* and *phyB2* single mutants, especially for the mesocotyl. These results suggest that *PhyB1* and *PhyB2* are redundant in mediating EOD-FR responses in the seedling, but with a predominant role for *PhyB1* over *PhyB2*. This is consistent with previous studies of *phyB1* and *phyB2* mutants that show *PhyB1* has a greater influence on mesocotyl elongation under W and R than *PhyB2* (Sheehan et al., 2007). The mesocotyl response to EOD-FR of the *phyB1 phyB2* double mutant demonstrates that other photoreceptors also control, to a lesser degree, FR-mediated elongation.

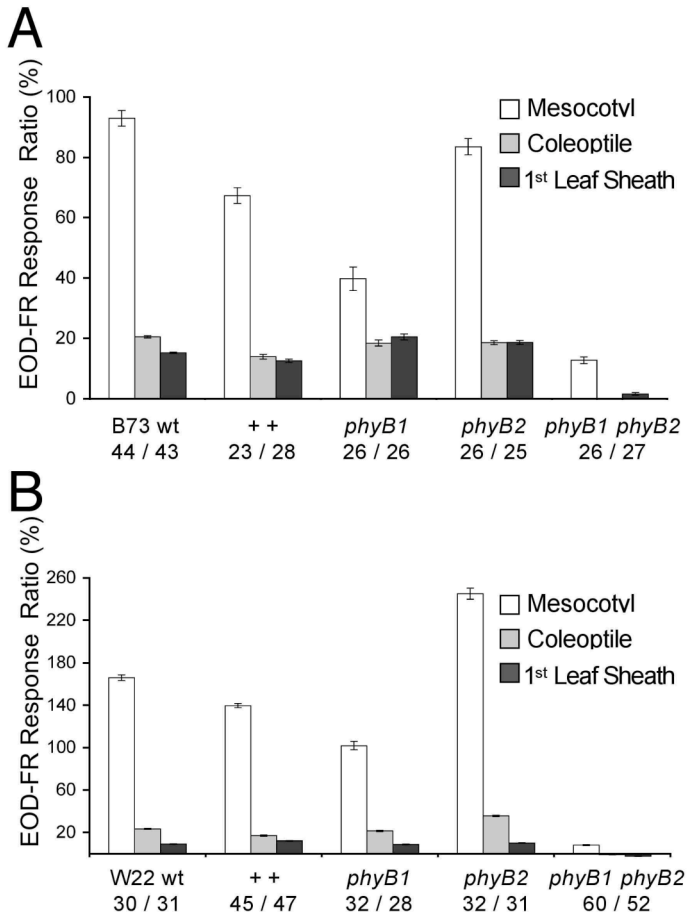

Figure 2.9 EOD-FR response ratios of the *phyB* mutant series. Responses are shown for mutants introgressed into A, B73 and B, W22. The number of seedlings measured at 10 dap is shown below each genotype as W/EOD-FR treatments. wt, wild-type; SE, standard error; + +, *PhyB1 PhyB2* non-mutant segregant.

The response to EOD-FR was also examined in the phytochromobilin deficient *elm1* mutant (Fig. 2.10). The *elm1* mutant is homologous to the Arabidopsis *hy2* mutant and both condition a pale green, elongated seedling phenotype (Kohchi et al., 2001; Sawers et al., 2002). In the B73 introgressions the mesocotyl of *elm1* seedlings was longer than the *phyB1 phyB2* double mutant, but non-responsive to EOD-FR. The length of the coleoptile was not significantly different than the *phyB1 phyB2* double mutant under W but significantly longer under EOD-FR. The 1st leaf sheath of *elm1* was longer than the *phyB1 phyB2* double mutant under both light treatments and was also responsive to EOD-FR. In the W22 introgressions, the *elm1* mutant mesocotyl was responsive to the EOD-FR, the coleoptile was non-responsive, while the 1st leaf sheath was shorter following EOD-FR treatments than when grown under W only. The reduction in the apparent length of the 1st leaf sheath under EOD-FR may be a consequence of the slightly greater extension of the mesocotyl, resulting in less resource committed to sheath tissues. In both inbred backgrounds, reduced but detectable EOD-FR responses may be attributed to the presence of low levels of PHYB1 and PHYB2, as the *elm1* allele is not a complete loss-of-function mutation (Sawers et al., 2004).

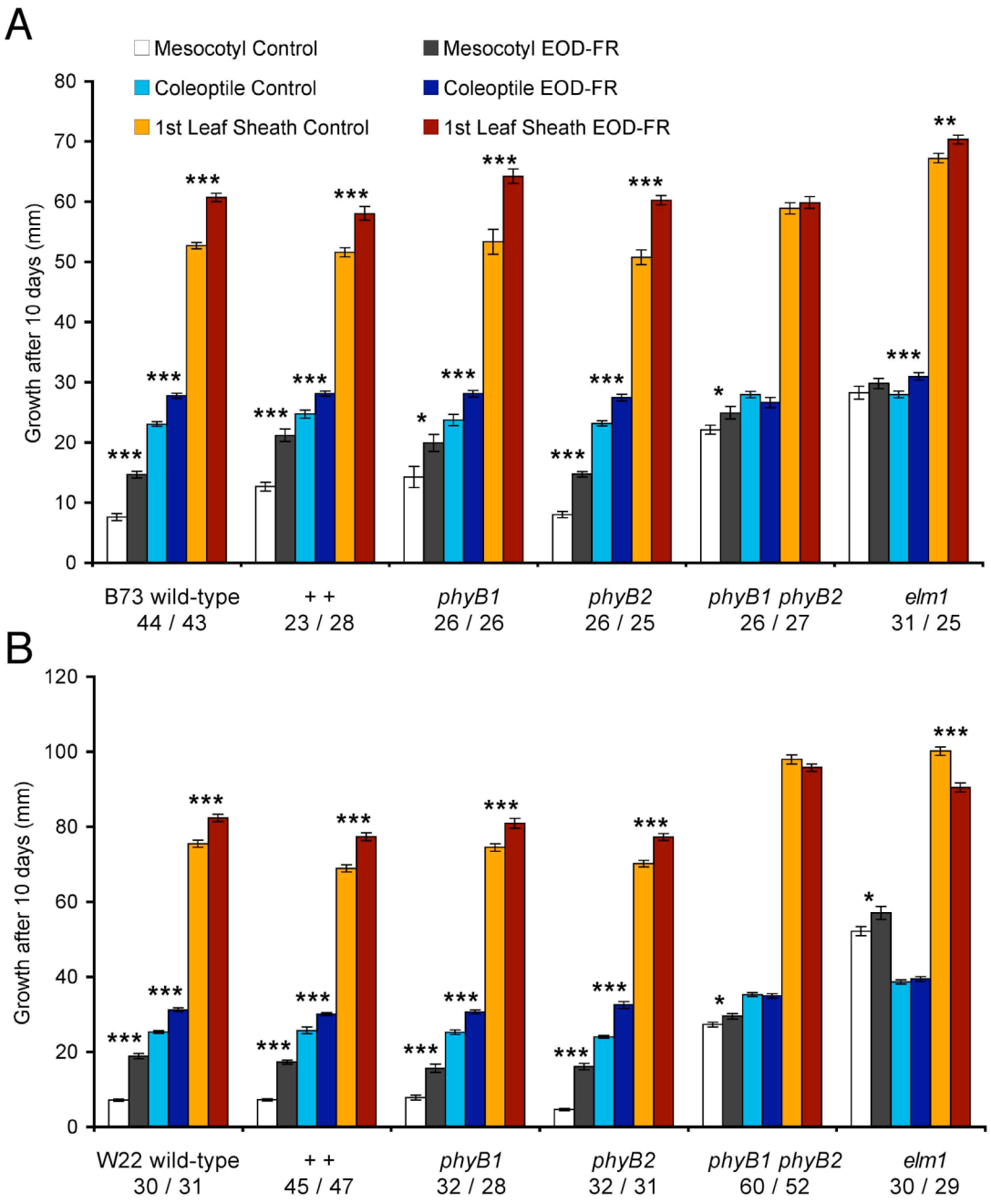

Figure 2.10 EOD-FR response in *phyB1*, *phyB2*, *phyB1 phyB2* and *elm1* mutants. A, Mutants introgressed into a B73 inbred line. B, Mutants introgressed into a W22 inbred line. The values are representative of the mean ± SE. The numbers below each genotype correspond to the number of seedlings measured for the W control / EOD-FR treatment. Asterisks indicates significance between the two light treatments (Student's t test * $P < 0.05$, ** $P < 0.01$, *** $P < 0.001$). + +, *PhyB1 PhyB2* non-mutant segregant.

2.2.5 Tissue-Specific Regulation of EOD-FR Responses by GA

The role of GA in the downstream transduction of FR signaling was investigated by pharmacological treatments using synthetic GA_3 and the GA biosynthesis inhibitor paclobutrazol (PBZ). The effectiveness of a 50 μg mL^{-1} PBZ seed imbibition treatment (Pinhero et al., 1997) was confirmed in wild-type W22 and *elm1* mutant seedlings, and through comparisons with a mock-treated *dwarf1* (*d1*) mutant (Emerson, 1912). The *d1* mutation has not been defined molecularly, but the homozygous mutant is impaired in the conversion of GA_{20} to GA_1, GA_{20} to GA_5 and GA_5 to GA_3 (Spray et al., 1996). The *d1* mutant can be restored to a stature similar to wild-type by exogenous application of GA_3. PBZ-treated seedlings had thicker and greener tissues, characteristic features of dwarf mutants (Neuffer et al., 1997). Both wild-type W22 and *elm1* PBZ-treated seedlings were phenotypically similar to *d1* (Fig. 2.11). To establish whether exogenous GA_3 would enhance seedling EOD-FR responses, seedlings were treated with 50 μM GA_3 (Ogawa et al., 1999) by daily soil drench. Morphological responses to PBZ and GA_3 treatments are presented in Figure 2.11. GA_3 caused exaggerated elongation of the mesocotyl, coleoptile, and 1st leaf sheath, and a delay in leaf blade emergence. Leaf blades were paler, narrower and hyponastic: responses similar to the ones caused by EOD-FR.

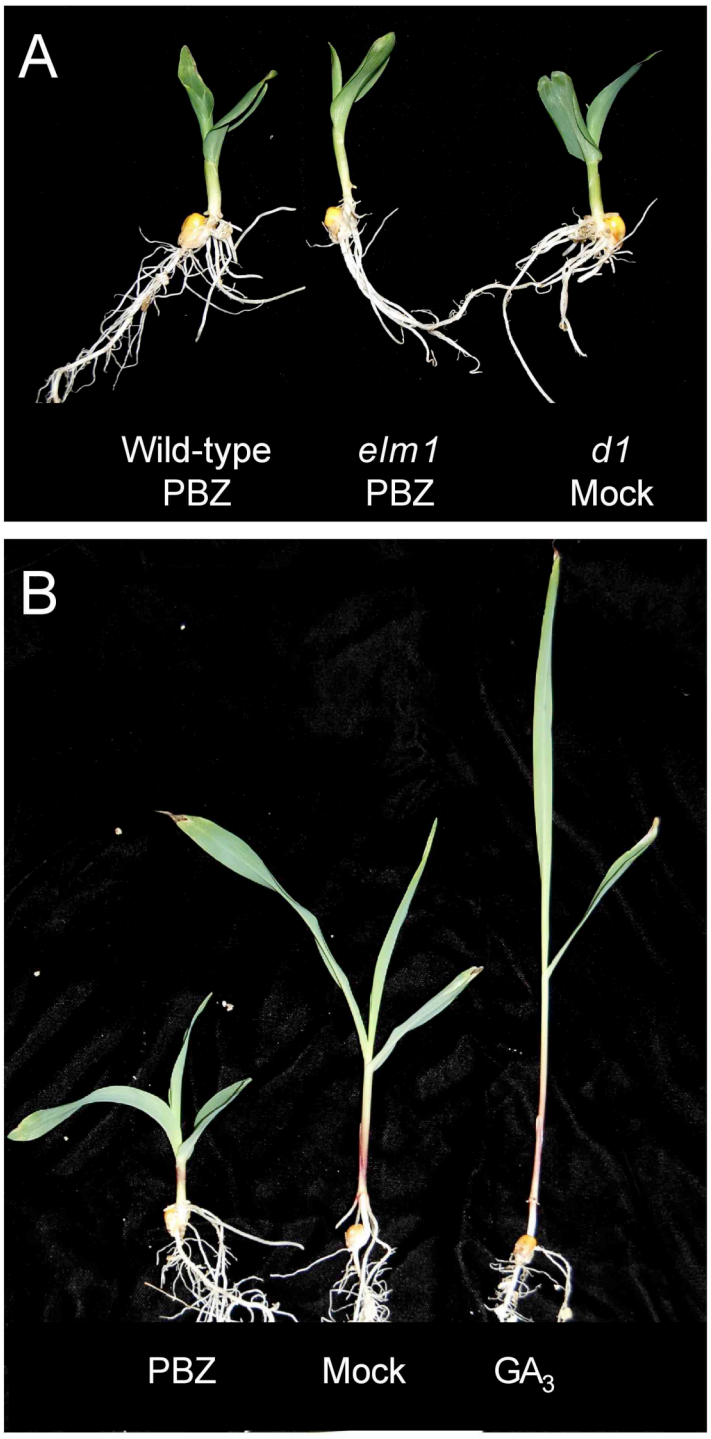

Figure 2.11 Effects of pharmacological treatments on maize seedling development. A, 10 day old W22 seedlings grown from PBZ-treated seed, wild-type + PBZ, *elm1/elm1* + PBZ, and the mock-treated *d1/d1*. B, 10 day old B73 seedlings grown from seed treated with PBZ, mock (control), or GA_3.

To further investigate the role of GA in EOD-FR responses, we examined the effects of EOD-FR when combined with GA_3 and PBZ treatments in B73 wild-type and *phyB1 phyB2* double mutant (Fig. 2.12A). Wild-type mesocotyl, coleoptile and 1st leaf sheath tissues were all significantly longer in GA_3-treated seedlings relative to a mock treatment and all responded to EOD-FR despite significant elongation responses induced by GA_3. Thus, at this concentration of GA_3, EOD-FR-mediated responses are not saturated by GA_3 treatments. In wild-type, PBZ treatment repressed mesocotyl elongation, under both light treatments, indicating that GA is required for elongation of mesocotyl tissues. The coleoptile and 1st leaf sheath responded to EOD-FR following PBZ treatment. As seedling tissues were capable of responding to EOD-FR following PBZ treatments, other growth stimulating factors (such as auxins) likely contribute to EOD-FR responses. These results also suggest that GA plays a predominant role in mediating FR-induced mesocotyl elongation relative to coleoptile and sheath tissues.

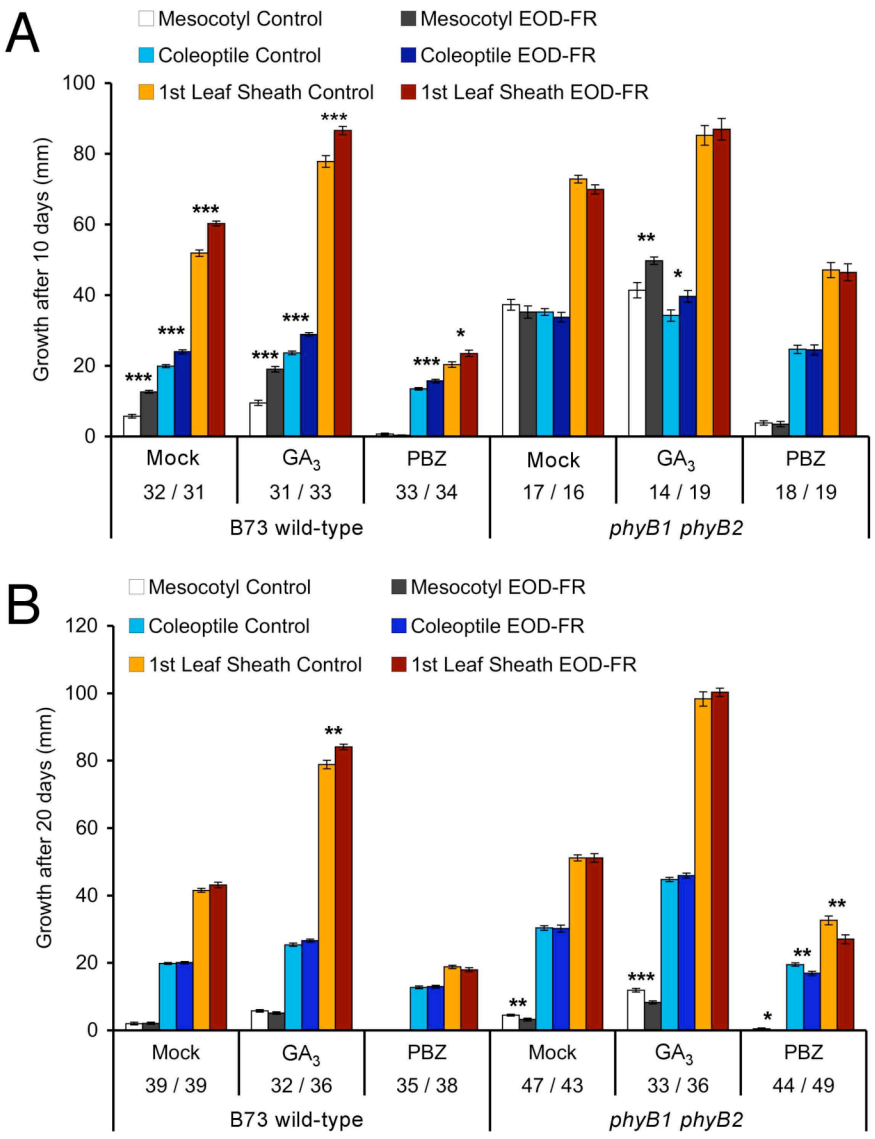

Figure 2.12 Effects of GA and chilling temperatures on EOD-FR-mediated elongation response. Mock-, GA_3- and PBZ-treated B73 wild-type and *phyB1 phyB2* double mutant seedlings were used. A, Seedlings were grown at a constant temperature of 28ºC and measurements taken 10 dap. B, Seedlings were subjected to a nightly chilling temperature of 10ºC and grown at 28°C during the photoperiod. Measurements were taken 20 dap. The values are representative of the mean ± SE. The number of seedlings measured for W / EOD-FR are shown below each treatment. Asterisks indicate Student's *t* test significance between the two light treatments for each line (* $P < 0.05$, ** $P < 0.01$, *** $P < 0.001$).

The *phyB1 phyB2* double mutant was also evaluated for its response to GA_3 and PBZ (Fig. 2.12A). While double mutants failed to respond to EOD-FR, they responded to EOD-FR following GA_3 applications. This response was observed for mesocotyl and coleoptile tissues but not first leaf sheath tissue. This suggests that in addition to PHYB-mediated EOD-FR responses, PHYA and/or PHYC may contribute to EOD-FR response when GA_3 is not limiting. PBZ treatments inhibited responsiveness of the double mutants to EOD-FR, but all tissues were significantly taller than wild-type PBZ-treated seedlings. These results suggest that the double mutants are either more responsive to endogenous GA or produce more active GA than wild-type. Furthermore, GA regulation is tissue-specific, with the greatest effect in mesocotyl tissues.

2.2.6 Chilling Temperatures Applied During Dark Breaks Modulate EOD-FR Responses

To investigate the effect of temperature on EOD-FR response growth temperature was alternated between 28°C during the photoperiod and a chilling temperature of 10°C during dark breaks. This chill treatment was made in combination with EOD-FR, GA_3 and PBZ treatments. Growth chamber temperature was reduced only during dark breaks to simulate the broad daily fluctuations that can take place in early field season under temperate climates. To ensure robust germination, maize seeds were imbibed in soil at a constant temperature of 28°C for two days prior to the first chill treatment. Coleoptiles had not emerged from the soil at this time. The duration of the experiment under chill treatments was extended to 20 d to allow sufficient development of the seedlings prior to measurements.

The chill treatment attenuated the EOD-FR response in wild-type B73 for all three traits measured (mock treatment, Fig. 2.12B). Coleoptiles and 1st leaf sheaths in the *phyB1 phyB2* double mutant were non-responsive to EOD-FR. However, mesocotyl tissues were significantly shorter following EOD-FR treatments in the *phyB1 phyB2* double mutants. In addition, seedlings were more similar in appearance to wild-type (Fig. 2.13) than when grown at constant 28º C. Surprisingly, both GA and PBZ treatments enhanced the effect of EOD-FR in *phyB1 phyB2* seedlings, resulting in less elongation following EOD-FR treatments. These results suggest a complex interplay between temperature and GA-mediated elongation. They also suggest a role for *PhyA* or *PhyC* in the regulation of EOD-FR response under low temperatures in the absence of *PhyB*.

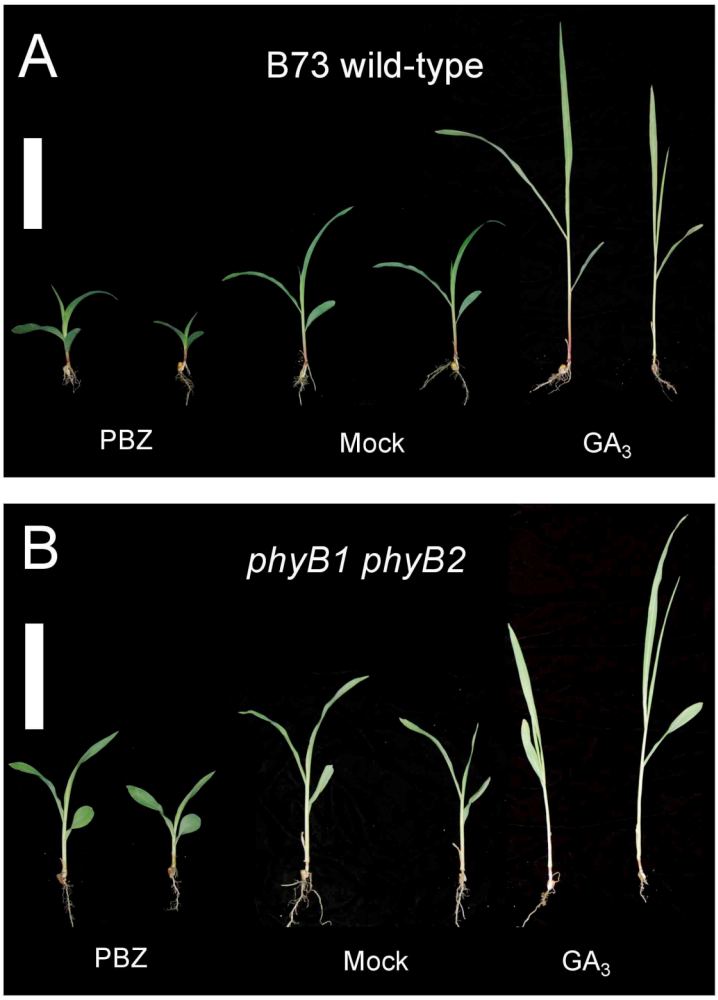

Figure 2.13 Pharmacological and chill treatments of maize seedlings. A, B73 wild-type and B, *phyB1 phyB2* double mutants were subjected to a nightly chill temperature of 10ºC and received either exogenous applications of PBZ, mock-treatments, or GA_3. For each treatment, a single representative seedling is shown. W control is on the left and EOD-FR treated plant is on the right. Vertical bar = 10 cm.

2.2.7 FR-mediated Regulation of ABA Levels in the Mesocotyl

Transient exposure to cold is associated with increased levels of ABA (Penfield, 2008) and in Arabidopsis, *PhyB* was identified as the primary light receptor for the activation of cold-dependent light signaling (Kim et al., 2002). To evaluate the

role of ABA in modulating maize seedling development in response to transient chilling temperatures and EOD-FR, mesocotyl and leaf blade tissues of B73 wild-type and *phyB1 phyB2* double mutant were harvested at subjective dawn and ABA content measured. All tissues were harvested within 30 min from the beginning of the photoperiod. ABA content was assayed by indirect enzyme-linked immunosorbent assay (ELISA; see Materials and Methods). At constant 28°C, EOD-FR reduced ABA levels approximately 50% ($P = 0.09$) in wild-type B73 seedlings (Fig. 2.14A). When a chill treatment was applied during dark breaks, ABA levels in wild-type remained at similar levels to seedlings grown in W at 28ºC (Fig. 2.14A). The EOD-FR treatment of *phyB1 phyB2* double mutants caused a 50% reduction in mesocotyl levels of ABA ($P = 0.02$) at 28ºC but had little effect with chill treatments, suggesting a role for *PhyA* or *PhyC* in regulating ABA levels in the mesocotyl at 28ºC in addition to contributing to elongation under chill treatments as discussed above. In contrast to mesocotyl tissues, ABA levels in the leaf blades (Fig. 2.14B) of both wild-type and *phyB1 phyB2* double mutant appeared to increase in response to chilling, but failed to respond to EOD-FR. In summary, these results reveal a temperature-dependent and phyB-independent pathway that regulates ABA levels in response to EOD-FR treatments.

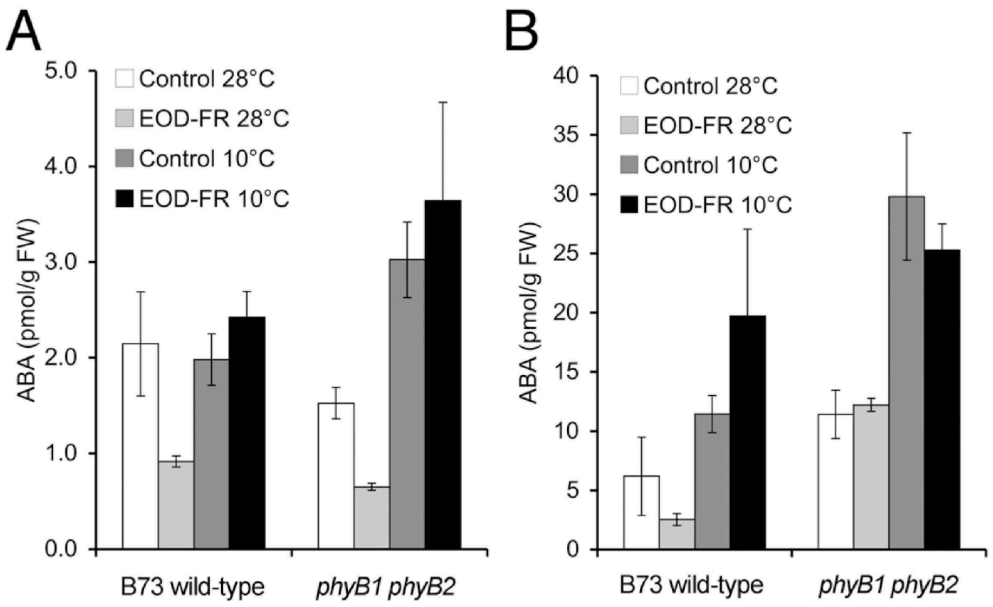

Figure 2.14 ABA concentration in A, mesocotyl and B, leaf blade of B73 wild-type and *phyB1 phyB2* double mutants grown under two different temperature regimes. All seedling tissues were harvested at the beginning of the photoperiod (dawn) 10 days (28°C constant) or 15 days (10°C dark chill) after planting. Each measurement consists of a mean (± SE) derived from three biological replicates (each from a pool of 8 seedlings). FW, fresh weight.

2.3 Discussion

Early detection of FR reflected by surrounding vegetation is an important factor influencing plant development (Ballare et al., 1990; Rajcan et al., 2004). To examine this process in maize, a crop grown at high planting density, we developed an EOD-FR assay that mimics several developmental responses caused by low R:FR as previously described (Fankhauser and Casal, 2004). The light treatment offers the benefit of using a uniform controlled environment to simultaneously conduct screens on large numbers of seedlings and minimizes environmental differences between control and treated plants as only a 15 min pulse of daily FR differentiates the

treatments. Previous studies have shown that coleoptile and mesocotyl tissues are responsive to EOD-FR through a LFR mode of PHY action (Gorton and Briggs, 1980). Here, we show that elongation responses, triggered by the EOD-FR treatment are completely reversible through a PHYB-mediated LFR and validated on two different inbred lines. The two maize paralogs PHYB1 and PHYB2 are largely redundant in mediating the elongation responses of all three seedling tissues measured, likely as a result of similar structural characteristics and expression profiles (Sheehan et al., 2004).

Natural variation has been used to define components of the light signal transduction pathway in Arabidopsis and demonstrated the role of variation at phytochromes and cryptochromes in mediating light response (Maloof et al., 2001; Wolyn et al., 2004). Surveys of Arabidopsis accessions exposed to low R:FR revealed wide variations in hypocotyl elongation and flowering time, but no correlations were observed between the two traits (Botto and Smith, 2002). To explore the variation in responses to EOD-FR in maize, we evaluated a genetically diverse panel of inbred lines largely comprised of the founders of the NAM population (McMullen et al., 2009). A wide range of responses to EOD-FR was observed for all three tissues measured, suggesting genetic variation is present in the panel. For mesocotyl, an association between EOD-FR responsiveness and population structure was established, as TS lines were the least responsive to EOD-FR. A previous study demonstrated that TS seedlings were more photomorphogenic and displayed less mesocotyl elongation upon light exposure (Markelz et al., 2003). Thus, it appears that mesocotyl tissues are highly responsive to R and W light in TS but EOD-FR responses have been partially attenuated. Robust EOD-FR responses of mesocotyl tissues were observed for teosinte and a commercial hybrid, suggesting EOD-FR response may have fitness benefits under both natural and artificial selection.

To gain a better understanding of the genetic architecture of EOD-FR and the loci underlying its control, the IBM mapping population (Lee et al., 2002) was screened for responses to EOD-FR. This population has been used to map QTL for cell wall composition, flowering time, and resistance to southern leaf blight (Hazen et al., 2003; Balint-Kurti et al., 2007). In our analysis, none of the 16 QTL identified mapped to phytochrome gene family or *Elm1* loci. This was somewhat unexpected, as photoreceptors have been identified as QTL for light response and flowering time in Arabidopsis (Wolyn et al., 2004). Furthermore, association analysis in Arabidopsis identified *phyB* as a target of natural selection in regulating R responses (Filiault et al., 2008) and *PhyC* as a source of flowering time variation (Balasubramanian et al., 2006). In maize, variation in photoreceptors may modulate FR responses but allelic variation is likely not present or was undetected in our study. Only two significant QTL for EOD-FR elongation ratio were identified in the analysis, where the peaks coincided with two QTL specific to EOD-FR but not to elongation in W. Unfortunately, the low resolution of the mapping population precludes speculation on candidate genes in these intervals. However, the heritability of the mesocotyl and 1st leaf sheath traits mapped for EOD-FR are both high (0.87 and 0.90 respectively), which should greatly facilitate the fine mapping effort that is currently underway. The inability to capture the majority of the QTL that were found for elongation in EOD-FR as response ratio QTL suggests that many of these QTL mediate elongation independent of FR signaling. Alternatively, the lower heritability inherent to response ratios between two light treatments results in less power in detection and precludes the mapping of small effect QTL.

A teosinte x maize NIL was used to further investigate the QTL located within bin 9.03. This QTL was first identified in the IBM population as specific to mesocotyl elongation but the teosinte introgression also revealed that the same or linked region

may also affect coleoptile and 1st leaf sheath. This result suggests that the tissue-specific nature of QTL may also be influenced by genetic variation segregating in mapping populations. At present, it is unclear if QTL that affect elongation responses to EOD-FR in seedlings also exert control of leaf growth and canopy morphology in later stages of plant growth. A study using B73 x Mo17 RIL planted at two different densities identified several QTL associated with traits affecting light penetration in the canopy (Mickelson et al., 2002). Two of these QTL, one for tassel branch number and the other for leaf angle are located in close proximity to the bin 4.09 QTL that controls 1st leaf sheath EOD-FR elongation and response ratio. A similar study, also using a B73 x Mo17 RIL population, identified QTL associated with mature plant height in regions overlapping the 4.09 and 9.03 seedling QTL. As in our study, it was the Mo17 parent that contributed the responsive allele (Gonzalo et al., 2010). In a separate study, the density response of several Tx303 x B73 segmental introgression lines was evaluated (Gonzalo et al., 2006) and several density-dependent QTL were identified, one of which mapped to 4.03, a location where we identified a QTL for 1st leaf sheath elongation under EOD-FR. Further investigations should help reveal if EOD-FR responses in the seedling can be used as a proxy for high-density responses. If so, the co-location of QTL across these studies suggests some pleiotropic regulation of the R/FR signaling throughout development.

Characterization of *phyB* single and double mutants revealed the primary role of *PhyB* in regulating responses to EOD-FR. However, as was observed for seedling responses to R and W (Sheehan et al., 2007), *PhyB1* plays a more prominent role in regulating the response. Furthermore, introgressions into two different inbreds revealed distinct genetic modifiers in B73 and W22. The *elm1* mutant, which is a weak allele (Sawers et al., 2004), is still responsive to EOD-FR, likely because of the presence of low levels of *PhyB1* and *PhyB2*. It is also interesting to note that roles for

PhyA or *PhyC* in EOD-FR response were revealed only in the double mutants. These included an EOD-FR response to chill treatments and the suppression of ABA accumulation following EOD-FR treatments. It is likely that in wild-type plants these roles for PHYA and PHYC are largely masked by *PhyB*. However, under conditions where PHYB is inactivated (e.g. FR treatments) or in accessions with non-functional alleles of *PhyB* (e.g. France 2), *PhyA* or *PhyC* may play a more important role in regulating responses to FR light signals.

The role of GA in mediating elongation response to EOD-FR was investigated using GA_3 and PBZ. Previous studies demonstrated that GA_3 combined with EOD-FR had a synergistic effect on elongation in *Phaseolus vulgaris* (Downs et al., 1957) and on the induction of flowering in sorghum (Williams and Morgan, 1979). The accumulation profile of bioactive GA's is disrupted in the sorghum *phyB* mutant and biosynthesis inhibitors can reduce shoot elongation in both wild-type and the *phyB* mutant (Lee et al., 1998). The responses observed in this report were consistent with the possibility that there are additive signaling pathways for EOD-FR response, one with GA involvement and the other independent of GA. Additional hormones such as abscisic acid, auxin and ethylene also likely to be involved in these responses (Vandenbussche et al., 2005). GA-stimulated elongation was greater in the mesocotyl than in either the coleoptile or 1st leaf sheath as elongation responses were completely suppressed in PBZ-treated wild-type mesocotyl. It is possible that the endogenous GA profiles are also altered in the *phyB1 phyB2* double mutant. The tissue-specific control of EOD-FR response by different hormones is likely to complicate the analysis of mutant phenotypes, particularly when whole seedlings are used for molecular studies. Our results suggest, the responses in mesocotyl may be distinct from leaf blade or sheath tissues and warrant a fine-grain (e.g. tissue-specific) analysis of the molecular signaling networks.

The effect of a chilling temperature during dark breaks on EOD-FR-induced responses was also investigated. A previous study identified European flint and highland tropical lines as having a greater chilling tolerance than Corn Belt dent material (Leipner and Stamp, 2009) and chilling tolerant maize genotypes accumulate higher amounts of ABA during cold weather periods (Janowiak et al., 2003). Chilling temperatures are also associated with prolonged cell cycle progression and reduced cell production in maize leaves (Rymen et al., 2007). Thus, there is evidence for both genetic variation and a molecular mechanism for cold tolerance in maize. In Arabidopsis, there is also good evidence supporting a role for phytochromes in regulating responses to cold stress that involve ABA signaling (Franklin and Whitelam, 2007). Previous studies in maize and Arabidopsis have shown an antagonism of ABA and GA signaling in the regulation of seed germination (White and Rivin, 2000; Seo et al., 2006; Oh et al., 2007; Sawada et al., 2008). In Arabidopsis, phytochromes can modulate endogenous levels of both GA and ABA (Seo et al., 2009) and we have shown here that ABA levels in mesocotyl tissues are negatively regulated by EOD-FR. R promotes Arabidopsis germination through activation of genes that encode GA biosynthetic enzymes and the repression of genes involved in GA catabolism. Red light also induces the expression of genes required for the repression of ABA biosynthesis, whereas FR light promotes ABA accumulation (Seo et al., 2006). Here, our data suggest a similar antagonism between ABA and GA signaling, but the control of ABA and GA levels is likely mediated through an alternative mode of phytochrome control. That is, R is likely to repress GA accumulation in the mesocotyl and result in increased levels of ABA. In the absence of PHYB, seedlings displayed an increased sensitivity to chilling resulting in less elongation following FR light treatments. This response is likely mediated by PHYA acting to increase ABA levels. Further studies, however, will be necessary to

characterize these interactions in detail that are likely to be mediated in part through transcriptional changes (Seo et al., 2009).

A model integrating these data is presented in Figure 2.15. In this model both ABA and GA contribute to mesocotyl elongation, but the contribution of each is modulated by temperature. Under low temperatures ABA signaling predominates and under constant temperatures GA signaling through PHYB predominates. This fine-tuning of mesocotyl elongation by temperature through hormone regulation is likely an important component of seedling emergence in temperate environments.

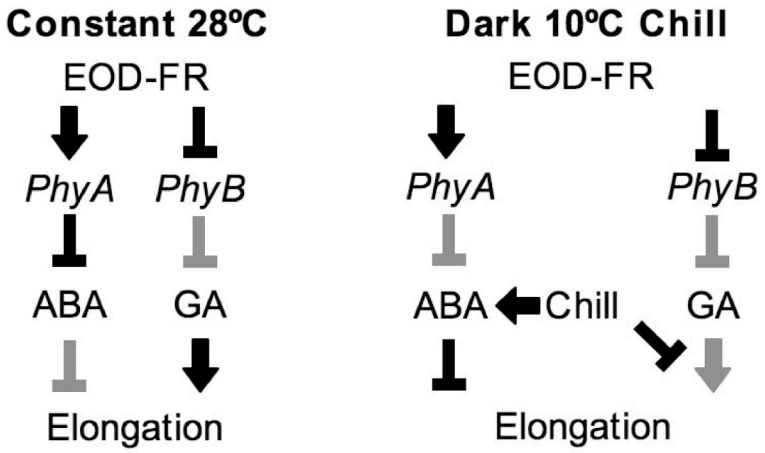

Figure 2.15 Interaction between light, temperature, and hormonal pathways in the control of maize mesocotyl elongation. At constant 28ºC (left panel), FR photoconverts PhyB-Pfr to PhyB-Pr resulting in a de-repression of elongation mediated by GA. In addition, ABA levels are reduced following EOD-FR exposure during night breaks in a PHYB-independent but FR-dependent manner, which strongly suggest a PHYA-mediated response. When a chilling treatment is applied during night breaks (right panel) ABA levels remain high and result in the repression of mesocotyl elongation. It is unclear if chilling reduces GA response directly or through an independent pathway (e.g. PHYA or ABA). As mesocotyl tissues are longer in the *phyB1 phyB2* double mutants than wild-type following chilling treatments, some GA signaling likely persists following chill treatments. Grey arrows indicates minor pathway and black arrows the predominant pathway.

2.4 Materials and Methods

2.4.1 Plant Materials

Inbred maize lines used in these experiments include B73, B97, CML52, CML69, CML103, CML288, CML247, CML277, CML322, CML333, HP301, Il14H, Ki3, Ki11, Ky21, M162W, M37W, Mo17, Mo18W, MS71, NC350, NC358, Oh43, Oh7B, P39, Tx303, Tzi8, W22, and the hybrid 34P88 (Pioneer Hi-Bred). The *phyB1* (*phyB1*::*Mu*563) allele carries a *Mu* insertion and was identified from the Pioneer Trait Utility System for Corn (TUSC) collection (Bensen et al., 1995; Sheehan et al., 2007). The *phyB2* (*phyB2*::*Mu*12058) allele also carries a *Mu* insertion and was identified from the Cold Spring Harbor MTM collection (May et al., 2003). The *phyB1* and *phyB2* loss-of-function alleles were introgressed into B73 (backcrossed four times for the EOD-FR *phyB* mutant series analysis and three times for the remaining experiments except for the GA_3 and PBZ experiment at constant temperature where, due to limited availability, the seeds used for the analysis were backcrossed only two times) and into W22 (backcrossed four times) inbred backgrounds. The *elm1* mutant was initially identified in the W22 background (Sawers et al., 2002) and was also introgressed into the B73 background by backcrossing five times. The *d1* mutant was introgressed into the W22 background by backcrossing five times. A subset of 272 of the 302 IBM lines (Lee et al., 2002) was used in this analysis and corresponds to the lines capable of flowering in Upstate New York. Teosinte-maize NILs were derived from crosses between teosinte and B73, followed by backcrossing to B73 four times. The BC4 plants were self-pollinated twice (BC4S2) and genotyped using 768 SNP markers (www.panzea.org).

2.4.2 PCR-based Genotyping

The *phyB1* and *phyB2* alleles respectively refer to *phyB1*::*Mu*563 and *phyB2*::*Mu*12058 loss-of-function alleles. All introgressions of the *phyB1*::*Mu*563 and *phyB2*::*Mu*12058 insertions and their corresponding segregant wild-type alleles were confirmed using PCR-based genotyping. A 950 bp fragment specific to the *phyB1*::*Mu*563 allele was amplified using the *Mu*-specific primer MuMTM (5'-GCCTCCATTTCGT-CGAATC-3') located in the transposon inverted terminal repeat and the *PhyB1*-specific primer 563Mu-R1 (5'-CAATTCTAGCTCCCGAAGCTGAAC-3'). A 979 bp *PhyB1* wild-type allele fragment was amplified using the *PhyB1*-specific primer 563Mu-NegF1 (5'-GAACCGCGTGCGAATGATTGCCGAT-3') and 563Mu-R1. Both *phyB1*::*Mu*563 and *PhyB1* alleles were amplified using these PCR conditions: 95°C for 3 min followed by 35 cycles of 95°C for 30 sec, 57°C for 30 sec and 72°C for 3 min. The presence of the *phyB2*::*Mu*12058 insertion allele was assayed using MuMTM and the *PhyB2*-specific primer 12058-R3 (5'-AGTAGCTTTTCGACTATATCA-TCAC-3'). Amplification conditions for the 1450 bp fragment were 95°C for 3 min followed by 35 cycles of 95°C for 30 sec, 57°C for 30 sec and 72°C for 3 min. The presence of the *PhyB2* wild-type allele was assayed using the *PhyB2*-specific primer 12058Mu-F1 (5'-CCGTTCCCTCGCTCGACTCCGTG-3') and the *PhyB* (non homeolog-specific) primer 12058Mu-NegR2 (5'-CATGCTCCACGACTGTGTCGC-3'). Amplification conditions for the 357 bp fragment were: 95°C for 3 min followed by 7 cycles of 95°C for 30 sec, 67°C for 30 sec (decreasing by 1°C at each subsequent cycle) and 72°C for 1:30 min, followed by 28 cycles of 95°C for 30 sec, 61°C for 30 sec and 72°C for 1:30 min. Introgression of the *elm1* allele were confirmed as previously described (Sawers et al., 2004). Genomic DNA was isolated from leaf tissue (Ahern et al., 2009) and

DNA fragments were amplified using GoTaq DNA polymerase according to the manufacturer's recommendations (Promega).

2.4.3 Growth Conditions and Light Treatments

All seeds were uniformly sown at a depth of 2 cm in germination trays with internal plastic cell dividers (6 cm x 6 cm) filled to the top with a soil mixture composed of 35% peat moss, 10% vermiculite, 35% baked clay, 10% sand, and 10% topsoil. The same planting density of 4 kernels per cell divider was used for all experiments. All kernel pedicels were oriented toward the bottom of the tray to improve emergence uniformity. All experiments were conducted using a complete random block design in a Conviron TC30 growth chamber. For each experiment, seeds were planted at the same time and the randomization pattern was identical between the upper (treatment) and lower (control) sections of the growth chamber to minimize possible positional effect inside the chamber when comparing light treatments. Phenotypic data were collected using an electronic caliper (Fowler) with direct data entry to a computer. Seedling trays awaiting measurements were kept at 4°C to halt growth. Four replicates were used for density experiments comprised of 488 seedlings for W and 481 seedlings for EOD-FR (B73) or 6 replicates and 324 seedlings (hybrid).

Plants were grown under a 10 h photoperiod of W, 28°C temperature, and 40% relative humidity. Each section was fitted with 8 fluorescent bulbs (cool white F72T8-CW, General Electric) emitting a PAR photon flux of 133.2 μmol m^{-2} sec^{-1} in the lower section (W control) and 130.0 μmol m^{-2} sec^{-1} in the upper section (treatment). The R and FR treatments were performed using LED module banks (2:1 R:FR, Quantum Devices) positioned at the left and right edges of the upper section. Since

LED modules and cables were found to absorb a significant amount of W, a similar W photon flux for the control section was obtained with the addition of mock equipment similar to that used in the treatment section. Each light module (15 cm x 15 cm) was positioned approximately 15 cm above soil level. Spectral irradiances of each light treatment were measured using a spectroradiometer (Apogee Instruments) and results are presented in Figure 2.1. The FR-R reversal experiment was performed using 2 R LED modules (47.4 μmol m^{-2} sec^{-1}) and 4 FR LED modules (51.1 μmol m^{-2} sec^{-1}). All EOD-FR experiments were conducted using 6 FR modules (76.7 μmol m^{-2} sec^{-1}) with the exception of the IBM screen where 4 FR LED modules were used. The EOD-FR treatment consisted of a pulse 15 min of FR immediately following each W photoperiod (including an overlap of 1 min where both W and FR were on). The FR-R reversal treatment consisted of the aforementioned EOD-FR treatment immediately followed by a 15 min pulse of R. Synchronization of all the light treatments was made by connecting the digital controls of the growth chamber to a remote power supply controlling the LED system. The growth conditions for the chill temperature treatment were similar as previously stated with the exception of imposing, beginning at the end of the second day of growth, a temperature of 10°C during the 14 h dark period until seedlings were measured. The temperature was maintained at 28°C for the first two days so as to not interfere with germination. The transition between 28°C and 10°C was made over a 1 h period at the beginning and end of each photoperiod.

2.4.4 Pharmacological Treatments and ABA Assay

Paclobutrazol (PBZ; Phytotechnology Laboratories) was dissolved in 100% DMSO (dimethyl sulfoxide) to a concentration of 50 mg mL^{-1} (170 mM) and seeds were imbibed for 18 h in a solution of 50 μg mL^{-1} PBZ (Pinhero et al., 1997) prior to

planting. Seeds not treated with PBZ were imbibed with a mock solution of 0.1% (v / v) DMSO. GA_3 (Phytotechnology Laboratories) was dissolved in 100% ethanol and a dilution of 50 μM (0.1%, v / v) (Ogawa et al., 1999) was applied daily by soil drench using 50 mL per cell divider. Non GA_3-treated seedlings received mock soil drench treatment using water supplemented with 0.1% (v / v) ethanol. ABA content was assayed by indirect ELISA. Mesocotyl and leaf blade tissue samples were harvested within a half hour from the beginning of the photoperiod (dawn) and immediately flash frozen in liquid nitrogen and ground with a mortar and pestle. Three biological replicates were harvested, each consisting of pooled seedling tissues from 8 seedlings. A powder aliquot was weighed and extracted three times with 80% (v / v) methanol; the extracts were pooled. Chromatographic separation and ABA determination purification was performed according to the procedure of (Setter and Parra, 2010). Briefly, compounds were separated with reverse-phase flash chromatography on columns packed with C18-silica material, and ABA was quantified by indirect ELISA with monoclonal antibody specific to (+) ABA (Agdia Inc.).

2.4.5 Statistical Analysis

The EOD-FR screen of the IBM population was repeated 4 times, each time using 4 kernels per line and per light treatment. Since germination rate and seed quality was highly variable, a single median value was derived for each RIL from all 4 replicates to attenuate the effect of outliers. The traits analyzed included the 4 primary measurements: total mesocotyl length and 1st leaf sheath length, for both control and EOD-FR treatments. Median lengths of mesocotyl of B73 in W was 17.14 and EOD-FR was 23.97 mm. Median length of mesocotyl of Mo17 in W was 12.94 mm and EOD-FR was 18.35 mm. Median values for 1st leaf sheath lengths for W control and

EOD-FR were 49.76 and 58.72 mm (B73 inbred) and 49.31 mm and 62.09 mm (Mo17 inbred), respectively. Two additional traits were derived from these initial measurements representing the elongation ratios of mesocotyl and 1st leaf sheath caused by the EOD-FR treatment relative to the W control. Defined as the EOD-FR response ratio, it was calculated for each line using the equation (EOD-FR − control) / control and expressed as a percentage. EOD-FR response ratios for the mesocotyl were 39.8% (B73 inbred) and 41.8% (Mo17 inbred) and for the 1st leaf sheath were 18.0% (B73 inbred) and 25.9% (Mo17 inbred). Broad-sense heritability (H^2) was estimated using a one-way ANOVA for the each trait measured or derived. For mesocotyl and 1st leaf sheath elongation, all data were used for estimates of heritability. Heritability of the EOD-FR response ratios was estimated using the median values of each repetition. For estimates of primary trait heritability, effects included in the model were lines, repetitions and the line x repetition interaction (the interaction was excluded for the EOD-FR response ratio estimates as a median value was used for each repetition). The mean square value of the model (between line variability) over the mean square values of both model and error (between and within line variability) was used to estimate the heritability. QTL analysis was conducted using the composite interval mapping module in the QTL Cartographer software version 2.5 (Basten et al., 1994; Wang et al., 2007). The genotypic data used for the analysis consisted of 1339 publicly available markers (www.maizegdb.org). Marker distances were based on the IBM version 1 map. LOD (logarithm of the odds) threshold significance level was set at $\alpha = 0.05$ and calculated from 1,000 permutations.

Statistical analyses were performed using JMP software version 7.0 (SAS Institute). With the exception of the IBM screen, analyses were based on averages and their corresponding standard errors. EOD-FR response ratios were also calculated

using the mean value of each light treatment. A standard error for each ratio was estimated using a bootstrap permutation analysis, where each of the two datasets used to calculate a EOD-FR response ratio were re-sampled 10,000 times to sizes of n_1 and n_2 and for each of the 10,000 iterations, a ratio was calculated. The distribution of this bootstrap sample of ratios was used estimate a standard deviation. A standard error was then calculated by dividing the standard deviation by the square root of the smallest of the two sample sizes: n_1 or n_2. Significant differences between lengths or ratios were calculated using Student's *t* test.

2.5 Acknowledgments

We thank Dr. Marty Sachs for providing the *d1* mutant, Dr. Edward Buckler for providing the NAM founder inbred lines, Dr. John Doebley for the teosinte seeds, Mr. Donald Slocum for the customization of the growth chamber, Mr. Matthias Kormaksson for assistance with statistical analysis, Mr. Karl Kremling for technical assistance, and Dr. Ruairidh Sawers for critical reading of the manuscript.

REFERENCES

Ahern KR, Deewatthanawong P, Schares J, Muszynski M, Weeks R, Vollbrecht E, Duvick J, Brendel VP, Brutnell TP (2009) Regional mutagenesis using *Dissociation* in maize. Methods **49:** 248-254

Balasubramanian S, Sureshkumar S, Agrawal M, Michael TP, Wessinger C, Maloof JN, Clark R, Warthmann N, Chory J, Weigel D (2006) The PHYTOCHROME C photoreceptor gene mediates natural variation in flowering and growth responses of *Arabidopsis thaliana*. Nat Genet **38:** 711-715

Balint-Kurti PJ, Zwonitzer JC, Wisser RJ, Carson ML, Oropeza-Rosas MA, Holland JB, Szalma SJ (2007) Precise mapping of quantitative trait loci for resistance to southern leaf blight, caused by Cochliobolus heterostrophus race O, and flowering time using advanced intercross maize lines. Genetics **176:** 645-657

Ballare CL, Scopel AL, Sanchez RA (1990) Far-red radiation reflected from adjacent leaves: an early signal of competition in plant canopies. Science **247:** 329-332

Bensen RJ, Johal GS, Crane VC, Tossberg JT, Schnable PS, Meeley RB, Briggs SP (1995) Cloning and characterization of the maize *An1* gene. Plant Cell **7:** 75-84

Bliss D, Smith H (1985) Penetration of light into soil and its role in the control of seed germination. Plant Cell Environ **8:** 475-483

Borthwick HA, Hendricks SB, Parker MW, Toole EH, Toole VK (1952) A reversible photoreaction controlling seed germination. Proc Natl Acad Sci U S A **38:** 662-666

Botto JF, Smith H (2002) Differential genetic variation in adaptive strategies to a common environmental signal in Arabidopsis accessions: phytochrome-mediated shade avoidance. Plant Cell Environ **25:** 53-63

Childs KL, Miller FR, Cordonnier-Pratt MM, Pratt LH, Morgan PW, Mullet JE (1997) The sorghum photoperiod sensitivity gene, Ma_3, encodes a phytochrome B. Plant Physiol **113:** 611-619

de Lucas M, Daviere JM, Rodriguez-Falcon M, Pontin M, Iglesias-Pedraz JM, Lorrain S, Fankhauser C, Blazquez MA, Titarenko E, Prat S (2008) A molecular framework for light and gibberellin control of cell elongation. Nature **451:** 480-484

Djakovic-Petrovic T, de Wit M, Voesenek LA, Pierik R (2007) DELLA protein function in growth responses to canopy signals. Plant J **51:** 117-126

Doebley JF, Gaut BS, Smith BD (2006) The molecular genetics of crop domestication. Cell **127:** 1309-1321

Downs RJ, Hendricks SB, Borthwick HA (1957) Photoreversible control of elongation of pinto beans and other plants under normal conditions of growth. Bot Gazette **118:** 199-208

Dubois PG, Brutnell TP (2009) Light signal transduction networks in maize. *In* S Hake, JL Bennetzen, eds, Handbook of Maize. Its Biology, Vol 1. Springer, New York, pp 205-228

Duek PD, Fankhauser C (2005) bHLH class transcription factors take centre stage in phytochrome signalling. Trends Plant Sci **10:** 51-54

Emerson RA (1912) The inheritance of certain "abnormalities" in maize. Am. Breeder's Assoc. Annu. Rep. **8:** 385-399

Fankhauser C, Casal JJ (2004) Phenotypic characterization of a photomorphogenic mutant. Plant J **39:** 747-760

Feng S, Martinez C, Gusmaroli G, Wang Y, Zhou J, Wang F, Chen L, Yu L, Iglesias-Pedraz JM, Kircher S, Schafer E, Fu X, Fan LM, Deng XW (2008) Coordinated regulation of *Arabidopsis thaliana* development by light and gibberellins. Nature **451:** 475-479

Filiault DL, Wessinger CA, Dinnery JR, Lutes J, Borevitz JO, Weigel D, Chory J, Maloof JN (2008) Amino acid polymorphisms in *Arabidopsis* phytochrome B cause differential responses to light. Proc Natl Acad Sci U S A **105:** 3157-3162

Franklin KA (2009) Light and temperature signal crosstalk in plant development. Curr Opin Plant Biol **12:** 63-68

Franklin KA, Whitelam GC (2007) Light-quality regulation of freezing tolerance in *Arabidopsis thaliana*. Nat Genet **39:** 1410-1413

Franklin KA, Whitelam GC (2007) Red:far-red ratio perception and shade avoidance. *In* B Publishing, ed, Light and Plant Development, Vol 31

Gonzalo M, Holland JB, Vyn TJ, McIntyre LM (2010) Direct mapping of density response in a population of B73 x Mo17 recombinant inbred lines of maize (*Zea mays* L.). Heredity **104:** 583–599

Gonzalo M, Vyn TJ, Holland JB, McIntyre LM (2006) Mapping density response in maize: a direct approach for testing genotype and treatment interactions. Genetics **173:** 331-348

Gorton HL, Briggs WR (1980) Phytochrome responses to end-of-day irradiations in light-grown corn grown in the presence and absence of Sandoz 9789. Plant Physiol **66:** 1024-1026

Halliday KJ, Salter MG, Thingnaes E, Whitelam GC (2003) Phytochrome control of flowering is temperature sensitive and correlates with expression of the floral integrator FT. Plant J **33:** 875-885

Hazen SP, Hawley RM, Davis GL, Henrissat B, Walton JD (2003) Quantitative trait loci and comparative genomics of cereal cell wall composition. Plant Physiol **132:** 263-271

Holland JB, Goodman MM (1995) Combining ability of tropical maize accessions with U.S. germplasm. Crop Sci **35:** 767-773

Janowiak F, Luck E, Dorffling K (2003) Chilling tolerance of maize seedlings in the field during cold periods in spring is related to chilling-induced increase in abscisic acid level. J. Agromony & Crop Science **189:** 156-161

Kasperbauer MJ (1971) Spectral distribution of light in a tobacco canopy and effects of end-of-day light quality on growth and development. Plant Physiol **47:** 775-778

Kebrom TH, Brutnell TP, Finlayson SA (2010) Suppression of sorghum axillary bud outgrowth by shade, phyB and defoliation signaling pathways. Plant Cell Environ **33:** 48-58

Kelly JM, Lagarias JC (1985) Photochemistry of 124-kilodalton Avena phytochrome under constant illumination in vitro. Biochemistry **24:** 6003–6010

Khanna R, Shen Y, Marion CM, Tsuchisaka A, Theologis A, Schafer E, Quail PH (2007) The basic helix-loop-helix transcription factor PIF5 acts on ethylene biosynthesis and phytochrome signaling by distinct mechanisms. Plant Cell **19:** 3915-3929

Kim HJ, Kim YK, Park JY, Kim J (2002) Light signalling mediated by phytochrome plays an important role in cold-induced gene expression through the C-repeat/dehydration responsive element (C/DRE) in Arabidopsis thaliana. Plant J **29:** 693-704

Kohchi T, Mukougawa K, Frankenberg N, Masuda M, Yokota A, Lagarias JC (2001) The Arabidopsis HY2 gene encodes phytochromobilin synthase, a ferredoxin-dependent biliverdin reductase. Plant Cell **13:** 425-436

Lee IJ, Foster KR, Morgan PW (1998) Photoperiod control of gibberellin levels and flowering in sorghum. Plant Physiol **116:** 1003-1011

Lee M, Sharopova N, Beavis WD, Grant D, Katt M, Blair D, Hallauer A (2002) Expanding the genetic map of maize with the intermated B73 x Mo17 (IBM) population. Plant Mol Biol **48:** 453-461

Leipner J, Stamp P (2009) Chilling stress in maize seedlings. *In* S Hake, JL Bennetzen, eds, Handbook of maize. Its biology, Vol 1. Springer, New York, pp 291-310

Liu JB, Mahoney KJ, Sikkema PH, Swanton CJ (2009) The importance of light quality in crop-weed competition. Weed Sci **49:** 217-224

Liu K, Goodman M, Muse S, Smith JS, Buckler E, Doebley J (2003) Genetic structure and diversity among maize inbred lines as inferred from DNA microsatellites. Genetics **165:** 2117-2128

Lorrain S, Allen T, Duek PD, Whitelam GC, Fankhauser C (2008) Phytochrome-mediated inhibition of shade avoidance involves degradation of growth-promoting bHLH transcription factors. Plant J **53:** 312-323

Maloof JN, Borevitz JO, Dabi T, Lutes J, Nehring RB, Redfern JL, Trainer GT, Wilson JM, Asami T, Berry CC, Weigel D, Chory J (2001) Natural variation in light sensitivity of Arabidopsis. Nat Genet **29:** 441-446

Mancinelli A (1994) The physiology of phytochrome action. *In* RE Kendrick, GHM Kronenberg, eds, Photomorphogenesis in Plants, Ed 2. Kluwer, Dordrecht, pp 211-269

Markelz NH, Costich DE, Brutnell TP (2003) Photomorphogenic responses in maize seedling development. Plant Physiol **133:** 1578-1591

May BP, Liu H, Vollbrecht E, Senior L, Rabinowicz PD, Roh D, Pan X, Stein L, Freeling M, Alexander D, Martienssen R (2003) Maize-targeted mutagenesis: A knockout resource for maize. Proc Natl Acad Sci U S A **100:** 11541-11546

McMullen MD, Kresovich S, Villeda HS, Bradbury P, Li H, Sun Q, Flint-Garcia S, Thornsberry J, Acharya C, Bottoms C, Brown P, Browne C, Eller M, Guill K, Harjes C, Kroon D, Lepak N, Mitchell SE, Peterson B, Pressoir G, Romero S, Oropeza Rosas M, Salvo S, Yates H, Hanson M, Jones E, Smith S, Glaubitz JC, Goodman M, Ware D, Holland JB, Buckler ES (2009) Genetic properties of the maize nested association mapping population. Science **325:** 737-740

Mickelson SM, Stuber CS, Senior L, Kaeppler SM (2002) Quantitative trait loci controlling leaf and tassel traits in a B73 x Mo17 population of maize. Crop Sci **42**

Moreno JE, Tao Y, Chory J, Ballare CL (2009) Ecological modulation of plant defense via phytochrome control of jasmonate sensitivity. Proc Natl Acad Sci U S A **106:** 4935-4940

Neuffer MG, Coe EH, Wessler SR (1997) Mutants of maize. Cold Spring Harbor Laboratory Press, Cold Spring Harbor, NY, USA.

Ogawa M, Kusano T, Koizumi N, Katsumi M, Sano H (1999) Gibberellin-responsive genes: high level of transcript acumulation in leaf sheath meristematic tissue from *Zea mays* L. Plant Mol Biol **40:** 645-657

Oh E, Yamaguchi S, Hu J, Yusuke J, Jung B, Paik I, Lee HS, Sun TP, Kamiya Y, Choi G (2007) PIL5, a phytochrome-interacting bHLH protein, regulates gibberellin responsiveness by binding directly to the GAI and RGA promoters in Arabidopsis seeds. Plant Cell **19:** 1192-1208

Penfield S (2008) Temperature perception and signal transduction in plants. New Phytol **179:** 615-628

Pinhero RG, Rao MV, Paliyath G, Murr DP, Fletcher RA (1997) Changes in activities of antioxidant enzymes and their relationship to genetic and paclobutrazol-induced chilling tolerance of maize seedlings. Plant Physiol **114:** 695-704

Piskurewicz U, Tureckova V, Lacombe E, Lopez-Molina L (2009) Far-red light inhibits germination through DELLA-dependent stimulation of ABA synthesis and ABI3 activity. Embo J **28:** 2259-2271

Rajcan I, Chandler KJ, Swanton CJ (2004) Red-far-red ratio of reflected light: a hypothesis of why early season weed control is important in corn. Weed Sci **52:** 774-778

Rajcan I, Swanton CJ (2001) Understanding maize-weed competition: resource competition, light quality and the whole plant. Field Crops Res **71:** 139-150

Rymen B, Fiorani F, Kartal F, Vandepoele K, Inze D, Beemster GT (2007) Cold nights impair leaf growth and cell cycle progression in maize through transcriptional changes of cell cycle genes. Plant Physiol **143:** 1429-1438

Salter MG, Franklin KA, Whitelam GC (2003) Gating of the rapid shade-avoidance response by the circadian clock in plants. Nature **426:** 680-683

Sawada Y, Aoki M, Nakaminami K, Mitsuhashi W, Tatematsu K, Kushiro T, Koshiba T, Kamiya Y, Inoue Y, Nambara E, Toyomasu T (2008) Phytochrome- and gibberellin-mediated regulation of abscisic acid metabolism during germination of photoblastic lettuce seeds. Plant Physiol **146:** 1386-1396

Sawers RJ, Linley PJ, Farmer PR, Hanley NP, Costich DE, Terry MJ, Brutnell TP (2002) *elongated mesocotyl1*, a phytochrome-deficient mutant of maize. Plant Physiol **130:** 155-163

Sawers RJ, Linley PJ, Gutierrez-Marcos JF, Delli-Bovi T, Farmer PR, Kohchi T, Terry MJ, Brutnell TP (2004) The *Elm1* (Zm*Hy2*) gene of maize encodes a phytochromobilin synthase. Plant Physiol **136:** 2771-2781

Sawers RJ, Sheehan MJ, Brutnell TP (2005) Cereal phytochromes: targets of selection, targets for manipulation? Trends Plant Sci **10:** 138-143

Seo M, Hanada A, Kuwahara A, Endo A, Okamoto M, Yamauchi Y, North H, Marion-Poll A, Sun TP, Koshiba T, Kamiya Y, Yamaguchi S, Nambara E (2006) Regulation of hormone metabolism in Arabidopsis seeds: phytochrome regulation of abscisic acid metabolism and abscisic acid regulation of gibberellin metabolism. Plant J **48:** 354-366

Seo M, Nambara E, Choi G, Yamaguchi S (2009) Interaction of light and hormone signals in germinating seeds. Plant Mol Biol **69:** 463-472

Setter TL, Parra R (2010) Relationship of carbohydrate and abscisic acid levels to kernel set in maize under postpollination water deficit. Crop Sci **50:** 980-988

Sheehan MJ, Farmer PR, Brutnell TP (2004) Structure and expression of maize phytochrome family homeologs. Genetics **167:** 1395-1405

Sheehan MJ, Kennedy LM, Costich DE, Brutnell TP (2007) Subfunctionalization of *PhyB1* and *PhyB2* in the control of seedling and mature plant traits in maize. Plant J **49:** 338-353

Smith H (1994) Sensing the light environment: the functions of the phytochrome family. *In* RE Kendrick, GMH Kronenberg, eds, Photomorphogenesis in Plants, Ed 2. Kluwer

Smith H (1995) Physiological and ecological function within the phytochrome family. Annu Rev Plant Physiol Plant Mol Biol **46:** 289-315

Smith H, Whitelam GC (1997) The shade avoidance syndrome: multiple responses mediated by multiple phytochromes. Plant Cell Environ **20:** 840-844

Spray CR, Kobayashi M, Suzuki Y, Phinney BO, Gaskin P, MacMillan J (1996) The *dwarf-1 (d1)* mutant of *Zea mays* blocks three steps in the gibberellin-biosynthetic pathway. Proc Natl Acad Sci U S A **93:** 10515-10518

Takano M, Inagaki N, Xie X, Yuzurihara N, Hihara F, Ishizuka T, Yano M, Nishimura M, Miyao A, Hirochika H, Shinomura T (2005) Distinct and cooperative functions of phytochromes A, B, and C in the control of deetiolation and flowering in rice. Plant Cell **17:** 3311-3325

Tao Y, Ferrer JL, Ljung K, Pojer F, Hong F, Long JA, Li L, Moreno JE, Bowman ME, Ivans LJ, Cheng Y, Lim J, Zhao Y, Ballare CL, Sandberg G, Noel JP, Chory J (2008) Rapid synthesis of auxin via a new tryptophan-dependent pathway is required for shade avoidance in plants. Cell **133:** 164-176

Vandenbussche F, Pierik R, Millenaar FF, Voesenek LA, Van Der Straeten D (2005) Reaching out of the shade. Curr Opin Plant Biol **8:** 462-468

White CN, Rivin CJ (2000) Gibberellins and seed development in maize. II. Gibberellin synthesis inhibition enhances abscisic acid signaling in cultured embryos. Plant Physiol **122:** 1089-1097

Williams EA, Morgan PW (1979) Floral initiation in sorghum hastened by gibberellic acid and far-red light. Planta **145:** 269-272

Wolyn DJ, Borevitz JO, Loudet O, Schwartz C, Maloof J, Ecker JR, Berry CC, Chory J (2004) Light-response quantitative trait loci identified with composite interval and eXtreme array mapping in Arabidopsis thaliana. Genetics **167:** 907-917

CHAPTER THREE

SUBFUNCTIONAILIZATION OF *PHYB1* AND *PHYB2* IN THE CONTROL OF MATURE TRAITS: A COMPARATIVE ANALYSIS OF THE B73 AND W22 *PHYB* MUTANTS INTROGRESSION SERIES

Abstract

The subfunctionalization between the two maize (*Zea mays* ssp. *mays*) paralogs *PhyB1* and *PhyB2* was investigated in two inbred backgrounds. The *Mutator* (*Mu*) insertion alleles *phyB1*::*Mu*563 and *phyB2*::*Mu*12058 were introgressed in the stiff stalk B73 and the non-stiff stalk W22 inbreds. The two *phyB* mutant series (which include the wild-type segregant, the two single mutants and the double mutant) were grown in a nursery field and phenotyped at maturity. Traits measured included plant height, ear node height, tassel length, leaf sheath and internode lengths and their length difference, leaf blade width, days to anthesis, upper leaf angle, and stem diameter. Each inbred background revealed distinct subfunctionalization patterns between the two *PhyB* paralogs. For the majority of the traits measured, the *phyB1 phyB2* double mutant displayed significant reduction in size compared to the wild-type segregant. This result confirms that maize PHYB act upstream of transduction pathways controlling several aspects of vegetative and reproductive development. Specific subfunctionalization between the two *PhyB* paralogs, among the different traits measured but also between inbred backgrounds, suggests the presence of background-specific genetic modifiers acting downstream the phytochrome transduction pathway.

3.1 Introduction

The maize (*Zea mays* ssp. *mays*) research community has long-appreciated the value of modifiers in the characterization of mutant phenotypes (Freeling and Fowler, 1993; Neuffer et al., 1997). Introgressions of mutants into multiple genetic backgrounds can potentially allow the identification of background-specific phenotypes and thus a more throughout characterization of the physiological and developmental impact a mutation has on plant development. The effect of these modifiers on the expression of a mutant phenotype can vary greatly between inbreds background. The role of trans modifiers (i.e. genotype-specific modifiers that do not reside in the recombining interval) was shown to modulate internal recombination rates of a 140 kb interval form W22, delimitated by markers *a1* and *sh2*, introgressed into the inbred lines A632, Oh43, and W64A (Yandeau-Nelson et al., 2006). In addition, the recent sequencing of a series of twenty-seven haplotypes of maize has begin to reveal the extend of the genome diversity across inbreds (Gore et al., 2009).

Furthermore, a large-scale program is underway to identify and clone modifiers of gene expression in maize (Johal et al., 2008). The dominant *Les* mutant *Rp1-D21*, which cause spontaneous cell death patches on leaves resembling pathogen attack, sees the expression of its phenotype highly dependent of the maize background used. In a proof of concept study, the *Rp1-D21* mutant was crossed to the IBM (Intermated B73 x Mo17) recombinant inbred line (RIL) mapping population (Lee et al., 2002), allowing the identification of a major quantitative trait loci controlling the expression of the *Rp1-D21* phenotype. Crosses of *Rp1-D21* to the 25 founders of the NAM (Nested Association Mapping) population (McMullen et al., 2009) showed a wide array of enhancement and suppression of the *Les* phenotype (Johal et al., 2008).

The use of common inbreds facilitates comparison between mutants and two of the most widely used in maize genetics are B73 and W22, both North American temperate inbreds. B73 belongs to the Iowa stiff stalk (SS) synthetic heterotic group (primarily composed of Reid Yellow Dent) and was developed by G.F. Sprague at Iowa State University to improve stalk quality (Troyer, 1999). W22 (Wisconsin 22) is a non-stiff stalk (NSS) derived from the Minnesota 13 lineage (Troyer, 1999) and is the recurrent parent of many genetic stocks. Heterotic groups, such as SS and NSS, were empirically created by relating the level of heterosis of crosses and the parents used in these crosses, therefore inbreds of related ancestry are often associated together (Troyer, 2006; Hallauer and Carena, 2009).

To survey the extent of the role of *PhyB1* and *PhyB2* in modulating maize development, the *phyB* mutant series, which was initially characterized in the France 2 background (Sheehan et al., 2007), was also introgressed in the B73 and W22 inbreds. The series includes the two single mutants *phyB1* and *phyB2*, the *phyB1 phyB2* double mutant, and the wild-type segregant *PhyB1 PhyB2*. The *phyB1* mutant was initially identified through a *Mutator* (*Mu*) transposon insertion mutagenesis screen (*phyB1*::*Mu*563). Because the mutation was in an undefined mixed background, the mutant allele was introgressed into several inbred backgrounds before initiating its characterization, including France 2. Interestingly, the introgression into the European flint France 2 revealed the presence of a non-functional *phyB2* allele (Sheehan et al., 2007).

When a second *Mu* insertion was identified in *PhyB2* (*phyB2*::*Mu*12058), introgressions of the *phyB1*::*Mu*563 and *phyB2*::*Mu*12058 alleles into B73 and W22 were initiated. Recurrent introgressions in both backgrounds were performed four times (see Chapter Two, sections 2.5.1 and 2.5.2 for a complete description of the plant materials and PCR-based genotyping). For four rounds of introgressions,

individuals homozygous for both *phyB1* and *phyB2* are expected to have approximately 93.75 % of their genome from the recurrent parent. The *phyB1 phyB2* mutant series, introgressed four time each in B73 and W22 backgrounds, was planted in a nursery field and evaluated for the presence of background-specific genetic modifiers on the expression and subfunctionalization of ten traits measured at maturity.

3.2 Results and Discussion

For the W22 introgressions, individual plants homozygous for each member of the *phyB* mutant series were identified by PCR-based genotyping during the summer of 2008. Homozygous individuals were self-pollinated and seed stocks increased during the following winter nursery. For the B73 introgressions, segregating families were screened and therefore individual plants were genotyped for the presence of *phyB1*::*Mu*563 or *phyB2*::*Mu*12058 alleles. Screens were performed in a 2009 nursery in Aurora, NY. The traits measured are described in Figure 3.1 and were chosen because most of them have been previously used to characterize the *phyB1 phyB2* mutant series in the France 2 background (Sheehan et al., 2007). Additional traits such as leaf number and leaf blade width were also measured, as they are common in the phenotypic characterization of maize plants (Neuffer et al., 1997; Kiesselbach, 1999). Phenotypic surveys were conducted at maturity (post-anthesis) with the exception of flowering time, which was measured throughout the growing season. All measurements were compared using a Tukey-Kramer statistical test with a *P*-value set at 0.05. Plant height was defined as the length from the ground up to the ligule of the flag leaf (Fig. 3.2A) and does not include the tassel main axis. Measurements were made using a PVC (polyvinyl chloride) pipe of 5 cm diameter to which a ruler with 1

cm increments was added. A summary of all the measurements is presented in Table 3.1.

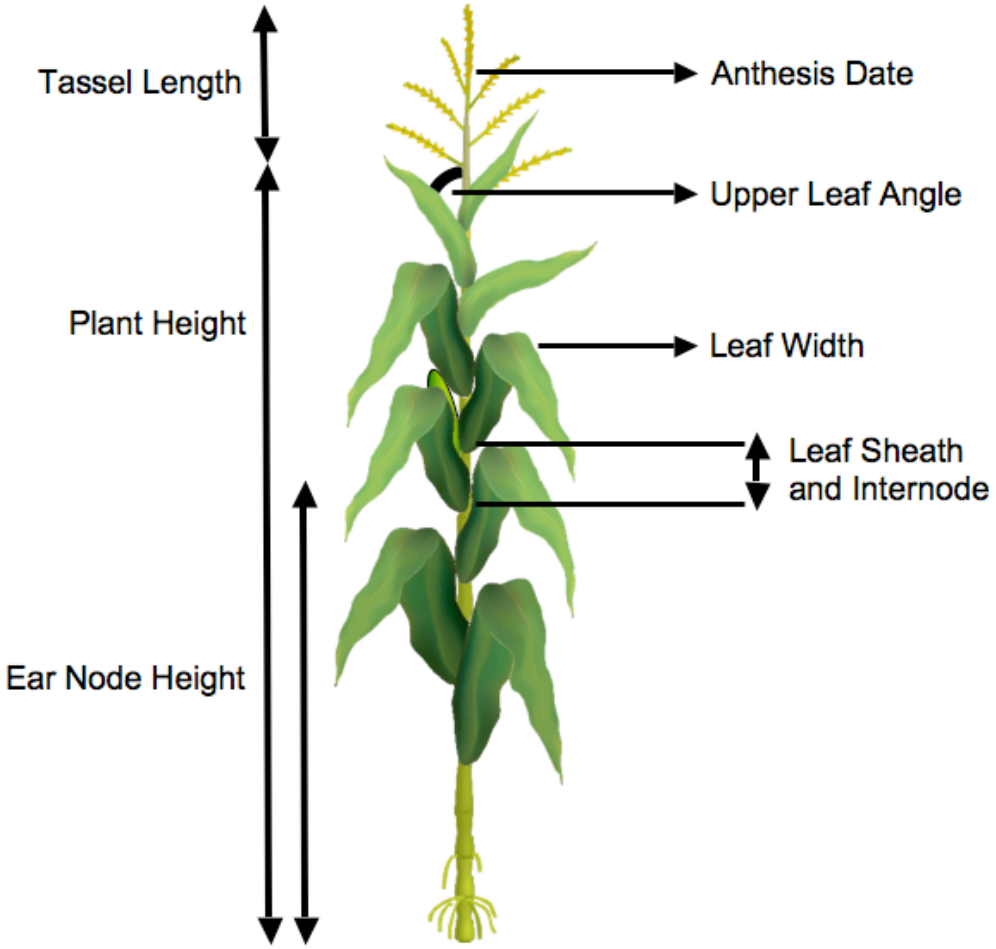

Figure 3.1 Phenotypic traits measured at maturity (post anthesis) on a maize plant. Presented on this rendition of a maize plant are the traits; plant height, ear node height, tassel length, days to anthesis, upper leaf angle, leaf width, leaf sheath length, and internode length. Also measured at maturity were the stem diameter of the ear internode and the leaf sheath-internode length difference.

Table 3.1. Phenotypic measurements performed on the *phyB* mutant series at maturity. *n*, number of observations; Diff (%), percentage difference between wild-type segregant (+ / +) and each of the other three members of the mutant series. Values in bold are significantly different than the wild-type segregant (Tukey-Kramer, $P = 0.05$)

		***phyB* Series [B73^4]**				***phyB* Series [W22^4]**			
Trait	**Genotype**	***n***	**Mean**	**St. Err.**	**Diff (%)**	***n***	**Mean**	**St. Err.**	**Diff (%)**
Plant Height (cm)	+ / +	33	199.3	3.3	- -	35	115.8	1.8	- -
	phyB1	75	194.8	1.3	-2.3	34	119.8	2.8	3.4
	phyB2	45	150.0	3.3	**-24.7**	40	103.3	2.4	**-10.9**
	phyB1 phyB2	19	156.7	10.2	**-21.3**	40	94.1	1.3	**-18.8**
Leaf Number	+ / +	17	21.6	0.2	- -	9	18.9	0.7	- -
	phyB1	37	20.4	0.1	**-6.0**	6	18.3	0.2	-2.9
	phyB2	27	18.9	0.2	**-12.7**	14	19.1	0.1	1.3
	phyB1 phyB2	11	16.5	0.5	**-23.6**	16	15.1	0.2	**-19.9**
Ear Node Height (cm)	+ / +	34	87.5	2.0	- -	15	37.5	2.0	
	phyB1	66	90.6	1.1	3	16	40.6	2.7	8.2
	phyB2	16	58.6	2.5	**-33**	15	36.6	2.0	-2.5
	phyB1 phyB2	20	57.9	4.7	**-34**	16	23.8	1.3	**-36.6**
Leaf Blade Width (cm)	+ / +	31	9.4	0.1	- -	9	7.9	0.4	- -
	phyB1	73	8.9	0.1	-5.2	6	6.8	0.2	-13.4
	phyB2	27	7.5	0.2	**-20.6**	14	7.6	0.3	-3.1
	phyB1 phyB2	16	5.8	0.3	**-38.3**	16	6.3	0.2	**-20.0**
Days to Anthesis	+ / +	34	90.5	0.4	- -	34	85.6	0.4	- -
	phyB1	86	92.0	0.4	**1.7**	38	87.2	0.4	**1.9**
	phyB2	42	93.0	0.5	**2.7**	45	83.7	0.3	**-2.2**
	phyB1 phyB2	11	88.5	0.7	-2.2	40	74.8	0.3	**-12.7**
Internode Length (cm)	+ / +	34	15.1	0.3	- -	15	10.5	0.4	- -
	phyB1	66	16.2	0.2	**7.0**	16	11.0	0.4	4.4
	phyB2	16	15.1	0.4	0.0	15	8.1	0.4	**-23.4**
	phyB1 phyB2	20	17.3	0.6	**14.1**	16	10.5	0.6	-0.6
Leaf Sheath Length (cm)	+ / +	34	12.5	0.1	- -	15	14.1	0.3	- -
	phyB1	66	12.1	0.1	-2.7	16	14.4	0.4	2.2
	phyB2	16	12.2	0.1	-2.3	15	11.7	0.5	**-17.0**
	phyB1 phyB2	20	11.2	0.3	**-10.6**	16	11.6	0.2	**-18.2**
Sheath - Internode Difference (cm)	+ / +	34	-2.6	0.3	- -	15	3.6	0.5	- -
	phyB1	66	-4.0	0.2	**52.8**	16	3.4	0.6	-4.5
	phyB2	16	-2.9	0.4	11.0	15	3.7	0.6	1.8
	phyB1 phyB2	20	-6.1	0.7	**130.4**	16	1.1	0.6	**-69.6**
Tassel Length (cm)	+ / +	33	36.7	0.7	- -	35	22.8	0.5	- -
	phyB1	75	33.3	0.6	**-9.3**	34	24.9	0.6	9.1
	phyB2	45	26.9	1.0	**-26.6**	40	22.2	0.6	-2.6
	phyB1 phyB2	19	12.6	1.9	**-65.6**	40	22.0	0.7	-3.6
Stem Diameter (cm)	+ / +	34	2.2	0.0	- -	15	1.8	0.1	- -
	phyB1	66	2.0	0.0	**-8.6**	16	1.6	0.1	**-15.4**
	phyB2	16	1.8	0.1	**-18.1**	15	1.8	0.1	-5.2
	phyB1 phyB2	20	1.3	0.1	**-42.4**	16	1.3	0.1	**-28.9**

In the B73 background, plant height appears to be controlled exclusively by *PhyB2*, as no significant difference between the wild-type segregant and *phyB1* single mutant was found. Furthermore, the *phyB2* single mutant is non-distinguishable from the double *phyB1 phyB2* mutant and both are shorter than the wild-type segregant. In W22, *phyB1* is not significantly different than the wild-type segregant, while the *phyB2* mutant has an intermediate height between the *phyB1 phyB2* double and *phyB1* and the wild-type segregant.

These findings suggest that *PhyB2* contributes to the regulation of plant height in both W22 and B73 inbreds. However, it is important to note that it is possible that a locus closely linked to the *phyB2* mutant allele is contributing to plant height (i.e. cis modifiers). As the *phyB2* allele was isolated from a mutagenized background of unknown ancestry, introgression blocks (1 to 10 cM) are likely to carry tens or hundreds of alleles from the original mutant background. Nevertheless, these results suggest subfunctionalization of the two *PhyB* paralogs in the regulation of plant height with *PhyB2* contributing significantly more than *PhyB1* to this trait. This result is in contrast to seedling length, where *PhyB1* appears to play a predominant role in regulating mesocotyl elongation (Sheehan, et al. 2007 and Chapter Two, Section 2.2.4). These findings also suggest that modifier loci do influence the expression of *Phy* genes. In B73, *PhyB1* did not contribute significantly to plant height, but in the W22 inbred *PhyB1* was partially redundant with *PhyB2* in the control of elongation responses. In the France 2 background, results suggest additive roles for the two *Phy* paralogs in the control of plant height (Sheehan et al., 2007).

Leaves were counted and tagged at three intervals during the growth season and results are presented in Figure 3.2B. These data show that in B73, both *PhyB1* and *PhyB2* additively control total leaf number. In W22, both *phyB1* and *phyB2* single

mutants are equivalent to the wild-type segregant and thus demonstrate a redundancy between the two *PhyB* paralogs.

Ear node height was measured using a measuring stick from ground level up to the node at the base of the most upper ear (Fig. 3.2C). In B73, *PhyB2* solely controls the trait, while in W22 both *PhyB1* and *PhyB2* act redundantly. The width of the leaf blade opposite to the ear was measured using a ruler (Fig. 3.2D). Measurements were taken at the widest section across the length of the blade. In B73, the subfunctionalization between *PhyB1* and *PhyB2* appears to give a greater role to *PhyB2* over *PhyB1*. In W22, the roles are reversed, this time with a preponderant role for *PhyB1*.

Days to anthesis were scored when approximately half of the anthers along the primary axis of the tassel had dehisced (Fig. 3.2E). In B73, results are inconclusive over the role of each *PhyB* paralog, and their subfunctionalization remains unresolved based on this analysis. While the *phyB1 phyB2* double mutant was the earliest to flower, the *phyB2* single mutant had its anthesis after both the wild-type segregant and the double mutant. The subfunctionalization in W22 presented the *phyB1 phyB2* double mutant with the shortest anthesis date, followed by the *phyB2* single, the wild-type segregant and finally the *phyB1* single mutant. These results suggest a preponderant role for *PhyB2* over *PhyB1*. A similar conclusion was initially derived from analysis in the France 2 background (Sheehan et al., 2007).

The two stem nodes used for the measurement of the internode length are located respectively at the base and immediately above the most upper ear (Fig. 3.2F). The B73 introgressions present a preponderant role for *PhyB1*, while the W22 introgressions are inconclusive in regard to the subfunctionalization the two *PhyB* paralogs. Interestingly, only the *phyB2* single mutant shows a significant reduction in

the internode length while the three remaining members of the mutant series are not significantly different from each other.

The leaf sheath selected for the measurement of its length is located at the base of the most upper ear on the opposite side of the stem (Fig. 3.2G). The B73 introgressions present a redundant role for *PhyB1* and *PhyB2* in the control of this trait. In W22, the PHYB-mediated elongation of the sheath is solely due to *PhyB2*. A feature of the *phyB1 phyB2* double mutant, as originally described in the France 2 inbred background, is the presence of a longer internode than the sheath surrounding it. This trait was calculated using the sheath length minus the internode length (Sheehan et al., 2007). Using the internode and sheath length measurements originally presented in Figure 3.2F and Figure 3.2G, the comparison between the two traits in presented in Figure 3.2H. Similarly to France 2, the four members of the B73 mutant series have a shorter sheath than their internode. The *phyB1 phyB2* double mutant has the largest difference of the four, followed by *phyB1*, suggesting a preponderant role for *PhyB1* in the expression of this phenotype. Surprisingly, the W22 series showed longer sheath lengths than internode length for all four members. The wild-type segregant and both *phyB* single mutants are not significantly different from each other. Only the *phyB1 phyB2* double mutant display a significantly smaller length difference then the three other members of the series, making the two *PhyB* paralogs redundant in the control of this trait. In France 2, the subfunctionalization is additive (Sheehan et al., 2007).

Tassel lengths were measured from the ligule of the flag leaf to the tip of the main axis of the tassel. Results are presented in Figure 3.2I, and shows additive roles for the two *PhyB* paralogs in the B73 background. The results observed in the W22 background do not allow any conclusions on the subfunctionalization of *PhyB1* and *PhyB2*. Finally, the stem diameter was measured at the internode above the ear (Fig.

3.2J). An additive role the two *PhyB* paralogs is distinguishable in B73, while a preponderant role for *PhyB1* over *PhyB2* in the control of the trait takes place in the W22 background.

A summary of the subfunctionalization between *PhyB1* and *PhyB2* for the control of mature traits is compiled in Table 3.2. It should be noted that for the vast majority of traits measured, the *phyB1 phyB2* double mutant displayed a phenotype not only significantly different but also smaller that the wild-type segregant. It is the case for plant height, leaf number, ear node height, leaf blade width, days to anthesis (W22 only), leaf sheath length, sheath – internode length difference, tassel length (B73 only), and stem diameter. This common characteristic confirm that PHYB1 and PHYB2 act upstream of major transduction pathways controlling several aspects of plant growth and reproduction. Only the internode length of the *phyB1 phyB2* double mutant (in both B73 and W22), days to anthesis (B73 only), and tassel length (W22 only) did not show a significant reduction in comparison to the wild-type segregant. Taken together, these results present an important role for the two *PhyB* paralogs in the development of a maize plant. When one or two members are non-functional, plant height and tassel length are generally shorter, the stem is narrower and internodes are longer. Leaf architecture of *phyB* mutants has a reduced number of leaves, narrower leaf blades and shorter sheaths. Furthermore, the introgression in two inbred backgrounds revealed distinct subfunctionalization between the two *PhyB* paralogs. When comparing results between B73, W22, and France 2 introgressions, subfunctionalization between the two *PhyB* paralogs is not constant. Only days to anthesis shares a preponderant role for *PhyB2* in W22 and France 2, and stem diameter have an additive role for *PhyB1* and *PhyB2* in B73 and France 2 (Table 3.2). This specificity in the subfunctionalization, both within inbred background at the trait level and also between inbred backgrounds, can also suggest the action of modifiers acting

downstream the phytochrome and light signal transduction pathway. The result presented here are likely a combination of phytochrome-specific modifiers and trait-specific ones.

Table 3.2 Summary of the subfunctionalization of *PhyB1* and *PhyB2* between B73, France 2, and W22 in the control of different maize traits at maturity. Results from the France 2 introgressions were previously published (Sheehan et al., 2007). NA, not available. Symbols < and > indicate a preponderant role for one paralog over the other. The symbol ^ and the number that follow indicate the number of times the mutant alleles were introgressed the inbred background.

	Inbred and introgression number		
Mature Traits	B73 ^4	W22^4	France 2^4
Plant Height	*PhyB2*	*B1 < B2*	*Additive*
Leaf Number	*Additive*	*Redundant*	NA
Ear Node Height	*PhyB2*	*Redundant*	NA
Blade Width	*B1 < B2*	*B1 > B2*	NA
Anthesis	Unresolved	*B1 < B2*	*B1 < B2*
Internode Length	*B1 > B2*	Unresolved	NA
Sheath Length	*Redundant*	*PhyB2*	NA
(Internode – Sheath)	*B1 > B2*	*Redundant*	*Additive*
Tassel Length	*Additive*	Unresolved	NA
Stem Diameter	*Additive*	*B1 > B2*	*Additive*

To uncover second-site enhancers and suppressors, Johal and colleagues (2008) have proposed a strategy to cross a single mutation to a large series of lines (either association- or RIL-based mapping populations) and generate novel variations of the mutant allele. Furthermore, some of these variants can have an agronomically useful phenotype and eventually be included to a breeding program. Genetics

modifiers of phytochromes can be proved useful to crop improvements as one or several of them can specifically target one or few phytochrome-mediated responses and not the complete light signal transduction pathway. Such strategy should also be considered considering the broad spectrum of variation these two mutations can cause to several aspects of maize development.

Figure 3.2 Phenotypic measurements of the maize *phyB1 phyB2* mutant series at maturity.

A

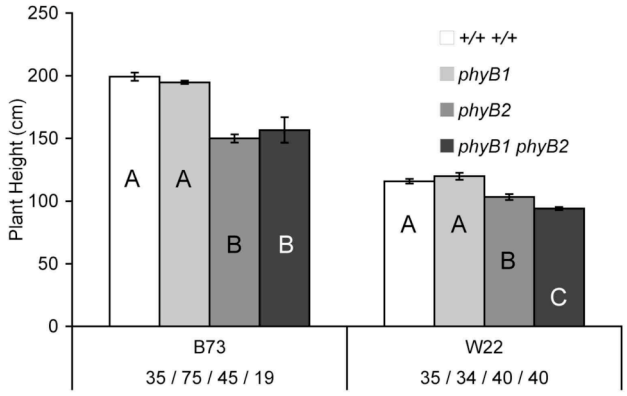
Plant Height (cm)
250
200
150
100
50
0
+/+ +/+
phyB1
phyB2
phyB1 phyB2
A
A
B
B
A
A
B
C
B73
35 / 75 / 45 / 19
W22
35 / 34 / 40 / 40

B

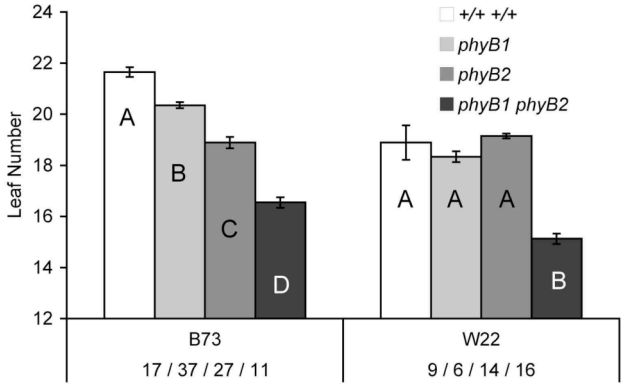
Leaf Number
24
22
20
18
16
14
12
+/+ +/+
phyB1
phyB2
phyB1 phyB2
A
B
C
D
A
A
A
B
B73
17 / 37 / 27 / 11
W22
9 / 6 / 14 / 16

C

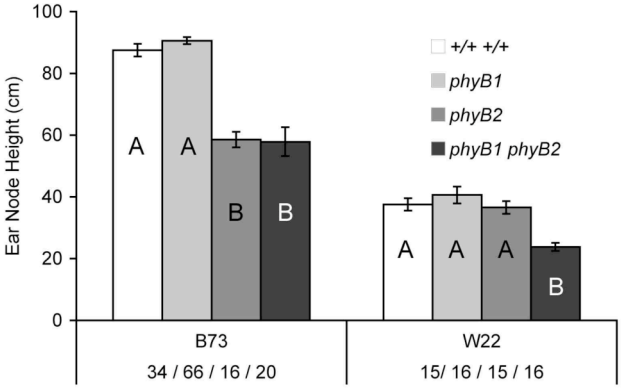
Ear Node Height (cm)
100
80
60
40
20
0
+/+ +/+
phyB1
phyB2
phyB1 phyB2
A
A
B
B
A
A
A
B
B73
34 / 66 / 16 / 20
W22
15/ 16 / 15 / 16

Figure 3.2 (Continued)

D

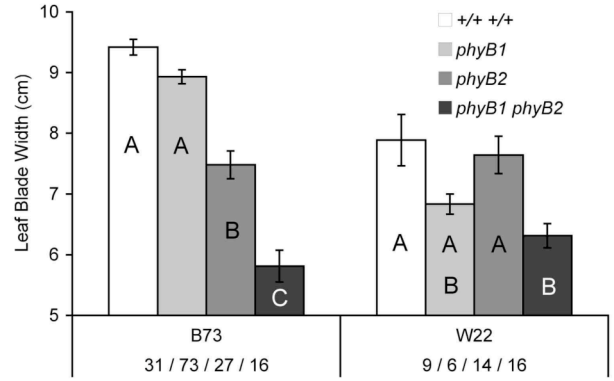

E

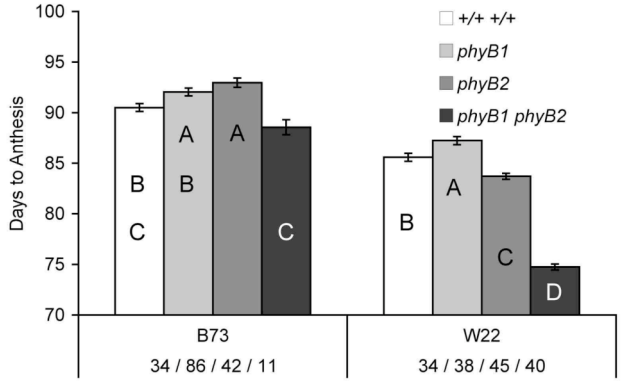

F

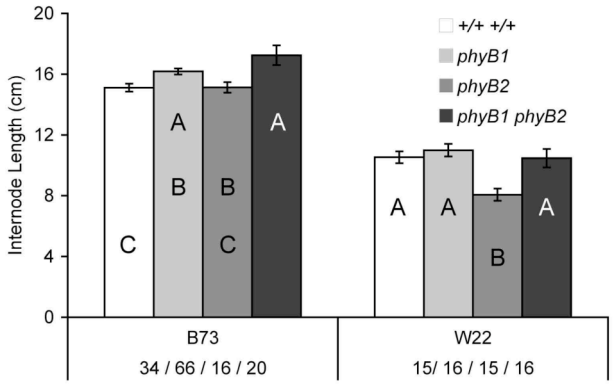

Figure 3.2 (Continued)

G

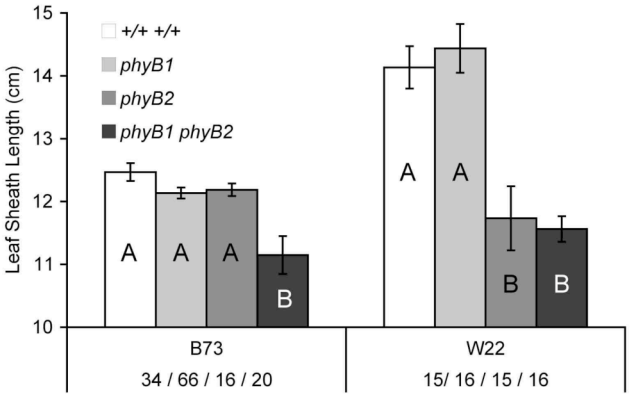

H

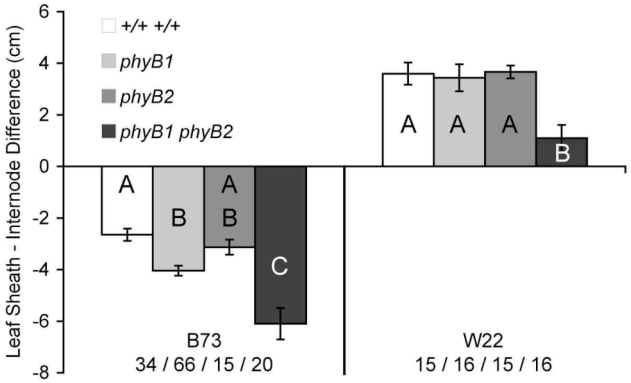

I

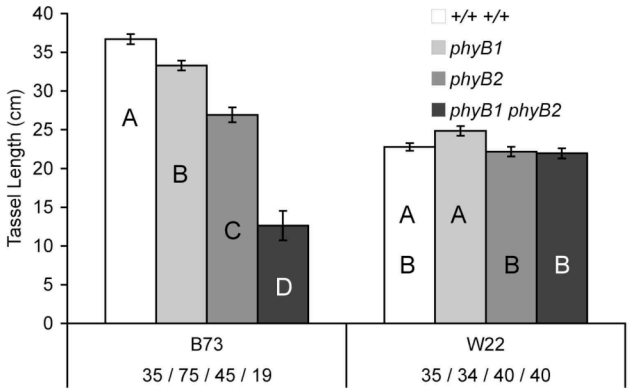

Figure 3.2 (Continued)

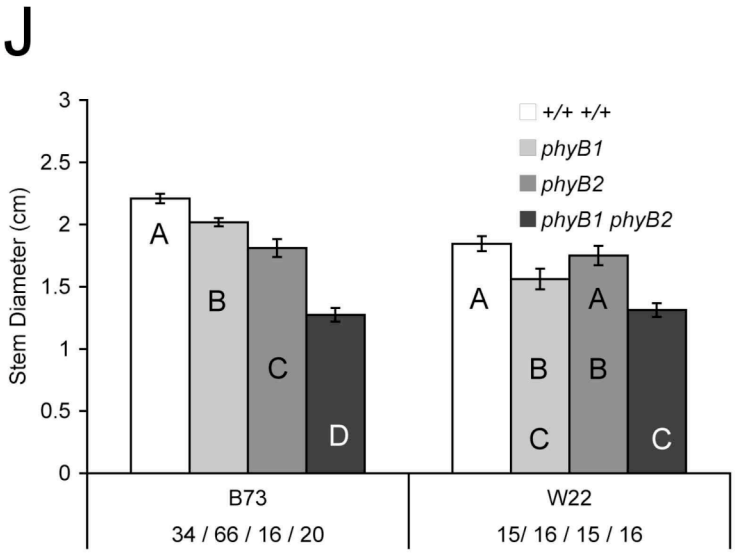

Phenotypic measurements of the maize *phyB1 phyB2* mutant series at maturity. All the traits were measured post-anthesis, with the exception of days to anthesis. All measurements were made in a nursery field in Aurora, NY, in the summer of 2009. A, Plant height. B, Leaf number. C, Ear node height. D, Leaf blade width. E, Days to anthesis. F, Internode length. G, Leaf sheath length. H, Leaf sheath length – Internode length difference. I, Tassel length. J, Stem diameter. Below each bar is the number of individuals that were measured. Error bar is the standard error. All statistical comparisons within inbred backgrounds were made using the Tukey-Kramer test. Different letters within each introgression indicate a *P*-value smaller than 0.05.

Current large scale mapping of modifiers have solely focus on single dominant alleles (Johal et al., 2008). In the case of *PhyB*, the mapping effort would be more complex, as two recessive alleles need to be cross to obtain homozygous F_2 individuals in sufficient number to perform a precise phenotyping. But since the phenotypic characterization of the *phyB1 phyB2* double mutant suggests that the absence of both PHYB1 and PHYB2 is detrimental to normal growth and development, and because several traits appear to be controlled predominantly or

totally by only one of the two *PhyB* paralogs, the introgression of a single *phyB* mutant might be sufficient to identify useful variants.

REFERENCES

Freeling M, Fowler J (1993) A nine-step way to characterize a morphological mutant. *In* M Freeling, V Walbot, eds, The maize handbook. Springer, New York, pp 209–211

Gore MA, Chia JM, Elshire RJ, Sun Q, Ersoz ES, Hurwitz BL, Peiffer JA, McMullen MD, Grills GS, Ross-Ibarra J, Ware DH, Buckler ES (2009) A first-generation haplotype map of maize. Science **326:** 1115-1117

Hallauer AR, Carena MJ (2009) Maize breeding. *In* MJ Carena, ed, Handbook of Breeding: Cereals. Springer, pp 1-98

Johal GS, Balint-Kurti PJ, Weil CF (2008) Mining and harnessing natural variation: a little MAGIC. Crop Sci **48:** 2066–2073

Kiesselbach TA (1999) The structure and reproduction of corn, 50th anniversary edition. Cold Spring Harbor Laboratory Press, Cold Spring Harbor, NY.

Lee M, Sharopova N, Beavis WD, Grant D, Katt M, Blair D, Hallauer A (2002) Expanding the genetic map of maize with the intermated B73 x Mo17 (IBM) population. Plant Mol Biol **48:** 453-461

McMullen MD, Kresovich S, Villeda HS, Bradbury P, Li H, Sun Q, Flint-Garcia S, Thornsberry J, Acharya C, Bottoms C, Brown P, Browne C, Eller M, Guill K, Harjes C, Kroon D, Lepak N, Mitchell SE, Peterson B, Pressoir G, Romero S, Oropeza Rosas M, Salvo S, Yates H, Hanson M, Jones E, Smith S, Glaubitz JC, Goodman M, Ware D, Holland JB, Buckler ES (2009) Genetic properties of the maize nested association mapping population. Science **325:** 737-740

Neuffer MG, Coe EH, Wessler SR (1997) Mutants of maize. Cold Spring Harbor Laboratory Press, Cold Spring Harbor, NY, USA.

Sheehan MJ, Kennedy LM, Costich DE, Brutnell TP (2007) Subfunctionalization of *PhyB1* and *PhyB2* in the control of seedling and mature plant traits in maize. Plant J **49:** 338-353

Troyer AF (1999) Background of U.S. hybrid corn. Crop Sci **39:** 601-626

Troyer AF (2006) Adaptedness and heterosis in corn and mule hybrids. Crop Sci **46:** 528-543

Yandeau-Nelson MD, Nikolau BJ, Schnable PS (2006) Effects of trans-acting genetic modifiers on meiotic recombination across the *a1-sh2* interval of maize. Genetics **174:** 101-112

CHAPTER FOUR

INFLUENCE OF DIURNAL SUN PATH ON MAIZE PLANT HEIGHT

Abstract

The influence of the daily sun path on maize (*Zea mays* ssp. *mays*) plant height was evaluated in a nursery field. The lower red to far-red ratio (R:FR) at the west (W) side of the field at sunset (i.e. end-of-day twilight FR) was hypothesized to create a plant height gradient along the east-west (E-W) cardinal axis. After regressing plant height relative to cardinal position in the field, an E-W gradient was identified where plants were significantly taller on the W side of the field. The analysis also identified field edge effects which cause plants to be progressively shorter from the inner to outer four edge rows, presumably due to higher photosynthetically active radiation and R:FR exposures. This effect was measured at the E and W edges of the nursery field, within a strip comprising the four outmost rows. The end-of-day twilight FR explains respectively 3% and 6% of the variation in plant height measured for all the lines present in the field and for the B73 checks only. These observations are discussed in the context of the shade avoidance syndrome.

4.1 Introduction

The light environment of a typical maize field fluctuates constantly due to both the plant growth, which progressively closes the canopy, and also because of the daily movement of the sun. Seasonal and hourly changes of the sun position influence the direction, fluence, spectral composition, and duration of the incident light. At high latitude, the sun path describes an arch where its zenith is at its most perpendicular during the summer solstice (June 21st). At this date, the earth axis is most incline toward the sun (Fig. 4.1). The sun path then gradually moves toward the equator until the winter solstice (December 21st). The earth axis then adopts its most inclined position away from the sun. During twilight, the two periods of the day when the sun elevation is between - 10° and + 10°, light travels across a longer path length than at other times of the day, resulting in more scattering and greater absorption of energy by the atmosphere (Smith, 1982). The ozone layer removes most of the short wavelengths while longer wavelengths are absorbed by oxygen at both 688 and 762 nm, and water vapor absorb wavelengths at around 723 nm (Chapter One, Fig. 1.2). Furthermore, refraction of the sunlight by the atmosphere increases the amount of longer wavelengths to reach the earth surface and causing characteristic orange/red sky coloration. The red to far-red ratio (R:FR) is reduced from approximately 1.19 in the middle of the day to 0.96 at dusk (Smith, 1982). The length of the twilight interval and the extent of the R:FR reduction increases at higher latitudes. Both of them fluctuate seasonally, increasing in duration as day lengths get shorter in the fall (Hughes et al., 1984).

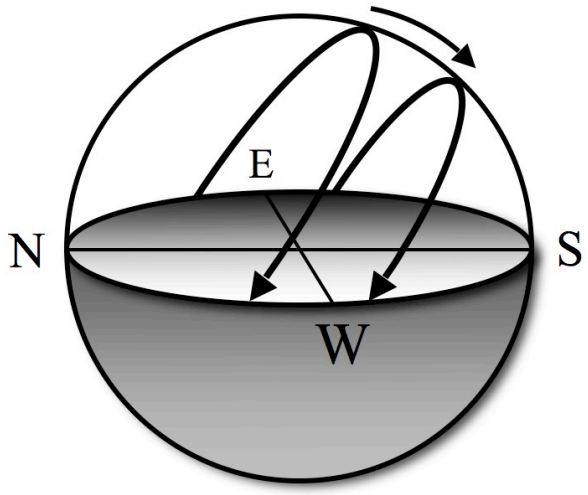

Figure 4.1 Diagram of the daily sun path at two different times of the year moving above a planar surface. The arched arrow on the left represents the sun path around the summer solstice. On the right, a second arched arrow represents the sun path later in the fall. In this second path, both a reduction in the duration of the daily exposure time and a more pronounced inclination toward the equator take place. The direction of each cardinal point is indicated (N, north; E, east; S, south; W, west).

The end-of-day twilight is highly reminiscent of end-of-day FR (EOD-FR) as both occur prior to a dark break and have similar spectral composition. Like EOD-FR, end-of-day twilight FR followed by darkness should photoconvert a large proportion of phytochromes to the inactive Pr form (Kelly and Lagarias, 1985). The subsequent darkness maintains an elevated pool of Pr and signals a de-repression of elongation. Conversely, at the beginning of the day, twilight precedes a period of high R:FR. Daylight is characterized by a higher R:FR converting the phytochrome pool back to the active Pfr, which repress elongation (Franklin and Whitelam, 2007). Unlike EOD-FR, daily beginning-of-day FR treatments failed to cause any significant impact on plant development (Kasperbauer, 1971). Examples of the application of an EOD-FR assay, primarily as a means to induced developmental responses similar to the shade

avoidance syndrome (SAS; Chapter One, Section 1.6), include the characterization of cold acclimation in red dogwood *Cornus stolonifera* (Michx) (McKenzie et al., 1974), maize seedling elongation and anthocyanin content of the coleoptile (Gorton and Briggs, 1980), and characterizing light responses of phytochrome mutants in Arabidopsis (*Arabidopsis thaliana*) (Nagatani et al., 1993; Robson et al., 1993; Wester et al., 1994; Casal, 1996; Devlin et al., 1998; Devlin et al., 1999; Franklin et al., 2003).

In a controlled environment, reduction in the R:FR during dawn and dusk twilight periods in addition to a lengthening of the photoperiod, was found to advance the seasonal developmental process of bud burst of silver birch plantlets (*Betula pendula*) (Linkosalo and Lechowicz, 2006). However, it remains unclear if dawn and dusk low R:FR treatments are additive it their contribution. In Arabidopsis, both low temperature and low R:FR at dusk can independently increase the expression of the *CBF* family of transcriptional activators that leads to enhanced freezing tolerance (Franklin and Whitelam, 2007). This result suggests that prolonged low R:FR at the end of the growth season acts as an environmental cue signaling the impending cold temperatures of winter. Thus, low R:FR present during twilight appears to have a biological relevance as a seasonal cue but no report exists on its capacity to induce SAS responses.

4.2 Results: Influence of daily end-of-day twilight low R:FR on maize plant height

The presence of a daily end-of-day twilight low R:FR effect was evaluated in maize using phenotypic data for plant height collected in a single field plot (Aurora, NY) in 2007. Increased plant height is a response associated with low R:FR and the SAS (Dubois and Brutnell, 2009). Based on the sun movement described previously and SAS-related plant height response, two positional effects were expected in the

field. In a N-S (north-south) axis, maize plants would be taller toward the N side of the field as they received less sunlight and lower R:FR ratios than southern positioned plants. In the E-W (east-west) axis, maize plants were expected to be taller toward the western edge of the field as they are exposed to higher irradiance of low R:FR at the end of the day. The fluence of the light gradually diminishes as it laterally penetrates into the field, reaching its lowest level at the east border. Another light effect expected to be detected is an "edge effect" causing plants grown at the fringe of a field to be shorter than then mean height due to grater access to higher photosynthetically active radiation (PAR) and R:FR (Dubois and Brutnell, 2009).

A diverse collection of maize germplasm including 5000 lines of the nested association mapping (NAM) population, 200 lines of the intermated B73 x Mo17 (IBM) population, and 300 lines of an association panel were evaluated. To serve as checks, rows of the B73 inbred were randomly planted 200 times within the field plot. Lines from the different populations were pooled and planted according to their flowering time in a N-S gradient. This was made as an attempt to minimize labor time during pollination. Overall, 5397 plant height measurements were collected. Each line was planted by half-row and a single plant representing the median height in each half-row was used for height measurements. To investigate the presence of N-S and E-W position effects, plant height data was assigned a location defined by Cartesian coordinates based on a X-Y matrix (Fig. 4.2).

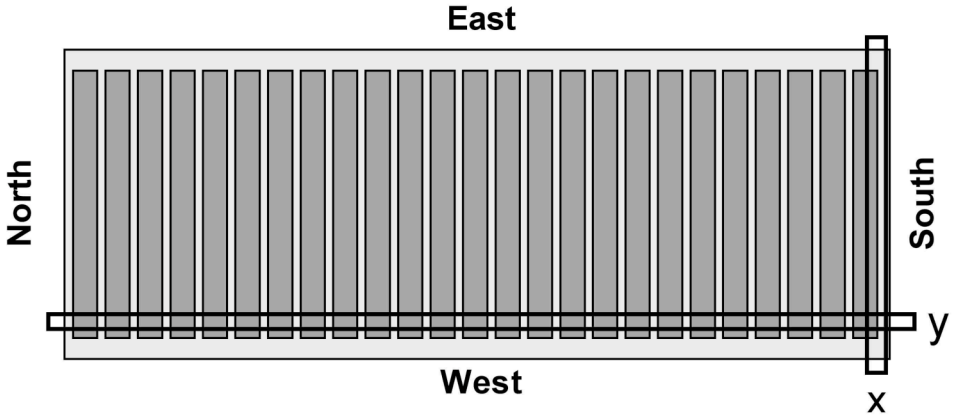

Figure 4.2 Diagram of a 2007 field nursery located in Aurora, N.Y. Each dark gray rectangle represents a range of plant rows. Ranges are oriented W-E and individual rows within a range are in a S-N orientation. Each row was divided in two at the center, each planted with a different line (a half-row facing N and the other facing S). For this analysis, each half-row height corresponding to a line was assigned X-Y matrix coordinates. Plant heights were scored using a plastic pipe labeled with barcodes in 1 cm increment and recorded with wireless laser scanner.

Plant height for each X and Y coordinate was pooled and an average calculated for each. In the E-W axis (Fig. 4.3A), an edge effect at each end of the field is clearly visible. Shorter plants were expected at each extremity, as higher PAR and R:FR are available due to better light penetration in the canopy. Lines located at the edge of the field therefore display attenuated SAS responses and plant heights are reduced relative to the remainder of the field. This gradient effect usually disappears at the fifth row within a field, a point where light under the canopy becomes uniform (P. Dubois, personal observations). When the four outmost rows at each extremity of the W-E axis are removed from the analysis, the remaining Y coordinates average heights are greater than the overall mean on the W side, and smaller on the E side. No edge or axis gradient is visually detectable for the X-axis (Fig. 4.3B). Although edge effects at the N and S are likely present, we were unable to detect these in the dataset. This can be explained by the orientation of individual rows, which were planted only in a S-N

orientation. Since the edge effect is most apparent in the plants closest to the field edge, the plant height gradient is within the first and last range of rows, thus undetectable with available measurements. If the field had its rows in a W-E orientation, the detection edge effects at the N and S extremities of the field would likely have been possible.

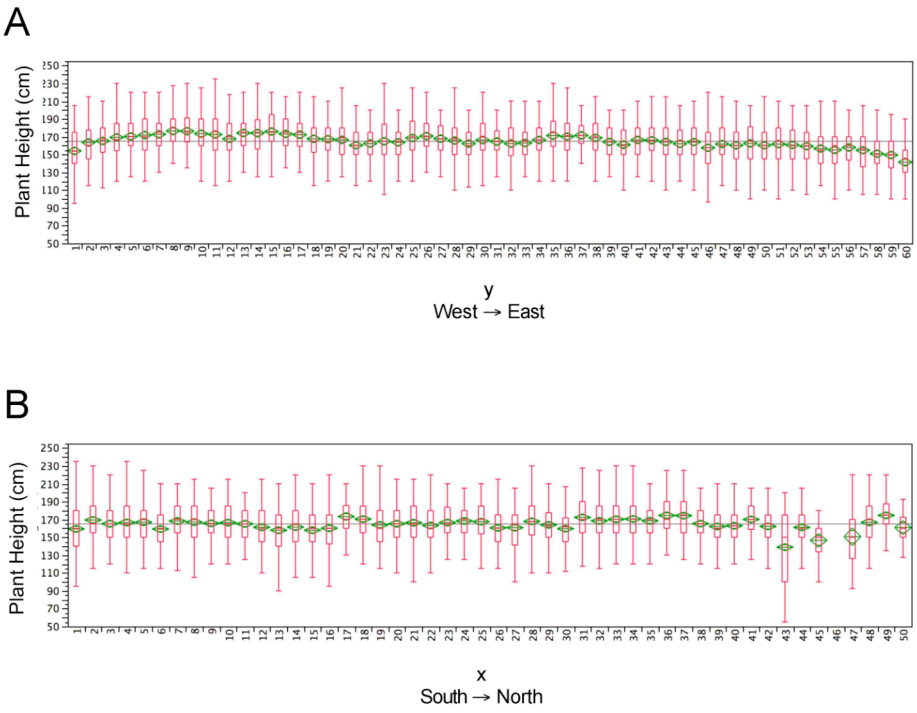

Figure 4.3 Box plot distributions of plant heights for the X- and Y- axis. The horizontal grey line represents the field mean for plant height. Each box plot consists of a green polygon representing the 95% confidence interval of the average. Box bottoms and tops represent the 25th and 75th percentile of that coordinate plant height respectively. A, W to E axis (Y). B, S to N axis (X).

To quantify in more detail the different positional effects present in the field, the E-W axis (Y) was divided into three sections based on the two edge responses observed in Figure 4.3A. A model defined as $y = \beta_0 + \beta_1 X + \beta_2 Y + \beta_3 XY + \varepsilon$ was used

to evaluate if Cartesian coordinates are significant. Both E and W edges had equivalent but inverse slopes: + 4.76 ($P < 0.0001$) at the W extremity and - 4.12 ($P = 0.0002$) at the E extremity. A *t* test was performed using the estimates and standard error of the two Y-axis slopes: $\beta_2^{East} = 4.76$, SE = 1.015 and $\beta_2^{West} = -4.12$, SE = 1.077 (DF = $n_2^{East} + n_2^{West} - 4$), and showed no significant difference between the two slopes despite their heterogeneous composition ($t = 0.435$ $P = 0.66$). Model summaries are presented in Table 4.1 for the E edge and in Table 4.2 for the W edge of the field.

Table 4.1. Model summary for plant height measurements based on field Cartesian coordinates for the W edge of the field (4 rows, all lines included). The model used is $y = \beta_0 + \beta_1 X + \beta_2 Y + \beta_3 XY + \varepsilon$.

R^2	0.118
R^2 Adjusted	0.111
Root Mean Square Error	21.53
Mean of Response	163.02
n	358

Source	**DF**	**Sum of Squares**	**Mean Square**	***F* Ratio**
Model	3	22034.99	7345.00	15.8474
Error	354	164073.06	463.48	**Prob > *F***
C. Total	357	186108.05		< 0.0001

Term	**Estimate**	**Std Error**	***t* Ratio**	**Prob > | *t* |**
Intercept	141.56	3.45	41.08	< 0.0001
X	0.40	0.08	4.73	< 0.0001
Y	4.76	1.01	4.69	< 0.0001
(X-23.8464)*(Y-2.5)	-0.14	0.08	-1.88	0.0608

Table 4.2. Model summary for maize plant height based on field Cartesian coordinates for the E edge of the field (4 rows, all lines included). The model used is $y = \beta_0 + \beta_1 X + \beta_2 Y + \beta_3 XY + \varepsilon$.

R^2	0.044
R^2 Adjusted	0.036
Root Mean Square Error	22.74
Mean of Response	149.26
n	359

Source	**DF**	**Sum of Squares**	**Mean Square**	***F* Ratio**
Model	3	8424.70	2808.23	5.43
Error	355	183487.49	516.87	**Prob > *F***
C. Total	358	191912.19		0.0012
Term	**Estimate**	**Std Error**	***t* Ratio**	**Prob > | *t* |**
Intercept	161.09	3.59	44.86	< 0.0001
X	-0.064	0.084	-0.76	0.44
Y	-4.12	1.08	-3.82	0.0002
(X-25.12)*(Y-2.48)	-0.074	0.075	-0.99	0.32

The effect of the X (W-E) and Y (S-N) coordinates and their interaction (X*Y) was tested using a standard least squares with the following model: $y = \beta_0 + \beta_1 X + \beta_2 Y + \beta_3 XY + \varepsilon$ (Tables 4.1 and 4.2). For the four rows at the W border, the model was significant (F ratio = 15.84, $P < 0.0001$). Both X and Y components were significant ($t = 4.73$ and 4.69 respectively, both with $P < 0.0001$), but not their interaction ($t = -1.88$, $P = 0.06$). For the four rows at the E border, the model was significant (F ratio = 5.43, $P = 0.001$), the Y-axis component was significant ($t = -3.82$, $P = 0.0002$), but not the X-axis ($t = -0.76$, $P = 0.45$) or their interaction ($t = -0.99$, $P = 0.32$). For the W border, the R^2 of the model was 0.118 and R^2 for the X and Y regressions were 0.055 and 0.054 respectively. At the east border, the R^2 of the model was 0.044 while the R^2 values of the X and Y regressions were 0.0018 and 0.040 respectively. All R^2 values for the X and Y regressions were calculated by removing from the model one of the two Cardinal axes and their interaction. The X-axis regression model was $y = \beta_0 + \beta_1 X + \varepsilon$, while the Y-axis regression model used was $y = \beta_0 + \beta_2 Y + \varepsilon$.

For the whole field, but excluding the eight Y-axis rows locates at the W and E edges, the model was significant (F ratio = 55.28, $P < 0.0001$). The X component was not significant (slope of -0.0008, Student's t = -0.33, $P = 0.74$) while the Y component was significant (slope of -0.28, Student's t = -12.69, $P < 0.0001$), but not the X*Y interaction (Student's t = -1.86, $P = 0.063$). A model summary for the whole field (minus W and E edges) is presented in Table 4.3. The W-E and S-N regressions are presented in Figure 4.4B. The R^2 value for the model is 0.034, while the R^2 values for the X and Y regressions are 0.00012 and 0.034 respectively.

Table 4.3. Model summary for maize plant height based on field Cartesian coordinates for the complete field, all lines (excluding both E and W 4 edges rows). The model used is $y = \beta_0 + \beta_1 X + \beta_2 Y + \beta_3 XY + \varepsilon$.

R^2	0.034
R^2 Adjusted	0.034
Root Mean Square Error	22.59
Mean of Response	166.22
n	4680

Source	**DF**	**Sum of Squares**	**Mean Square**	***F* Ratio**
Model	3	84605.7	28201.9	55.28
Error	4676	2385450.3	510.1	**Prob > *F***
C. Total	4679	2470056.0		< 0.0001
Term	**Estimate**	**Std Error**	***t* Ratio**	**Prob > | *t* |**
Intercept	175.02	0.94	186.18	0.0000
X	-0.008	0.024	-0.33	0.74
Y	-0.28	0.02	-12.69	< 0.0001
(X-22.02)*(Y-30.16)	-0.003	0.002	-1.86	0.063

To test if the B73 inbred checks scattered across the field behaved in a similar way as the population as a whole, heights and coordinates were extracted from the dataset and submitted to the same analysis. Because there was an insufficient number of B73 checks in the fourth first rows of the E and W field extremity, the two edges were omitted in the B73 checks analysis. As presented in Figure 4.5, the B73 checks behaved in a similar fashion as the complete dataset presented in Figure 4.4. Namely

that a slope is detectable in the W-E axis. The effect of the X (S-N) and Y (W-E) coordinates and their interaction (X *Y) was also tested using a standard least squares analysis using the model: $y = \beta_0 + \beta_1 X + \beta_2 Y + \beta_3 XY + \varepsilon$. Again using all the B73 height data, with the exception of the eight rows making the E and W field borders, the model was significant (F ratio = 4.11, $P = 0.0075$). The X component not was significant ($t = -0.24$, $P = 0.81$) while the Y component was significant ($t = -3.36$, $P = 0.001$) but not the X*Y interaction ($t = -0.89$, $P = 0.38$). Model summary for the B73 checks field (minus W and E edges) is presented in Table 4.4. The W-E axis (Y) has a slope of -0.24 ($P = 0.001$; Fig. 4.5A). The S-N axis (X) has a slope of -0.018 (non-significant; Fig. 4.5B). The R^2 value for the model was 0.066, while the R^2 values for the X and Y regressions were 0.0012 and 0.062 respectively.

Table 4.4. Model summary for maize plant height based on field Cartesian coordinates for the B73 checks (excluding both E and W edges rows). The model used is $y = \beta_0 + \beta_1 X + \beta_2 Y + \beta_3 XY + \varepsilon$.

R^2	0.066			
R^2 Adjusted	0.050			
Root Mean Square Error	13.89			
Mean of Response	175.63			
n	178			
Source	**DF**	**Sum of Squares**	**Mean Square**	***F* Ratio**
Model	3	2383.59	794.53	4.11
Error	174	33601.19	193.11	**Prob > *F***
C. Total	177	35984.78		0.0075
Term	**Estimate**	**Std Error**	***t* Ratio**	**Prob > | *t* |**
Intercept	183.66	2.97	61.76	< 0.0001
X	-0.018	0.076	-0.24	0.81
Y	-0.24	0.071	-3.36	0.001
(X-24.09)*(Y-31.54)	-0.0047	0.0053	-0.89	0.38

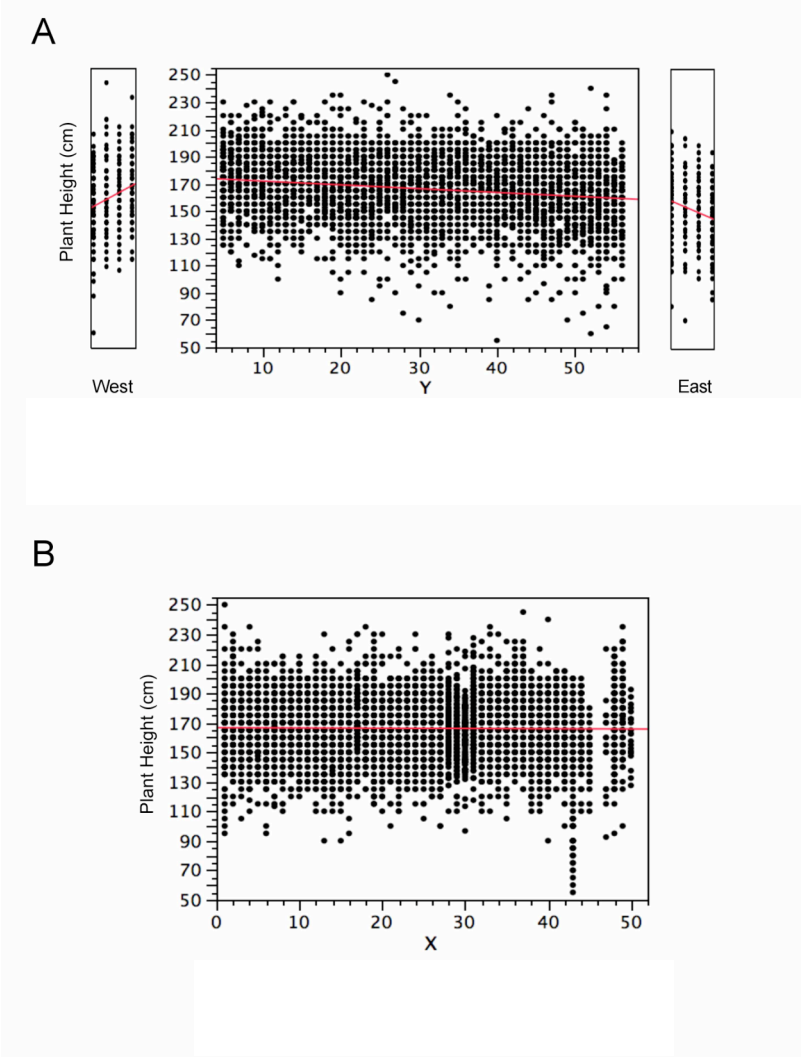

Figure 4.4 Regression plots of plant height measurements based on field position. Each data point is represented by a black dot and the red line represents the regression. A, W-E axis (Y). The four rows present at each edge were isolated from the inner field to account for the height edge effect seen in conventional maize fields. Thus distinct regressions were derived of each border rows and the inner field. B, S-N axis (X). Since rows are in a S-N orientation, plant height edge effects present at each field extremity cannot be measured and thus are not presented. The single regression includes all the coordinates of the X-axis. N, north; E, east; S, south; W, west.

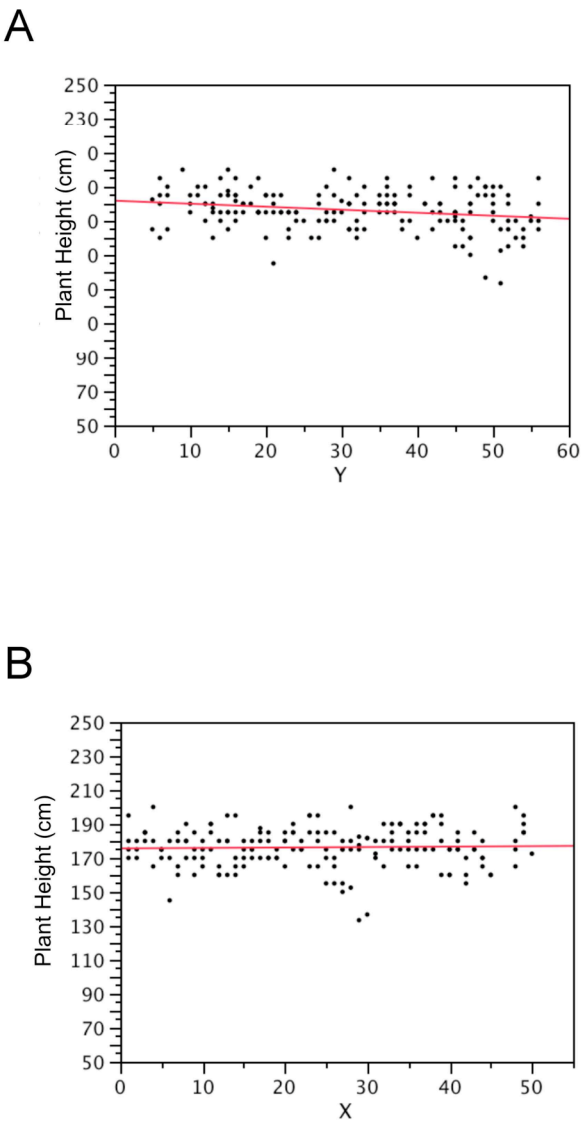

Figure 4.5 Regression analysis of the plant height of the B73 checks. Each data point is represented by a dot. A, W-E axis (Y). B, S-N axis (X). N, north; E, east; S, south; W, west.

4.3 Conclusions

Results presented in this chapter are in agreement with our hypothesis; namely that a low R:FR exposure originating at the W side of the field at sunset creates a height gradient along the W-E axis, with the tallest plants (or most SAS responsive) located at the W end of the field. The plant height data also revealed an edge effect at the E and W borders of the field. Across the four outmost rows, the reduction in height toward the last rows had equivalent but inverse slopes (+4.73 and -4.13). No N-S effect was detected, which suggest that the sun path inclination toward the south has no significant effect on plant height at this latitude. Excluding the last eight Y-axis rows located at the W and E edges, only the Y-axis (W-E) component ($P < 0.0001$) was significant. The exclusion of a line genotype effect by performing a separate analysis of the B73 checks again showed a significant effect only for the Y-axis ($P = 0.001$). A plant height slope similar to the whole line population (-0.28) could be generated with the B73 checks (-0.24), with the tallest individuals located in the W section of the field. The two slopes are not significantly different ($t = 1.699$, $P = 0.089$). In the W-E axis, both the whole line population and the B73 checks had R^2 values of 0.03 and 0.06 respectively. In the case of the B73 checks, the uniformity of the genetic material improves the proportion of the height variation explained by the W-E position. If a twilight end-of-day FR effectively influences plant height, it can explain approximately 5% of the total variation measured in the field.

Since this analysis is based solely on data collected from a single field plot and from a single year, it would not be prudent to generalize its conclusions. Additional measurements based on several locations and years will be necessary to strengthen this hypothesis. In addition to replication of the original field design, a screen of a uniform hybrid may provide an additional dataset that would eliminate genotype variance and

have implications for breeding efforts. Additional design considerations include sufficient distance from obstructions at the field margins and using a replicated block design in which blocks are planted in two different row orientations. Another open question is the biological significance of this developmental response. In a crop grown at high density such as maize, the twilight end-of-day low R:FR likely will have a marginal impact on plant development and yield in a production field. Nevertheless, the inclusion of light parameters such as cardinal row orientation and Cartesian coordinates should improve phenotypic data analysis in field experiments and yield trials. It is tempting to speculate that the W-E effect describes here is mediated by a similar mechanism as the EOD-FR response. The rationale being that the phytochrome photoreceptors and the light transduction networks are unable to differentiate them.

4.4 Acknowledgments

I thank Dr. Edward Bucker for sharing plant height measurements.

REFERENCES

Casal JJ (1996) Phytochrome A enhances the promotion of hypocotyl growth caused by reductions in levels of phytochrome B in its far-red-light-absorbing form in light-grown Arabidopsis thaliana. Plant Physiol **112:** 965-973

Devlin PF, Patel SR, Whitelam GC (1998) Phytochrome E influences internode elongation and flowering time in Arabidopsis. Plant Cell **10:** 1479-1487

Devlin PF, Robson PR, Patel SR, Goosey L, Sharrock RA, Whitelam GC (1999) Phytochrome D acts in the shade-avoidance syndrome in Arabidopsis by controlling elongation growth and flowering time. Plant Physiol **119:** 909-915

Dubois PG, Brutnell TP (2009) Light signal transduction networks in maize. *In* S Hake, JL Bennetzen, eds, Handbook of Maize. Its Biology, Vol 1. Springer, New York, pp 205-228

Franklin KA, Praekelt U, Stoddart WM, Billingham OE, Halliday KJ, Whitelam GC (2003) Phytochromes B, D, and E act redundantly to control multiple physiological responses in Arabidopsis. Plant Physiol **131:** 1340-1346

Franklin KA, Whitelam GC (2007) Light-quality regulation of freezing tolerance in *Arabidopsis thaliana*. Nat Genet **39:** 1410-1413

Franklin KA, Whitelam GC (2007) Red:far-red ratio perception and shade avoidance. *In* B Publishing, ed, Light and Plant Development, Vol 31

Gorton HL, Briggs WR (1980) Phytochrome responses to end-of-day irradiations in light-grown corn grown in the presence and absence of Sandoz 9789. Plant Physiol **66:** 1024-1026

Hughes JE, Morgan DC, Lambton PA, Black CR, Smith H (1984) Photoperiodic time signals during twilight. Plant Cell Environ **7:** 269-277

Kasperbauer MJ (1971) Spectral distribution of light in a tobacco canopy and effects of end-of-day light quality on growth and development. Plant Physiol **47:** 775-778

Kelly JM, Lagarias JC (1985) Photochemistry of 124-kilodalton Avena phytochrome under constant illumination in vitro. Biochemistry **24:** 6003–6010

Linkosalo T, Lechowicz MJ (2006) Twilight far-red treatment advances leaf bud burst of silver birch (*Betula pendula*). Tree Physiol **26:** 1249-1256

McKenzie JS, Weiser CJ, Burke MJ (1974) Effects of Red and Far Red Light on the Initiation of Cold Acclimation in Cornus stolonifera Michx. Plant Physiol **53:** 783-789

Nagatani A, Reed JW, Chory J (1993) Isolation and initial characterization of Arabidopsis mutants that are deficient in phytochrome A. Plant Physiol **102:** 269-277

Robson P, Whitelam GC, Smith H (1993) Selected components of the shade-avoidance syndrome are displayed in a normal manner in mutants of *Arabidopsis thaliana* and *Brassica rapa* deficient in phytochrome B. Plant Physiol **102:** 1179-1184

Smith H (1982) Light quality, photoperception and plant strategy. Annu Rev Plant Physiol **33:** 481-518

Wester L, Somers DE, Clack T, Sharrock RA (1994) Transgenic complementation of the hy3 phytochrome B mutation and response to PHYB gene copy number in Arabidopsis. Plant J **5:** 261-272

CHAPTER FIVE

EVALUATION OF DIFFERENT WITHIN-ROW PLANTING DENSITIES IN A NURSERY FIELD

Abstract

A pilot study was conducted to evaluate the feasibility of measuring density responses in a conventional maize (*Zea mays* ssp. *mays*) field nursery. A panel including three maize inbreds, the *phyB1 phyB2* mutant series and collection of teosinte near isogenic lines (NIL) was grown at two planting densities. Due to limitations in space and labor, measurements were taken on a single row per line at each density with the exception of days to anthesis which was measured on all plants in a row. Of the three inbreds evaluated, both B73 and W22 had significantly fewer days to anthesis at high density, while Mo17 was non responsive to the treatment. A subset of forty-one NILs, representing a minimum tiling path of the teosinte genome, had responses to high density ranging from non-responsive to an eight day hastening of flowering. The survey of the four members of the *phyB1 phyB2* mutant series revealed an additive role for the two *PhyB* paralogs in the control of leaf blade azimuthal orientation.

5.1 Introduction

The discovery of heterosis in maize (*Zea mays* ssp. *mays*) (Shull, 1908; East, 1909) led to the development of hybrid seed production (Jones, 1918). Since then, yield gains per year have consistently progressed in maize, now approaching 178 kg ha^{-1} $year^{-1}$ with the advent of molecular marker assisted selection and transgenic traits (Troyer, 2006). These gains can be attributed to both the genetic improvements of inbred parents and better agronomic practices. Improvements in performance under abiotic stress such as nitrogen deficiency, cold temperature, drought, and weed competition, together with an increase in tolerance to high planting densities accounts for the majority of the genetic gain (Lee and Tollenaar, 2007). Since the advent of commercially available maize hybrids in the 1930's, yields have increased from 1500 kg ha^{-1}, to exceeding 9000 kg ha^{-1} in the 2000's in the U.S. while average planting density has increased from 27 000 to more than 80 000 plants ha^{-1}. Through the years, yield has remained strongly associated with increases in planting density (Pearson's correlation coefficient $r = 0.97$) (based on USDA data, www.nass.usda.gov and Troyer, 2006). Following the example set by savvy farmers to increase their crop yield (John W. Dudley, personal communication), maize breeders also implemented very high densities in their selection program to increase variations between entries (Troyer and Resenbrook, 1983).

A major constraint associated with high plant density is the limited availability of light to each individual plants. The shade avoidance syndrome (SAS) is a developmental response to a reduction in both the photosynthetically active radiation (PAR) and the ratio of red (R) to far-red (FR) light the plant receives. A R:FR reduction is caused by the selective absorption of blue (B) and R by the chlorophyll and carotenoid pigments of neighboring vegetation. This alteration to the light

environment signals to the plant an imminent competitive threat. In response, elongation growth is enhanced at the expense of lateral meristem development (both ears and tillers), leaf angle increases and root development is impaired (Maddonni et al., 2002; Fellner et al., 2003). Prolonged exposure to canopy shade accelerates flowering and decreases seed set. Importantly, SAS responses are observable in modern maize fields, suggesting that several SAS-related traits represent attractive targets for further improvement of both grain and biomass yields (Dubois and Brutnell, 2009). While it is believed that most SAS responses are detrimental to grain yield per plant (Smith, 1982), others like increased hyponasty and the azimuthal orientation of leaf blades are likely beneficial. Together, they increase light penetration and limit physical interactions between adjacent plants (Maddonni et al., 2002). Thus, understanding the costs and benefits of SAS to crop yield is important when considering breeding programs that aim to increase planting densities even further.

In a dense stand of mixed vegetation competing for limited resources, the SAS contributes to adaptive plasticity and competitive fitness (Schmitt et al., 2003). But for a densely planted crop such as maize, the benefit of reallocating resources to compete with genetically identical neighbors are limited (Smith, 1994). If most SAS responses favor survival over prolificacy, some of the remnant plasticity present in modern hybrids appears to be paramount to sustain current yields.

Few attempts have been made to characterize the genetic basis of plant response to density in mature field-grown maize. The central role of light penetration in a dense stand of maize plants was demonstrated using the *liguleless2* mutant (Brink, 1933). The gene encodes a basic helix-loop-helix protein involved in the establishment of the ligule located at the junction between the sheath and blade of the leaf (Walsh et al., 1998). Without a proper ligule, the mutant plant is characterized by an upright leaf

stature (Neuffer et al., 1997). Leaf hyponasty such as the one caused by *liguleless2* increases sunlit leaf area per unit of land area, decreases leaf photon flux density and the radiation use efficiency increases. It also lowers leaf temperature and increases water use efficiency (Lambers et al., 2008).

A comparative analysis using isogenic hybrids with or without the *liguleless2* mutation showed that upright leaf orientation increased grain yield by 40% at a plant density of 59 300 plants ha^{-1} (Pendleton et al., 1968). Another study used hybrid lines created using the *liguleless1* and *liguleless2* mutants that were planted at densities of 60 000, 75 000 and 90 000 plants ha^{-1}. Each mutation was introgressed into four different inbred backgrounds and five hybrid combinations were derived from them. At the two highest densities, the *liguleless2* hybrids had significantly higher grain yield than the wild-type isogenic hybrids with conventional leaf morphology (Lambert and Johnson, 1978). These studies validate both hyponasty as a significant contributor to yield and the use of contrasting planting densities in characterizing light-related developmental responses in maize.

The genetic regulation of maize response to planting density was explored using a population of 186 B73 x Mo17 recombinant inbred lines (RIL) planted at densities of 50 000 and 100 000 plants ha^{-1} (Gonzalo et al., 2009). A total of six traits were measured: plant height, anthesis-silking interval, days to anthesis, barrenness, ear per plant, and yield per ear. The density treatment was significant for all traits except yield per plant. Increasing density significantly increased anthesis-silking interval, barrenness, and plant height. Days to anthesis also increased at higher density, perhaps due to limited availability of resources. It reduces both ears per plant and yield per plant. Quantitative trait loci (QTL) were identified for all traits measured, where some were recurrently identified at both densities while others were specific to one planting density.

The development of more precise mapping populations such as the Intermated B73 x Mo17 (IBM) (Lee et al., 2002) and the Nested Association Mapping (NAM) population (McMullen et al., 2009) have greatly increased the resolution of QTL and should help identify genes underlying density response in maize. Another mapping population that should prove to be valuable is a collection of B73 x teosinte near isogenic lines (NIL) recently developed by Dr. Flint-Garcia at the University of Missouri. In this mapping population, each NIL carries one or a few chromosomal segments of the maize wild ancestor teosinte (*Zea mays* ssp. *parviglumis*) introgressed into the B73 maize genome (Doebley et al., 2006). The population is made of 642 BC4S2 NILs (backcrossed four times into B73, followed by two generations of selfing) and was characterized with SNP markers to define the introgressed teosinte chromosomal segment(s). An Illumina Golden Gate assay of 768 SNP markers was developed to genotype each line (see Chapter 2 for a more detailed description on how the population was created). A minimum tiling path consisting of 41 teosinte x B73 NILs covering the whole teosinte genome was assembled and used for the dual purpose of evaluating the feasibility of density mapping in a field nursery and to survey a subset of the population for its developmental responses at high density. To complement this density survey, the maize inbred lines B73, Mo17, W22 and the *phyB1 phyB2* mutant series were also examined.

5.2 Results and Discussion

Experiments were performed during the 2009 growth season in Aurora (NY). Each row had a length of 418 cm (14 feet) and the distance between each row was 76 cm (2.5 feet). Maize lines were planted at a low density of 10 kernels per row and at a high density of 40 kernels per row. Rows to be grown at a same density were grouped together and two border rows of B73 inbred were planted at the same density at each end. Assuming 100% germination rate, 10 kernels per row correspond to 31 369 plants ha^{-1} while 40 kernels per rows correspond to 125 500 plants ha^{-1}. At low density, the germination rate was on average 69%, thus the actual density was of 21 500 plants ha^{-1}. Rows planted at high density had an average germination rate of 73%, making a density of approximately 92 200 plants ha^{-1}. The minimum tiling path of the teosinte x B73 NIL collection was also planted at these two densities. This subset of the population was assembled by Dr. Flint-Garcia and is composed of 41 lines. Taken together, these 41 lines allow a complete coverage of the teosinte genome in a minimal number of lines. Each NIL was planted in a single replicate at each density. Also included in the density pilot experiment were the maize inbreds B73, Mo17 and W22, planted in eight replicate rows at each density. The *phyB1 phyB2* mutant series, introgressed four times into the W22 background was also planted in four rows for each planting density (Chapter Two, Section 2.5.2)

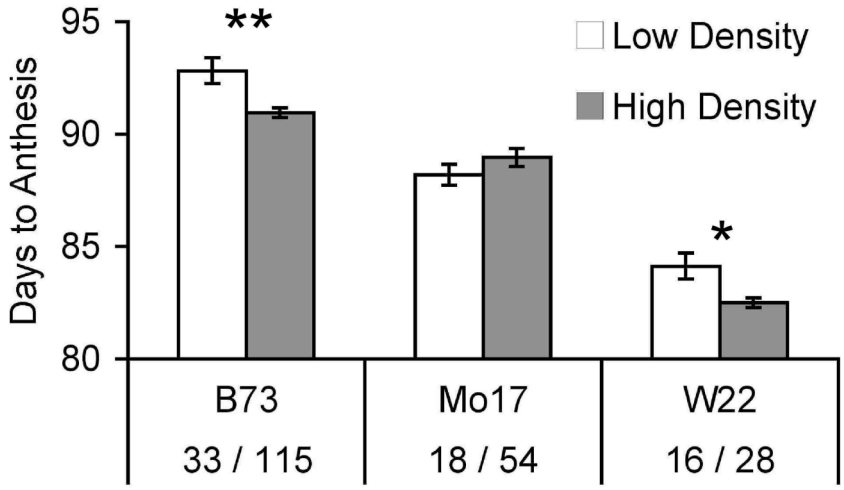

Figure 5.1 Days to anthesis was measured for three maize inbreds: B73, Mo17, and W22. The values are representative of the mean ± SE. The number of plants measured for low and high planting density respectively are shown below each inbred. Asterisks indicate Student's *t* test significance between the two planting densities for each inbred line (* $P < 0.05$, ** $P < 0.01$). SE, standard error.

Figure 5.2 A, Days to anthesis were measured for each teosinte x B73 NIL, and the B73 inbred. The values are representative of the mean ± standard error. B, Scatter plot of days to anthesis for each teosinte x B73 NIL. The red dot represents the B73 inbred. C, The hastening of days to anthesis caused by high density planting was calculated for each line by subtracting the low-density anthesis date from the high-density date. The distribution of the hastening of anthesis date ranges from 0 to 8 days.

A

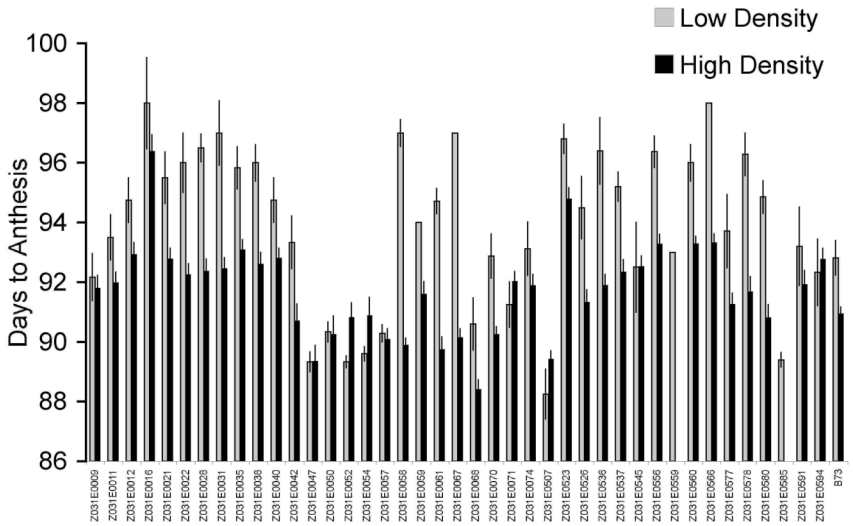
Low Density
High Density
Days to Anthesis
100
98
96
94
92
90
88
86

B

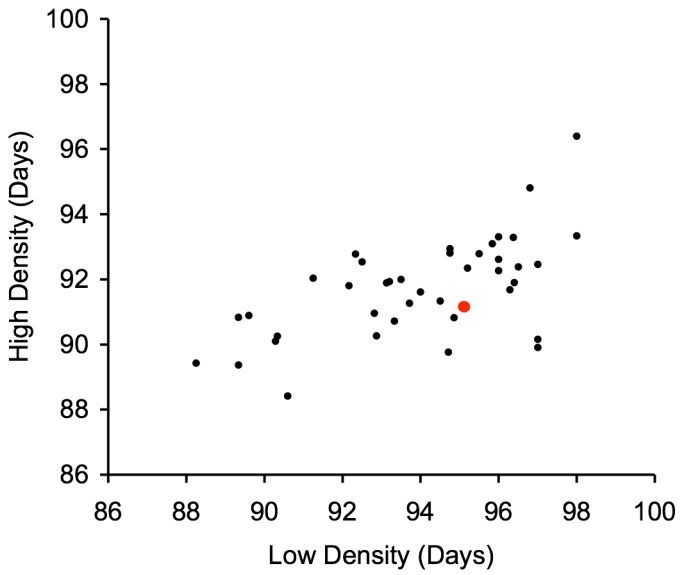
High Density (Days)
Low Density (Days)
100
98
96
94
92
90
88
86
86
88
90
92
94
96
98
100

C

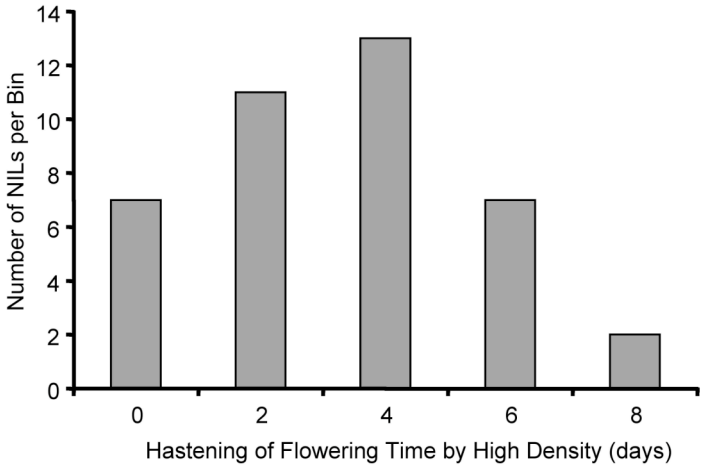
Number of NILs per Bin
Hastening of Flowering Time by High Density (days)
14
12
10
8
6
4
2
0
0
2
4
6
8

Days to anthesis are defined as the interval between the planting date and the date where approximately half of the male flowers located on the main tassel branch shed pollen. Results for the three inbred lines are presented in Figure 5.1. Both B73 and W22 show a significant reduction in the anthesis time at high density. The Mo17 inbred appears to be non-responsive to the treatment, suggesting that anthesis time in Mo17 is less sensitive to planting density than B73 and W22. Results for the 41 lines of the teosinte x B73 minimum tiling path are presented in Figure 5.2A. A wide range of responses can be observed among the 41 NIL. Some lines, such as Z031E0507, flowered between 89 and 90 days and was not responsive to the density treatment. The line Z031E0016 was one on the last ones to flower at 98 days and was also non-responsive to density. Most lines were responsive to density such as line Z031E0058, which flowered at high density 8 days earlier than at low density. The B73 controls planted across the NIL was also responsive to density and its response is somewhat intermediate among the different NIL.

A flowering time interval was calculated for each line and is defined as the difference in flowering date between low-density and high-density plantings. The distribution of these intervals is presented in Figure 5.2B. Flowering time responses to density ranged from non-responsive to up to eight days difference. The distribution is symmetrical and unimodal suggesting that it should be possible to map this trait in a larger set of NILs. Taken together, these results clearly demonstrate that genetic variation from teosinte contributes to flowering time variation under low- and high-density plantings. However, a better way to insure a precise density (and likely to increase heritability of the response) would be to plant at high density and then thin seedlings to the desired number. Thus, rows should be planted at approximately 40% higher density, and then thinned at an early seedling stage as not to interfere with later development. Mapping populations such as the complete set of teosinte x B73 NIL or

the IBM population can feasibly be planted at two densities and phenotyped. The thinning would need to be performed as soon as feasibly possible in order to avoid early SAS responses triggered by neighboring seedlings. For the same reason, a strict control of weeds would also need to be in place.

Non-random azimuthal distribution of the leaves across rows improves light interception at high density (Maddonni et al., 2001; Maddonni et al., 2002). This trait, which has never been measured in a mapping population or in a genetically diverse panel, was evaluated at the 16 leaf developmental stage. At this stage in development, plants are relatively short and thus it is easy to perform a visual scoring of the leaf orientation within a row by looking perpendicularly above it. The 41 lines of the minimum tiling path and three inbreds were visually evaluated for this trait using a visual rating scale. Lines were rated as 1) randomly oriented, 2) intermediate, or 3) perpendicular to the row. Among the three inbred lines evaluated, W22 had a strong perpendicular orientation, followed by B73, then Mo17. The *phyB1 phyB2* double mutant (introgressed four times into W22) lacks azimuthal orientation, while both *phyB1* and *phyB2* single mutants showed an intermediate orientation. These results strongly suggest that the trait is under the control of the phytochromes, with both *PhyB1* and *PhyB2* acting as primary receptors. Maddonni and colleagues (2002) have demonstrated, by using far-red (FR) filters, that maize plants re-orient their leaf blades away from FR by through unequal growth at internodes resulting in twisting of the leaf blades. This mechanism allows the plants to populate the inter-row space with blade tissue thus increasing leaf area index. Examples of azimuthal distribution at low and high densities are presented in Figure 5.3.

A

B

Figure 5.3 A, Example of two teosinte x B73 NILs at the 16 leaf stage and planted at 10 kernels per row (low density). In both rows, no leaf blade orientation is apparent (Z031E0507 and Z031E0523). B, Example of two teosinte x B73 NIL at the 16 leaf stage and planted at 40 kernels per row (high density). The top row shows a high level of blade orientation, where they are oriented perpendicular to the row (Z031E0067). The NIL planted in the bottom row has its leaf blades oriented randomly (Z031E0068).

This survey of the azimuthal orientation of a mapping population subset demonstrates that the trait is measurable and it is under genetic control. At a density close to 40 kernels per row, it should be feasible to map this trait in an appropriate population. The W22 inbred was identified as having a perpendicular orientation

versus the row while the *phyB1 phyB2* mutant had a random orientation, and both *phyB1* and *phyB2* single mutant had an intermediate orientation. These preliminary data strongly suggest that *PhyB1* and *PhyB2* act additively in the of control leaf azimuthal orientation.

Days to anthesis were measured for the *phyB1 phyB2* mutant series and a significant difference was only observed for the *phyB1 phyB2* double mutant (Fig. 5.4). This result was surprising as the double mutant was expected to display a

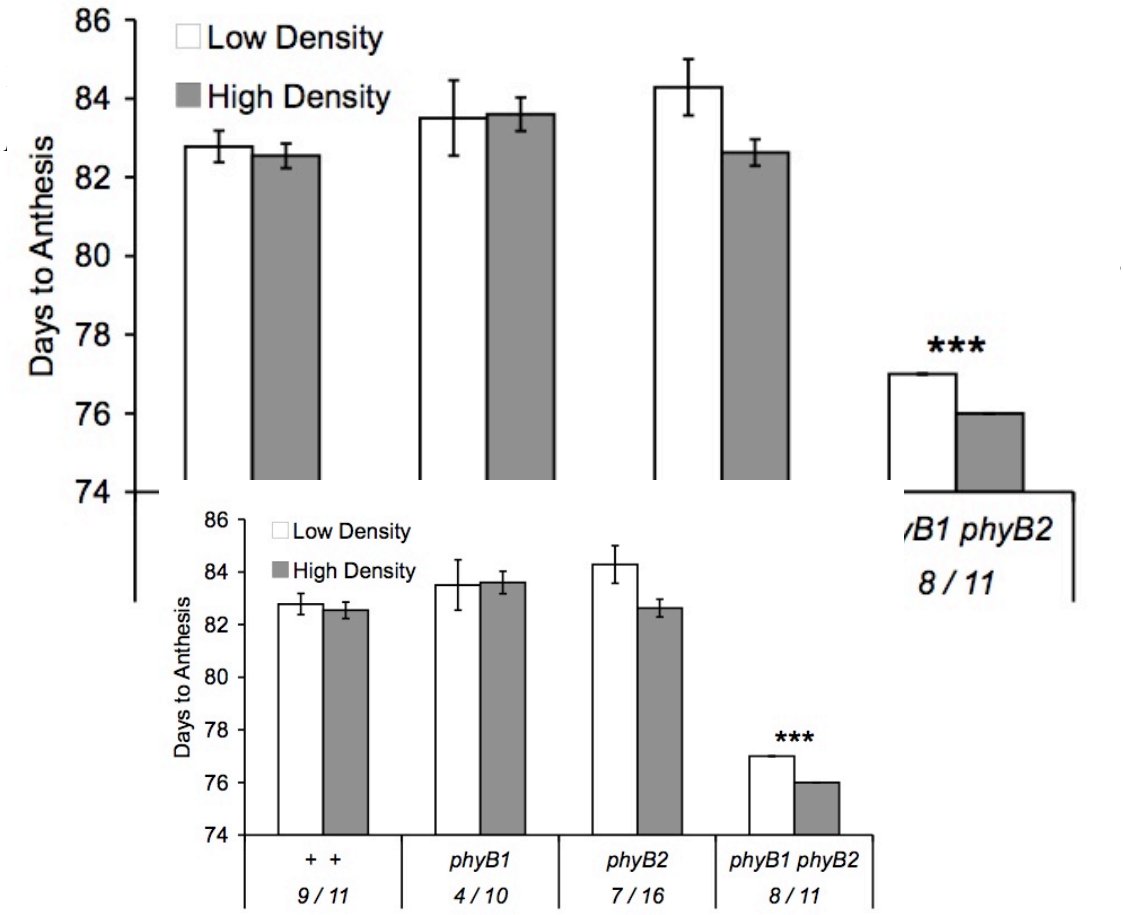

Figure 5.4. Days to anthesis was measured on *phyB1 phyB2* mutant series, introgressed four times into the W22 inbred background. The values are representative of the mean ± SE. Below each inbred is indicated the number of plants measured for low and high planting density respectively. Asterisks indicate Student's *t* test significance between the two densities for each line (*** $P < 0.001$). SE, standard error.

5.3 Material and Methods

The 41 teosinte x B73 NIL minimum tiling path stocks include: B73, Mo17, W22, Z031E0009, Z031E0011, Z031E0012, Z031E0016, Z031E0021, Z031E0022, Z031E0028, Z031E0031, Z031E0035, Z031E0038, Z031E0040, Z031E0042, Z031E0047, Z031E0050, Z031E0052, Z031E0054, Z031E0057, Z031E0058, Z031E0059, Z031E0061, Z031E0067, Z031E0068, Z031E0070, Z031E0071, Z031E0074, Z031E0507, Z031E0523, Z031E0526, Z031E0536, Z031E0537, Z031E0545, Z031E0556, Z031E0560, Z031E0566, Z031E0577, Z031E0578, Z031E0580, Z031E0585, Z031E0591, and Z031E0594.

RERERENCES

Brink RA (1933) Heritable characters in maize. XLVI. Liguleless-2. J Hered **24:** 325-326

Doebley JF, Gaut BS, Smith BD (2006) The molecular genetics of crop domestication. Cell **127:** 1309-1321

Dubois PG, Brutnell TP (2009) Light signal transduction networks in maize. *In* S Hake, JL Bennetzen, eds, Handbook of Maize. Its Biology, Vol 1. Springer, New York, pp 205-228

East EM (1909) Inbreeding in corn, 1907. Connecticut Agric Exp Stn Rep**:** 419-428

Fellner M, Horton LA, Cocke AE, Stephens NR, Ford ED, Van Volkenburgh E (2003) Light interacts with auxin during leaf elongation and leaf angle development in young corn seedlings. Planta **216:** 366-376

Gonzalo M, Holland JB, Vyn TJ, McIntyre LM (2009) Direct mapping of density response in a population of B73 x Mo17 recombinant inbred lines of maize (*Zea mays* L.). Heredity

Jones DF (1918) The effects of inbreeding and cross breeding upon development. Connecticut Agric Exp Stn Bull**:** 5-100

Lambers H, Chapin FS, Pons TL (2008) Plant physiological ecology, 2nd edition. Springer, New York

Lambert RJ, Johnson RR (1978) Leaf angle, tassel morphology, and the performance of maize hybrids. Crop Sci **18:** 499-502

Lee EA, Tollenaar M (2007) Physiological basis of successful breeding strategies for maize grain yield. Crop Sci **47(S3):** S202-S215

Lee M, Sharopova N, Beavis WD, Grant D, Katt M, Blair D, Hallauer A (2002) Expanding the genetic map of maize with the intermated B73 x Mo17 (IBM) population. Plant Mol Biol **48:** 453-461

Maddonni GA, Otegui ME, Andrieu B, Chelle M, Casal JJ (2002) Maize leaves turn away from neighbors. Plant Physiol **130:** 1181-1189

Maddonni GA, Otegui ME, Andrieu B, Chelle M, Casal JJ (2002) Maize leaves turn away from neighbors. Plant Physiol **130:** 1181-1189

Maddonni GA, Otegui ME, Cirilo AG (2001) Plant population density, row spacing and hybrid effects on maize canopy architecture and light attenuation. Field Crops Res **71:** 181-193

McMullen MD, Kresovich S, Villeda HS, Bradbury P, Li H, Sun Q, Flint-Garcia S, Thornsberry J, Acharya C, Bottoms C, Brown P, Browne C, Eller M, Guill K, Harjes C, Kroon D, Lepak N, Mitchell SE, Peterson B, Pressoir G, Romero S, Oropeza Rosas M, Salvo S, Yates H, Hanson M, Jones E, Smith S, Glaubitz JC, Goodman M, Ware D, Holland JB, Buckler ES (2009) Genetic properties of the maize nested association mapping population. Science **325:** 737-740

Neuffer MG, Coe EH, Wessler SR (1997) Mutants of maize. Cold Spring Harbor Laboratory Press, Cold Spring Harbor, NY, USA.

Pendleton JW, Smith GE, Winter SR, Johnson TJ (1968) Field investigations of the relationships of leaf angle in corn (*Zea mays* L.) to grain yield and apparent photosynthesis. Agron J **60:** 422-424

Schmitt J, Stinchcombe JR, Heschel MS, Huber H (2003) The adaptive evolution of plasticity:phytochrome-mediated shade avoidance responses. Integr Comp Biol **43:** 459-469

Shull GH (1908) The composition of a field of maize. Am. Breed. Assoc. **4:** 296-301

Smith H (1982) Light quality, photoperception and plant strategy. Annu Rev Plant Physiol **33:** 481-518

Smith H (1994) Phytochrome transgenics: functional, ecological and biotechnological applications. Semin Cell Biol **5:** 315-325

Troyer AF (2006) Adaptedness and heterosis in corn and mule hybrids. Crop Sci **46:** 528-543

Troyer AF, Resenbrook RW (1983) Utility of higher plant densities for corn performance testing. Crop Sci **23:** 863-867

Walsh J, Waters CA, Freeling M (1998) The maize gene liguleless2 encodes a basic leucine zipper protein involved in the establishment of the leaf blade-sheath boundary. Genes Dev **12:** 208-218

CHAPTER SIX

IDENTIFICATION OF PHYTOCHROME MUTANTS BY TILLING AND TRANSPOSON MUTAGENESIS

Abstract

Thus far, only *phyB1* and *phyB2* mutants have been characterized in maize (*Zea mays* ssp. *mays*). To identify additional mutants in phy family members (*PhyA1*, *PhyA2*, *PhyC1* and *PhyC2*), and also to identify new allelic mutants of *PhyB1* and *PhyB2* a reverse genetics approach was taken. The identification and characterization of a *Mutator* transposon insertion in *PhyA1* was undertaken and a series of EMS-induced mutations were identified through TILLING screenings. The *phyA1*::*Mu*4912 allele was introgressed into both B73 (one time) and W22 (five times) inbreds. Both a *phyA1 phyA2* and a *phyC1 phyC2* mutant series were generated and phenotypically characterized at maturity in a field nursery and under monochromatic light at the seedling stage. In *Arabidopsis thaliana*, phyA is the phytochrome that mediates responses to continuous far-red (FRc) light. In the absence of phyA, seedlings are etiolated under FRc. Unexpectedly, the *phyA1 phyA2* double mutant of maize failed to show an etiolated phenotype under FRc despite carrying a *Mutator* insertion at the *PhyA1* locus and an amino acid substitution predicted to be deleterious at the *PhyA2* locus. The *phyC1 phyC2* mutant series also failed to display any striking phenotypes, both at maturity and at seedling growth stages. These results are discussed in the context of phytochrome gene duplication and hetorodimer formation.

6.1 Introduction

In Arabidopsis (*Arabidopsis thaliana*), the availability of mutants was paramount to the elucidation of phytochrome function. Mutants were identified for each of the five phytochrome gene members: PhyA (Nagatani et al., 1993; Whitelam et al., 1993; Reed et al., 1994), PhyB (Somers et al., 1991), PhyC (Franklin et al., 2003), PhyD (Aukerman et al., 1997), and PhyE (Devlin et al., 1998). Single, double and higher order permutations of mutant alleles further defined functional redundancies and revealed the complex interplay between the phytochrome family members (Franklin et al., 2003). Recently, the assembly of a null quintuple *phy* mutant allowed the characterization of a plant developing in the absence of any phytochrome signal transduction (Strasser et al., 2010). Only capable of germinating in the *flowering locus T* mutant background, the *phy* null mutant allowed the demonstration that a photoreceptor other than the phytochrome mediates chlorophyll production in plants. It also showed that the cryptochrome photoreceptors operate independently of the phytochromes in mediating blue light signals. Phytochrome mutants have also been identified and characterized in other crops such as tomato (*Lycopersicon esculentum*) (Weller et al., 2000), rice (*Oryza sativa*) (Takano et al., 2005), pea (*Pisum sativum*) (Dalmais et al., 2008; Hofer et al., 2009) and maize (Sawers et al., 2002; Sawers et al., 2004; Sheehan et al., 2004) revealing conserved and novel functions associated with the diversification of the *Phy* gene family.

In order to perform a similar characterization of the phytochrome in maize (*Zea mays* ssp. *mays*), different strategies were employed to identify mutants for each member of its gene family. Grasses such as rice and sorghum contain only three phytochromes (*PhyA*, *PhyB*, and *PhyC*), but in maize, an ancient allopolyploidization event expanded the phytochrome members to six: *PhyA1, PhyA2, PhyB1, PhyB2,*

PhyC1, and *PhyC2* (Sheehan et al., 2004). To date, only two loss-of-function mutants have been identified in maize, *phyuB1* and *phyB2* (Sheehan et al., 2007). A *Mutator* (*Mu*) insertion was identified at the *PhyB1* locus (*phyB1*::*Mu*563) while a naturally occuring deletion in *PhyB2* was identified in the France 2 inbred background. A second *Mu* insertion has since been identified (*phyB2*::*Mu*12058) and the details of its characterization are presented in Chapter Two, Section 2.2.4 and Chapter Three, Section 3.2. The identification of mutant alleles for the remaining members *PhyA1, PhyA2, PhyC1* and *PhyC2* was pursued using two strategies. One was to complete the characterization of a third *Mu* insertion, for which a preliminary characterization attributed its insertion at one of the two *PhyA* paralogs. A second approach focused on the mining of a TILLING (Targeting Induced Local Lesions IN Genomes) mutant population developed at Purdue University by Dr. Cliff Weil (Till et al., 2004).

TILLING is a targeted screen of mutagenized population for mutations in genes of interest (McCallum et al., 2000). Point mutations are chemically induced by a mutagen such as ethylmethane sulfonate (EMS): a carcinogenic compound causing G to A transition mutations. The rate of mutation across the genome is a function of both the concentration and time of exposure to the reagent. Once created, the mutagenized population is indexed and pools are generated through sib-mating of M_2 (second generation of selfing a mutagenized plant) lines. Two different inbreds were used in the creation of TILLING population, the stiff stalk B73 and the non-stiff stalk W22. DNA pooled from the M_2 plants are screened using a PCR assay for a gene of interest. The amplification is followed by the denaturation and re-annealing of the amplified fragments. If a mutation is present within the amplified region, a single-stand "bubble" will be formed during the re-annealing process of heteroduplex DNA molecules. These mismatches can then be cleaved by the endonuclease *CEL*I and resolved on an acrylamide gel. Pools are then deconvoluted and individual mutant lines identified.

This approach, first developed in Arabidopsis (Colbert et al., 2001) has since been implemented in other plant species (Weil, 2009) including maize (Till et al., 2004), wheat (Slade et al., 2005), rice (Till et al., 2007), soybean (Cooper et al., 2008), and tomato (Minoia et al., 2010).

6.2 Results and Discussions

A *Mu* insertion at *PhyA* (*phyA*::*Mu*4912) was identified in screens of the Cold Spring Harbor MTM collection (May et al., 2003) by M. Sheehan and T. Brutnell (unpublished). Using both paralog-specific and *Mu*-specific primers, the 1.4 kb transposon insertion (Bennetzen, 1984) was confirmed to be in the GAF domain of *PhyA1* (see section 6.3 Material and Methods for the genotyping details). Thus far, the *phyA1*::*Mu*4912 allele was introgressed five times in the W22 background and one time into the B73 background (see Appendix One).

To identify mutants in the TILLING pipeline, primer sequences were designed and tested for each gene target. Genomic sequences for all six phytochrome gene members (Sheehan et al., 2004) were first screened using the CODDLe (Codon Optimized to Discover Deleterious Lesions) software which identifies regions of the peptide that are conserved across homologous protein from different genes and species (http://www.proweb.org/coddle/). Primers specific to each of the six phytochromes family members were validated for their paralog specificity by sequencing (results not shown) and submitted to Purdue University TILLING Service for screening. The PARSESNP (http://genome.purdue.edu/maizetilling/) application describes the potential effect of the mutation on a protein through a SIFT (Sorting Intolerant From Tolerant) score attributed to each substitution. Mutations with a SIFT score smaller than 0.05 are considered damaging to the protein. TILLING mutations identified for

the different phytochrome family members are summarized in Figure 6.1. The location of each mutation inside the phytochrome apoprotein and the peptide sequence comparison with other plant species are presented in Figure 6.2 for the two PHYA paralogs, Figure 6.3 for PHYB2, and Figure 6.4 for the two PHYC paralogs.

Table 6.1 Maize TILLING phytochrome mutants identified.

Mutants	Line Number	Inbred Background	Amino Acid Substitution	SIFT Score	Apoprotein Domain
phyA1	NW2160	B73	P66S	0.00	PHY
	PW1729	W22	G369D	0.00	GAF
	PW1145	W22	G456E	0.11	PHY
phyA2	PW1721	W22	E468K	0.01	PHY
	PW1067	W22	P499L	0.06	PHY
phyB2	3845	W22	G366R	0.01	GAF
	07534	W22	W398*	Stop Codon	GAF
phyC1	NW1036	B73	H370Y	0.00	GAF
	NW210	B73	R544K	NA	PHY
	PW1766	W22	M622I	0.03	PAS 1
	3916	W22	T653I	0.01	PAS 1
phyC2	PW900	W22	T431I	0.01	PHY
	PW11	W22	W645*	Stop Codon	PAS 1
	NW795	B73	E690K	0.02	PAS junction
	PW104	W22	Q738*	Stop Codon	PAS junction
	076-C7	B73	T746I1	0.5	PAS junction
	4711	W22	W778*	Stop Codon	PAS 2

Figure 6.1 Alignment of *PhyA* peptide sequences from maize (*Zm*PhyA1 and *Zm*PhyA2), sorghum (*Sb*PHYA), rice (*Os*PHYA), and Arabidopsis (*At*PHYA) and position of TILLING mutations. The red lettering denotes the GAF domain of the phytochrome apoprotein. The yellow lettering denotes the PHY domain. Olive green lettering highlighted in yellow is the chromophore attachment site. Green lettering denotes the two PAS domains. Purple lettering denotes the HIS-related kinase domain. Blue is a phytochrome-like ATPase domain. Red highlights are the TILLING mutations in PHYA1 or PHYA2.

```
ZmPhyA1  MSSLRPAQSSSSSSRTRQSSQARILAQTTLDAELNAEYEESGDSFDYSKLVEAQRSTPPEQQGRSGKVIA-YLQHIQRGK
ZmPhyA2  MSSSRPAHSSSSSSRTRQSSRARILAQTTLDAELNAEYEESGDSFDYSKLVEAQRSTPPEQQGRSGKVIA-YLQHIQRGK
SbPHYA   MSSSRPAHSSSSSSRTRQSSQARILAQTTLDAELNAEYEESGDSFDYSKLVEAQRSTPSEQQGRSGKVIA-YLQHIQRGK
OsPHYA   MSSSRPTQCSSSSSRTRQSSRARILAQTTLDAELNAEYEEYGDSFDYSKLVEAQRTTGPEQQARSEKVIA-YLHHIQRAK
AtPHYA   MSGSRPTQSSEGSRRSRHS--ARIIAQTTVDAKLHADFEESGSSFDYSTSVRVTGPVVENQPPRSDKVTTTYLHHIQKGK

ZmPhyA1  LIQPFGCLLALDEKSFRVIAFSENAPEMLTTVSHAVPNVDDPPKLGIGTNVRSLFTDPGATALQKALGFADVSLLNPILV
ZmPhyA2  LIQPFGCLLALDEKSFRVIAFSENAPEMLTTVSHAVPNVDDPPKLGIGTNVRSLFTDPGATALQKALGFADVSLLNPILV
SbPHYA   LIQPFGCLLALDEKSFRVIAFSENAPEMLTTVSHAVPNVDDPPKLGIGTNVRSLFTDPGATALQKALGFADVSLLNPILV
OsPHYA   LIQPFGCLLALDEKTFNVIALSENAPEMLTTVSHAVPSVDDPPKLRIGTNVWSLFTDPGATALQKALGFADVSLLNPILV
AtPHYA   LIQPFGCLLALDEKTFKVIAYSENASELLTMASHAVPSVGEHPVLGIGTDIRSLFTAPSASALQKALGFGDVSLLNPILV

ZmPhyA1  QCKTSGKPFYAIVHRATGCLVVDFEPVKPTEFPATAAGALQSYKLAAKAISKIQSLPGGSMQALCNTVVKEVFDLTGYDR
ZmPhyA2  QCKTSGKPFYAIVHRATGCLVVDFEPVKPTEFPATAAGALQSYKLAAKAISKIQSLPGGSMEALCNTVVKEVFDLTGYDR
SbPHYA   QCKTSGKPFYAIVHRATGCLVVDFEPVKPTEFPATAAGALQSYKLAAKAISKIQSLPGGSMEALCNTVVKEVFELTGYDR
OsPHYA   QCKTSGKPFYAIVHRATGCLVVDFEPVKPTEFPATAAGALQSYKLAAKAISKIQSLPGGSMEVLCNTVVKELFDLTGYDR
AtPHYA   HCRTSAKPFYAIIHRVTGSIIIDFEPVKPYEVPMTAAGALQSYKLAAKAITRLQSLPSGSMERLCDTMVQEVFELTGYDR

ZmPhyA1  VMAYKFHEDEHGEVFAEITKPGIEPYLGLHYPATDIPQAARFLFMKNKVRMICDCRARSVKIIEDEALSIDISLCGSTLR
ZmPhyA2  VMAYKFHEDEHGEVFAEITKPGIEPYIGLHYPATDIPQAARFLFMKNKVRMICDCRARSVKIIEDEALSIDISLCGSTLR
SbPHYA   VMAYKFHEDEHGEVFAEITKPGIEPYLGLHYPATDIPQAARFLFMKNKVRMICDCRAKSVKIIEDEALSIDISLCGSTLR
OsPHYA   VMAYKFHEDDHGEVFAEITKPGLEPYLGLHYPATDIPQAARFLFMKNKVRMICDCRARSIKIIEDESLHLDISLCGSTLR
AtPHYA   VMAYKFHEDDHGEVVSEVTKPGLEPYLGLHYPATDIPQAARFLFMKNKVRMIVDCNAKHARVLQDEKLSFDLTLCGSTLR
                                                      PW1729
                                                      (G369D)
ZmPhyA1  APHSCHLQYMENMNSIASLVMAVVVNENEDDDEPESEQPPQQQKRKKLWGLIVCHHESPRYVPFPLRYACEFLAQVFAVH
ZmPhyA2  APHSCHLKYMENMNSIASLVMAVVVNENEEDDEPEPEQPPQQQKKRLWGLIVCHHESPRYVPFPLRYACEFLAQVFAVH
SbPHYA   APHSCHLQYMENMNSIASLVMAVVVNENEEDDEPGPEQPPQQQKKRLWGLIVCHHESPRYVPFPLRYACEFLAQVFAVH
OsPHYA   APHSCHLQYMENMNSIASLVMAVVVNENEDDDEVGADQPAQQQKRKKLWGLLVCHHESPRYVPFPLRYACEFLAQVFAVH
AtPHYA   APHSCHLQYMANMDSIASLVMAVVVNEEDGEGDA-PDATTQPQKRKRLWGLVVCHNTTPRFVPFPLRYACEFLAQVFAIH
                                                      PW1145  NW2160 PW1067
                                                      (G456E)(P466S)(E468K)
ZmPhyA1  VNKEFELEKQIREKSILRMQTMLSDMLFKESSPLSIVSGSPNIMDLVKCDGAALLYGDKVWRLQTAPTESQIRDIAFWLS
ZmPhyA2  VNKEFELEKQIREKNILRMQTMLSDMLFKESSPLSIVSGSPNIMDLVKCDGAALLYGDKVWRLQTAPTPSQIRDIAFWLS
SbPHYA   VNKEFELEKQIREKSILRMQTMLSDMLFKEASPLSIVSGSPNIMDLVKCDGAALLYGDKVWRLQTAPTESQIRDIAFWLS
OsPHYA   VNKEFELERQVREKSILRMQTMLSDMLLRESSPLSIVSGTPNIMDLVKCDGAALLYGGKVWRLQNAPTESQIRDIAFWLS
AtPHYA   VNKEVELDNQMVEKNILRTQTLLCDMLMRDA-PLGIVSQSPNIMDLVKCDGAALLYKDKIWKLGTTPSEFHLQEIASWLC
                        PW1721
                        (P499L)
ZmPhyA1  EVHGDSTGLSTDSLQDAGYPGAASLGDMICGMAVAKITSKDILFWFRSHTAAEIKWGGAKHDPSDEDDSRRMHPRLSFKA
ZmPhyA2  EVHGDSTGLSTDSLQDAGYPGAASLGDMICGMAVAKITSKDILFWFRSHTAAEIKWGGAKHDPSDKDDNRRMHPRLSFKA
SbPHYA   EVHGDSTGLSTDSLQDAGYPGAASLGDMICGMAVAKITSKDILFWFRSHTAAEIKWGGAKHDPSDKDDNRRMHPRLSFKA
OsPHYA   DVHRDSTGLSTDSLHDAGYPGAAALGDMICGMAVAKINSKDILFWFRSHTAAEIRWGGAKHDPSDKDDSRRMHPRLSFKA
AtPHYA   EYHMDSTGLSTDSLHDAGFPRALSLGDSVCGMAAVRISSKDMIFWFRSHTAGEVRWGGAKHDPDDRDDARRMHPRSSFKA

ZmPhyA1  FLEVVKMKSLPWSDYEMDAIHSLQLILRGTLNDA-LKPAQSSGLDNQIGDLKLDGLAELQAVTSEMVRLMETATVPILAV
ZmPhyA2  FLEVVKTKSLPWSDYEMDAIHSLQLILRGTLNDA-SKPAQASGLDNQIGDLKLDGLAELQAVTSEMVRLMETATVPILAV
SbPHYA   FLEVVKMKSLPWSDYEMDAIHSLQLILRGTLNDA-LKPVQASGLDNQIGDLKLDGLAELQAVTSEMVRLMETATVPILAV
OsPHYA   FLEVVKMKSLPWNDYEMDAIHSLQLILRGTLNDD-IKPTRAASLDNQVGDLKLDGLAELQAVTSEMVRLMETATVPILAV
AtPHYA   FLEVVKTRSLPWKDYEMDAIHSLQLILRNAFKDSETTDVNTKVIYSKLNDLKIDGIQELEAVTSEMVRLIETATVPILAV

ZmPhyA1  DGNGLVNGWNQKVADLSGLRVDEAIGRHILTLVEDSSVPIVQRMLYLALQGREEKEVRFELKTHGSKRDDGPVILVVNAC
ZmPhyA2  DGNGLVNGWNQKVAELSGLRVDEAIGRHILTLVEDSSVSLVQRMLYLALQGREEKEVRFELKTHGSKRDDGPVILVVNAC
SbPHYA   DGNGLVNGWNQKVAELSGLRVDEAIGRHILTLVEDSSVSIVQRMLYLALQGKEEKEVRFELKTHGSKRDDGPVILVVNAC
OsPHYA   DSNGLVNGWNQKVAELTGLRVDEAIGRHILTVVEESSVPVVQRMLYLALQGKEEKEVKFEVKTHGSKRDDGPVILVVNAC
AtPHYA   DSDGLVNGWNTKIAELTGLSVDEAIGKHFLTLVEDSSVEIVKRMLENALEGTEEQNVQFEIKTHLSRADAGPISLVVNAC

ZmPhyA1  ASRDMHDHVVGVCFVAQDMTVHKLVMDKFTRVEGDYRAIIHNPNPLIPPIFGADQFGWCSEWNAAMTKLTGWHRDEVIDR
ZmPhyA2  ASRDLHDHVVGVCFVAQDMTVHKLVMDKFTRVEGDYKAIIHNPNPLIPPIFGADQFGWCSEWNAAMTKLTGWHRDEVVDK
SbPHYA   ASRDLHDHVVGVCFVAQDMTVHKLVMDKFTRVEGDYKAIIHNPNPLIPPIFGADQFGWCSEWNVAMTKLTGWHRDEVIDK
OsPHYA   ASRDLHDHVVGVCFVAQDMTVHKLVMDKFTRVEGDYKAIIHNPSPLIPPIFGADEFGWCSEWNAAMTKLTGWHRDEVINK
AtPHYA   ASRDLHENVVGVCFVAHDLTGQKTVMDKFTRIEGDYKAIIQNPNPLIPPIFGTDEFGWCTEWNPAMSKLTGLKREEVIDK

ZmPhyA1  MLLGEVFDSSNASCLLKSKDAFVRLCIIINSALAGEEAEKAPIGFFDRDGKYIECLLSVNRKVNADGVVTGVFCFIHVPS
ZmPhyA2  MLLGEVFNSSNASCLLKSKDAFVRLCIVINSALAGEEAEKASFGFFDRNEKYVECLLSVNRKVNADGVVTGVFCFIHVPS
SbPHYA   MLLGEVFDSSNASCLLKSKDDFVRLCIIINSALAGEEAENAPFGLFDRNGKYIECLLSVNRKVNADGVVTGVFCFIHVPS
OsPHYA   MLLGEVFDSTNASCLVKNKDAFVSLCILINSALAGDETEKAPFSFFDRNGKYIECLLSVNRKVNADGVITGVFCFIQVPS
AtPHYA   MLLGEVFGTQKSCCRLKNQEAFVNLGIVLNNAVTSQDPDKVSFAFFTRGGKYVECLLCVSKKLDRKGVVTGVFCFLQLAS

ZmPhyA1  DDLQHALHVQQASEQTALRRLKAFSYMRHAIDKPLSGMLYSRETLKGTDLDEEQMRQVRVADNCHRQLNKILADLDQDNI
ZmPhyA2  DDLQHALHVQQASEQTAQRKLKAFSYMRHAINKPLSGMLYSRETLKSTGLNEEQMRQVRVGDNCHRQLNKILADLDQDNI
SbPHYA   DDLQHALHVQQASEQTAQRRLKAFSYMRHAINKPLSGMLYSRETLKSTGLNEEQMRQVHVADSCHRQLNKILADLDQDNI
OsPHYA   HELQHALHVQQASQQNALTKLKAYSYMRHAINNPLSGMLYSRKALKNTGLNEEQMKEVNVADSCHRQLNKILSDLDQDSV
AtPHYA   HELQQALHVQRLAERTAVKRLKALAYIKRQIRNPLSGIMFTRKMIEGTELGPEQRRILQTSALCQKQLSKILDDSDLESI
```

Figure 6.1 (Continued)

```
ZmPhyA1  TDKSSCLDLDMAEFVLQDVVVSAVSQVLIGCQGKGIRVACNLPERSMKQKVYGDGIRLQQILSDFLFVSVKFSPAGGSVD
ZmPhyA2  TDKSSCLDLDMAEFVLQDVVVSAVSQVLIGCQAKGIRVACNLPERSMKQKVYGDGIRLQQIVSDFLFVSVKFSPAGGSVD
SbPHYA   TDKSSCLDLDMAEFVLEDVVVSAVSQVLIGCQGKGIRVACNLPERFMKQKVYGDGIRLQQILSDFLFVSVKFSPVGGSVD
OsPHYA   MNKSSCLDLEMVEFVLQDVFVAAVSQVLITCQGKGIRVSCNLPERYMKQTVYGDGVRLQQILSDFLFVSVKFSPVGGSVE
AtPHYA   IE--GCLDLEMKEFTLNEVLTASTSQVMMKSNGKSVRITNETGEEVMSDTLYGDSIRLQQVLADFMLMAVNFTPSGGQLT

ZmPhyA1  ISSKLTKNSIGENLHLIDFELRIKHQGAGVPAEILSQMYGEDNREQSEEGLSLLVSRNLLRLMNGDIRHLREAGMSTFIL
ZmPhyA2  ISSKLTKNSIGENLHLIDFELRIKHRGAGVPAEILSQMYEEDNKEQSEEGFSLAVSRNLLRLMNGDIRHLREAGMSTFIL
SbPHYA   ISSKLTKNSIGENLHLIDFELRIKHQGAGVPAEILSQMYEEDNKEPSEEGLSLLVSRNLLRLMNGNIRHIREAGMSTFIL
OsPHYA   ISCSLTKNSIGENLHLIDLELRIKHQGKGVPADLLSQMYEDDNKEQSDEGMSLAVSRNLLRLMNGDVRHMREAGMSTFIL
AtPHYA   VSASLRKDQLGRSVHLANLEIRLTHTGAGIPEFLLNQMFGTEE-DVSEEGLSLMVSRKLVKLMNGDVQYLRQAGKSSFII

ZmPhyA1  TAELAAAPSAAGH
ZmPhyA2  TAELAAAPSAVGR
SbPHYA   TAELAAAPSAVGQ
OsPHYA   SVELASAPA---K
AtPHYA   TAELAAA----NK
```

Figure 6.2 Alignment of PHYB peptide sequences from maize (*Zm*PhyB1 and *Zm*PhyB2), sorghum (*Sb*PHYB), rice (*Os*PHYB), and Arabidopsis (*At*PHYB) and position of TILLING mutations. Color-coding for Figure 6.2 is similar to the one described in Figure 6.1.

```
ZmPhyB1   MASGSRAT-PTRSPSSARPEAPRHAHHHHH--SQSSGGSTSRAGGG---------------AAATESVSKAVAQYTLDARLHAVFEQSGA
ZmPhyB2   MASDSRP--PKRSPS-ARRVAPRHAHHHHS---QSSGGSTSRAGAGGGGGG----------AAATESVSKAVAQYNLDARLHAVFEQSGA
SbPHYB    MASGSRAT-PTRSPSSARPEAPRHAHHHHHHHSQSSGGSTSRAGGGGGGGGGGGTAATATATATESVSKAVAQYTLDARLHAVFEQSGA
OsPHYB    MASGSRAT-PTRSPSSARPAAPRHQHHHSQ----SSGGSTSRAGGGGGGGGGGGG-----AAAAESVSKAVAQYTLDARLHAVFEQSGA
AtPHYB    MVSGVGGSGGGRGGGRGGEEEPSSSHTPNN----RRGGEQAQSSGTKSLRP----------RSNTESMSKAIQQYTVDARLHAVFEQSGE

ZmPhyB1   SGRSFDYSQSLRAPPT--PSSEQQIAAYLSRIQRGGHIQPFGCTLAVADDSSFRLLAFSENSPDLLDLSPHHSVPSLDSSAPP-HVSLGA
ZmPhyB2   SGRSFDYSQSLRAPPT--PSSEQQIAAYLSRIQRGGHIQPLGCTLAVADDSSFRLLAFSENAADLLDLSPHHSVPSLDSVALP-PVSLGA
SbPHYB    SGRSFDYSQSLRAPPT--PSSEQQIAAYLSRIQRGGHIQPFGCTLAVADDSSFRLLAFSENAADLLDLSPHHSVPSLDSAAPP-PVSLGA
OsPHYB    SGRSFDYTQSLRASPT--PSSEQQIAAYLSRIQRGGHIQPFGCTLAVADDSSFRLLAYSENTADLLDLSPHHSVPSLDSSAVPPPVSLGA
AtPHYB    SGKSFDYSQSLKTTTYGSSVPEQQITAYLSRIQRGGYIQPFGCMIAVDE-SSFRIIGYSENAREMLGIMP-QSVPTLE---KPEILAMGT

ZmPhyB1   DARLLFSPSSAVLLERAFAAREISLLNPIWIHSRVSSKPFYAILHRIDVGVVIDLEPARTEDPALSIAGAVQSQKLAVRAISRLQALPGG
ZmPhyB2   DARLYFSPSSAVLLERAFAAREISLLNPLWIHSRASSKPFYAILHRIDVGVVIDLEPARTEDPALSIAGAVQSQKLAVRAISRLQALPGG
SbPHYB    DARLLFSPSSAVLLERAFAAREISLLNPLWIHSRVSSKPFYAILHRIDVGVVIDLEPARTEDPALSIAGAVQSQKLAVRAISRLQALPGG
OsPHYB    DARLLFAPSSAVLLERAFAAREISLLNPLWIHSRVSSKPFYAILHRIDVGVVIDLEPARTEDPALSIAGAVQSQKLAVRAISRLQALPGG
AtPHYB    DVRSLFTSSSSILLERAFVAREITLLNPVWIHSKNTGKPFYAILHRIDVGVVIDLEPARTEDPALSIAGAVQSQKLAVRAISQLQALPGG

ZmPhyB1   DVKLLCDTVVEHVRELTGYDRVMVYRFHEDEHGEVVAESRRDNLEPYLGLHYPATDIPQASRFLFRQNRVRMIADCHATPVRVIQDPGLS
ZmPhyB2   DVKLLCDTVVEHVRELTGYDRVMVYKFHEDEHGEVVAESRRDNLEPYLGLHYPATDIPQASRFLFQQNRVRMIADCHAIPVRVIQDPGLS
SbPHYB    DIKLLCDTVVEHVRELTGYDRVMVYRFHEDEHGEVVAESRRDNLEPYLGLHYPATDIPQASRFLFRQNRVRMIADCHATPVRVIQDPGMS
OsPHYB    DVKLLCDTVVEYVRELTGYDRVMVYRFHEDEHGEVVAESRRNNLEPYIGLHYPATDIPQASRFLFRQNRVRMIADCHAAPVRVIQDPALT
AtPHYB    DIKLLCDTVVESVRDLTGYDRVMVYKFHEDEHGEVVAESKRDDLEPYIGLHYPATDIPQASRFLFKQNRVRMIVDCNATPVLVVQDDRLT
                                 3845                        07534
                                (G366R)                      (W398*)
ZmPhyB1   QPLCLVGSTLRAPHGCHAQYMANMGSIASLVMAVIISSGGDDEQTGRGGISSAMKLWGLVVCHHTSPRCIPFPLRYACEFLMQAFGLQL
ZmPhyB2   QQLCLVGSTLRAPHGCHAQYMANMGSIASLVMAVIISSGGDDERTGRGAISSSMKLWGLVVCHHTSPRCIPFPLRYACEFLMQAFGLQL
SbPHYB    QPLCLVGSTLRAPHGCHAQYMANMGSIASLVMAVIISSGGDDEQTGRGGISSAMKLWGLVVCHHTSPRCIPFPLRYACEFLMQAFGLQL
OsPHYB    QPLCLVGSTLRSPHGCHAQYMANMGSIASLVMAVIISSGGDDDHISRGSIPSAMKLWGLVVCHHTSPRCIPFPLRYACEFLMQAFGLQL
AtPHYB    QSMCLVGSTLRAPHGCHSQYMANMGSIASLAMAVIIN-GNEDDGSNVASGRSSMRLWGLVVCHHTSSRCIPFPLRYACEFLMQAFGLQL
NtPHYB    QPLCLVGSTLRAPHGCHAQYMANMGSIASLTLAVIIN-GNDEE--AVG-GRSSMRLWGLVVGHHTSARCIPFPLRYACEFLMQAFGLQL

ZmPhyB1   NMELQLAHQLSEKHILRTQTLLCDMLLRDSPTGIVTQSPSIMDLVKCDGAALYYHGKYYPLGVTPTESQIKDIIEWLTVFHGDSTGLSTD
ZmPhyB2   NMELQLAHQLSEKHILRTQTLLCDMLLRDSPAGIITQSPSVMDLVKCDGAALYYRGKYYPLGVTPTESQIKDIIEWLTVCHGDSTGLSTD
SbPHYB    NMELQLAHQLSEKHILRTQTLLCDMLLRDSPTGIVTQSPSIMDLVKCDGAALYYHGKYYPLGVTPTESQIKDIIEWLTVCHGDSTGLSTD
OsPHYB    NMELQLAHQLSEKHILRTQTLLCDMLLRDSPTGIVTQSPSIMDLVKCDGAALYYHGKYYPLGVTPTEVQIKDIIEWLTMCHGDSTGLSTD
AtPHYB    NMELQLALQMSEKRVLRTQTLLCDMLLRDSPAGIVTQSPSIMDLVKCDGAAFLYHGKYYPLGVAPSEVQIKDVVEWLLANHADSTGLSTD

ZmPhyB1   SLADAGYLGAAALGEAVCGMAVAYITPSDYLFWFRSHTAKEIKWGGAKHHPEDKDDGQRMHPRSSFKAFLEVVKSRSLPWENAEMDAIHS
ZmPhyB2   SLADAGYLGAVALGDAVCGMAVAYITPSDYLFWFRSHTAKEIKWGGAKHHPEDKDDGQRMHPRSSFKAFLEVVKSRSLSWENAEMDAIHS
SbPHYB    SLADAGYLGAAALGDAVCGMAVAYITPSDYLFWFRSHTAKEIKWGGAKHHPEDKDDGQRMHPRSSFKAFLEVVKSRSLPWENAEMDAIHS
OsPHYB    SLADAGYPGAAALGDAVSGMAVAYITPSDYLFWFRSHTAKEIKWGGAKHHPEDKDDGQRMHPRSSFKAFLEVVKSRSLPWENAEMDAIHS
AtPHYB    SLGDAGYPGAAALGDAVCGMAVAYITKRDFLFWFRSHTAKEIKWGGAKHHPEDKDDGQRMHPRSSFQAFLEVVKSRSQPWETAEMDAIHS

ZmPhyB1   LQLILRDSFRDAAEGTNNSKAIVNGQVQ--LRELELRGINELSSVAREMVRLIETATVPIFAVDTDGCINGWNAKIAELTGLSVEEAMGK
ZmPhyB2   LQLILRDSFRDAAEGTSNSKAIVNGQRQ--LGELELRGINELSSVAREMVRLIETATVPIFAVDTDGCINGWNAKIAELTGLSVEEAMGK
SbPHYB    LQLILRDSFRDAAEGTSNSKAIVNGQVQ--LGELELRGINELSSVAREMVRLIETATVPIFAVDTDGCINGWNAKIAELTGLSVEEAMGK
OsPHYB    LQLILRDSFRDSAEGTSNSKAIVNGQVQ--LGELELRGIDELSSVAREMVRLIETATVPIFAVDTDGCINGWNAKVAELTGLSVEEAMGK
AtPHYB    LQLILRDSFKESEAAMN--SKVVDGVVQPCRDMAGEQGIDELGAVAREMVRLIETATVPIFAVDAGGCINGWNAKIAELTGLSVEEAMGK

ZmPhyB1   SLVNDLIFKESEATVEKLLSRALRGEEDKNVEIKLKTFGSEQSKGPIFVVVNACSSRDYTQNIVGVCFVGQDVTGQKVVMDKFVNIQGDY
ZmPhyB2   SLVNDLIFKECDDIVEKLLSRALRGEEDKNVEIKLKTFGSEQSKGAIFVIVNACSSRDYTQNIVGVCFVGQDVTGQKVVMDKFINIQGDY
SbPHYB    SLVNDLIFKESEEIVEKLLSRALRGEEDKNVEIKLKTFGSEQSNGAIFVIVNACSSRDYTQNIVGVCFVGQDVTGQKVVMDKFINIQGDY
OsPHYB    SLVNDLIFKESEETVNKLLSRALRGDEDKNVEIKLKTFGPEQSKGPIFVIVNACSSRDYTKNIVGVCFVGQDVTGQKVVMDKFINIQGDY
AtPHYB    SLVSDLIYKENEATVNKLLSRALRGDEEKNVEVKLKTFSPELQGKAVFVVVNACSSKDYLNNIVGVCFVGQDVTSQKIVMDKFINIQGDY

ZmPhyB1   KAIVHNPNPLIPPIFASDENTSCSEWNTAMEKLTGWSRGEVVGKFLIGEVFGNCCRLKGPDALTKFMVIIHNAIGGQDYEKFPFSFFDKN
ZmPhyB2   KAIVHNPNPLLPPIFASDENTSCSEWNTAMEKLTGWSREEVVGKFLIGEVFGNCCRLKGPDALTKFMVVIHNAIEGHDSEKFPFSFFDKN
SbPHYB    KAIVHNPNPLIPPIFASDENTSCSEWNTAMEKLTGWSRGEVVGKFLIGEVFGSFCRLKGPDALTKFMVVIHNAIGGQDYEKFPFSFFDKN
OsPHYB    KAIVHNPNPLIPPIFASDENTCCSEWNTAMEKLTGWSRGEVVGKLLVGEVFGNCCRLKGPDALTKFMIVLHNAIGGQDCEKFPFSFFDKN
AtPHYB    KAIVHSPNPLIPPIFAADENTCCLEWNMAMEKLTGWSRSEVIGKMIVGEVFGSCCMLKGPDALTKFMIVLHNAIGGQDTDKFPFPFFDRN

ZmPhyB1   GKYVQALLTANTRSKMDGKSIGAFCFLQIASTEIQQAFEIQRQQEKKCYARMKELAYICQEIKNPLSGIRFTNSLLQMTDLNDDQRQFLE
ZmPhyB2   GKYVQALLTANTRSKMDGKSIGAFCFLQIASAEIQQAFEIQRQQEKKCYARMKELAYICQEIKNPLSGIRFTNSLLQMTDLNDDQRQFLE
SbPHYB    GKYVQALLTANTRSKMDGKSIGAFCFLQIASAEIQQAFEIQRQQEKKCYARMKELAYICQEIKNPLSGIRFTNSLLQMTDLNDDQRQFLE
OsPHYB    GKYVQALLTANTRSRMDGEAIGAFCFLQIASPELQQAFEIQRHHEKKCYARMKELAYIYQEIKNPLNGIRFTNSLLEMTDLKDDQRQFLE
AtPHYB    GKFVQALLTANKRVSLEGKVIGAFCFLQIPSPELQQALAVQRRQDTECFTKAKELAYICQVIKNPLSGMRFANSLLEATDLNEDQKQLLE

ZmPhyB1   TSSACEKQMSKIVKDASLQSIEDGSLVLEQSEFSLGDVMNAVVSQAMLLLRERDLQLIRDIPDEIKDASAYGDQCRIQQVLADFLLSMVR
ZmPhyB2   TSSACEKQMSKIVKDASLKSIEDGSLVLEKSEFSLGDVMNAVVSQTMSLLRERDLQLIRDIPDEIKDASAYGDQFRIQQVLADFLLSMAQ
SbPHYB    TCSACEEQMSKIVKDATLQSIEDGSLVLEKSEFSFGDVMNAVVSQAMLLLRERDLQLIRDIPDEIKDASAYGDQFRIQQVLADFLLSMVR
OsPHYB    TSTACEKQMSKIVKDASLQSIEDGSLVLEKGEFSLGSVMNAVVSQVMIQLRERDLQLIRDIPDEIKEASAYGDQYRIQQVLCDFLLSMVR
AtPHYB    TSVSCEKQISRIVGDMDLESIEDGSFVLKREEFFLGSVINAIVSQAMFLLRDRGLQLIRDIPEEIKSIEVFGDQIRIQQLLAEFLLSIIR
```

Figure 6.2 (Continued)

```
ZmPhyB1  SAPSENGWVEIQVRPNVKQNSDGTNTELFIFRFACPGEGLPADVVQDMFSNSQWSTQEGVGLSTCRKILKLMGGEVQYIRESERSFFLIV
ZmPhyB2  SAPSENGWVEIQVRPNVKQNYDGTDTELFIFRFACPGEGLPADIVQDMFSNSQWSTQEGVGLSTCRKILKLMGGEVQYIRESERSFFLIV
SbPHYB   SAPSENGWVEIQVRPNVKQNSDGTDTELFIFRFTYPGEGLPADIVQDMFSNSQWSTQEGVGLSTCRKILKLMGGEVQYIRESERSFFLIV
OsPHYB   FAPAENGWVEIQVRPNIKQNSDGTDTMLFLFRFACPGEGLPPEIVQDMFSNSRWTTQEGIGLSICRKILKLMGGEVQYIRESERSFFHIV
AtPHYB   YAPSQE-WVEIHLSQLSKQMADGFAAIRTEFRMACPGEGLPPELVRDMFHSSRWTSPEGLGLSVCRKILKLMNGEVQYIRESERSYFLII

ZmPhyB1  LEQPQPRPAAGREIV
ZmPhyB2  LELPQPRLAAGRENQLIC
SbPHYB   LELPQPRPAADREIS
OsPHYB   LELPQPQQAASRGTS
AtPHYB   LELPVPRKRPLSTASGSGDMMLMMPY
```

Figure 6.3 Alignment of PHYC peptide sequences from maize (*Zm*PhyC1 and *Zm*PhyC2), sorghum (*Sb*PHYC), rice (*Os*PHYC), and Arabidopsis (*At*PHYC) and position of TILLING mutations. Color-coding for Figure 6.3 is similar to the one described in Figure 6.1.

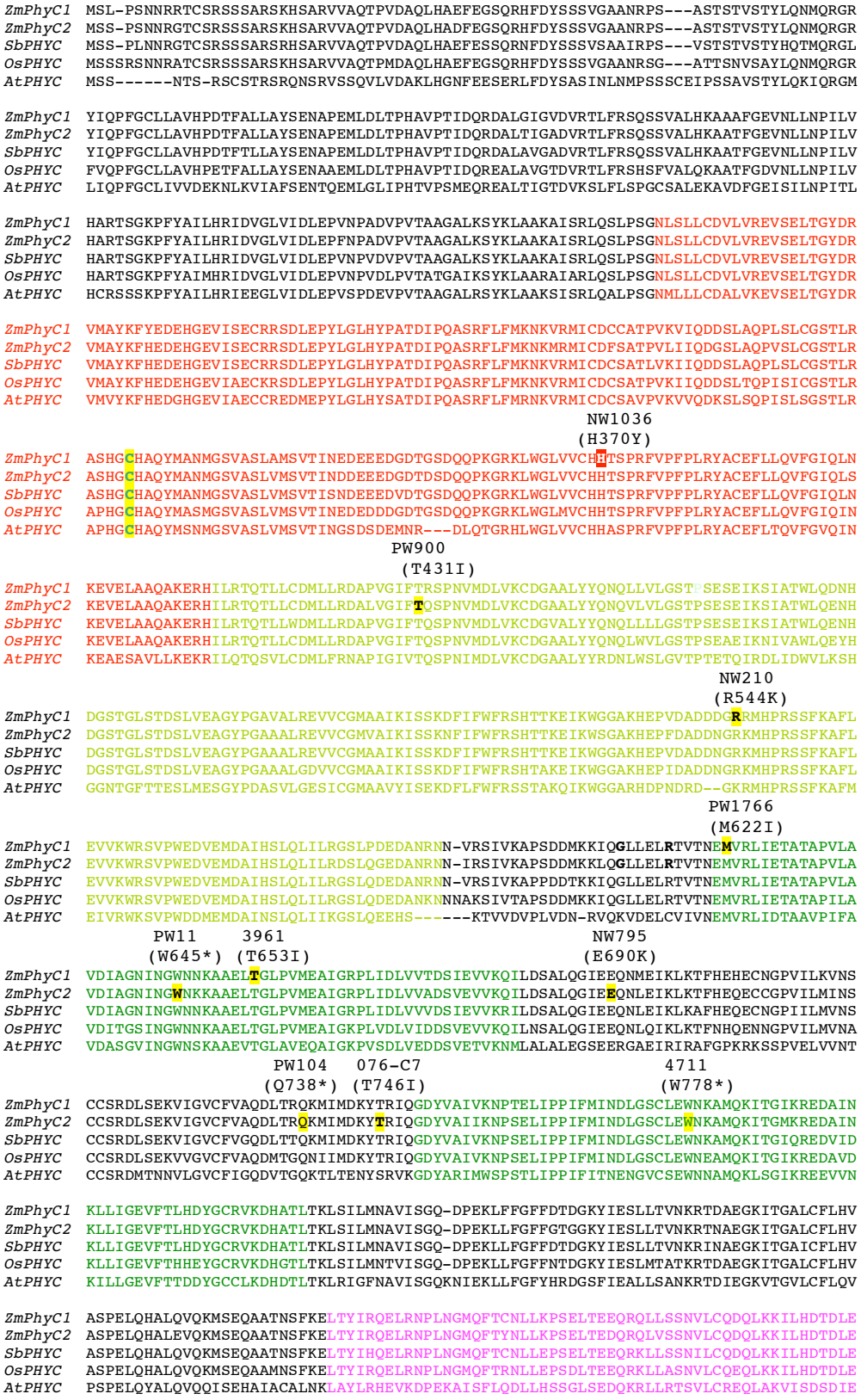
ZmPhyC1 MSL-PSNNRRTCSRSSSARSKHSARVVAQTPVDAQLHAEFEGSQRHFDYSSSVGAANRPS---ASTSTVSTYLQNMQRGR
ZmPhyC2 MSS-PSNNRGTCSRSSSARSKHSARVVAQTPVDAQLHADFEGSQRHFDYSSSVGAANRPS---ASTSTVSTYLQNMQRGR
SbPHYC MSS-PLNNRGTCSRSSSARSRHSARVVAQTPVDAQLHAEFESSQRNFDYSSSVSAAIRPS---VSTSTVSTYHQTMQRGL
OsPHYC MSSSRSNNRATCSRSSSARSKHSARVVAQTPMDAQLHAEFEGSQRHFDYSSSVGAANRSG---ATTSNVSAYLQNMQRGR
AtPHYC MSS------NTS-RSCSTRSRQNSRVSSQVLVDAKLHGNFEESERLFDYSASINLNMPSSSCEIPSSAVSTYLQKIQRGM
ZmPhyC1 YIQPFGCLLAVHPDTFALLAYSENAPEMLDLTPHAVPTIDQRDALGIGVDVRTLFRSQSSVALHKAAAFGEVNLLNPILV
ZmPhyC2 YIQPFGCLLAVHPDTFALLAYSENAPEMLDLTPHAVPTIDQRDALTIGADVRTLFRSQSSVALHKAATFGEVNLLNPILV
SbPHYC YIQPFGCLLAVHPDTFTLLAYSENAPEMLDLTPHAVPTIDQRDALAVGADVRTLFRSQSSVALHKAATFGEVNLLNPILV
OsPHYC FVQPFGCLLAVHPETFALLAYSENAAEMLDLTPHAVPTIDQREALAVGTDVRTLFRSHSFVALQKAATFGDVNLLNPILV
AtPHYC LIQPFGCLIVVDEKNLKVIAFSENTQEMLGLIPHTVPSMEQREALTIGTDVKSLFLSPGCSALEKAVDFGEISILNPITL
ZmPhyC1 HARTSGKPFYAILHRIDVGLVIDLEPVNPADVPVTAAGALKSYKLAAKAISRLQSLPSGNLSLLCDVLVREVSELTGYDR
ZmPhyC2 HARTSGKPFYAILHRIDVGLVIDLEPFNPADVPVTAAGALKSYKLAAKAISRLQSLPSGNLSLLCDVLVREVSELTGYDR
SbPHYC HARTSGKPFYAILHRIDVGLVIDLEPVNPVDVPVTAAGALKSYKLAAKAISRLQSLPSGNLSLLCDVLVREVSELTGYDR
OsPHYC HARTSGKPFYAIMHRIDVGLVIDLEPVNPVDLPVTATGAIKSYKLAARAIARLQSLPSGNLSLLCDVLVREVSELTGYDR
AtPHYC HCRSSSKPFYAILHRIEEGLVIDLEPVSPDEVPVTAAGALRSYKLAAKSISRLQALPSGNMLLLCDALVKEVSELTGYDR
NW1036
(H370Y)
ZmPhyC1 VMAYKFYEDEHGEVISECRRSDLEPYLGLHYPATDIPQASRFLFMKNKVRMICDCCATPVKVIQDDSLAQPLSLCGSTLR
ZmPhyC2 VMAYKFHEDEHGEVISECRRSDLEPYLGLHYPATDIPQASRFLFMKNKMRMICDFSATPVLIIQDGSLAQPVSLCGSTLR
SbPHYC VMAYKFHEDEHGEVISECRRSDLEPYLGLHYPATDIPQASRFLFMKNKVRMICDCSATLVKIIQDDSLAQPLSLCGSTLR
OsPHYC VMAYKFHEDEHGEVIAECKRSDLEPYLGLHYPATDIPQASRFLFMKNKVRMICDCSATPVKIIQDDSLTQPISICGSTLR
AtPHYC VMVYKFHEDGHGEVIAECCREDMEPYLGLHYSATDIPQASRFLFMRNKVRMICDCSAVPVKVVQDKSLSQPISLSGSTLR
PW900
(T431I)
ZmPhyC1 KEVELAAQAKERHILRTQTLLCDMLLRDAPVGIFTRSPNVMDLVKCDGAALYYQNQLLVLGSTPSESEIKSIATWLQDNH
ZmPhyC2 KEVELAAQAKERHILRTQTLLCDMLLRDALVGIFTQSPNVMDLVKCDGAALYYQNQVLVLGSTPSESEIKSIATWLQENH
SbPHYC KEVELAAQAKERHILRTQTLLWDMLLRDAPVGIFTQSPNVMDLVKCDGVALYYQNQLLLLGSTPSESEIKSIATWLQENH
OsPHYC KEVELAAQAKERHILRTQTLLCDMLLRDAPVGIFTQSPNVMDLVKCDGAALYYQNQLWVLGSTPSEAEIKNIVAWLQEYH
AtPHYC KEAESAVLLKEKRILQTQSVLCDMLFRNAPIGIVTQSPNIMDLVKCDGAALYYRDNLWSLGVTPTETQIRDLIDWVLKSH
NW210
(R544K)
ZmPhyC1 DGSTGLSTDSLVEAGYPGAVALREVVCGMAAIKISSKDFIFWFRSHTTKEIKWGGAKHEPVDADDDGRRMHPRSSFKAFL
ZmPhyC2 DGSTGLSTDSLVEAGYPGAAALREVVCGMVAIKISSKNFIFWFRSHTTKEIKWSGAKHEPFDADDNGRKMHPRSSFKAFL
SbPHYC DGSTGLSTDSLVEAGYPGAAALREVVCGMAAIKISSKDFIFWFRSHTTKEIKWGGAKHEPVDADDNGRKMHPRSSFKAFL
OsPHYC DGSTGLSTDSLVEAGYPGAAALGDVVCGMAAIKISSKDFIFWFRSHTAKEIKWGGAKHEPIDADDNGRKMHPRSSFKAFL
AtPHYC GGNTGFTTESLMESGYPDASVLGESICGMAAVYISEKDFLFWFRSSTAKQIKWGGARHDPNDRD--GKRMHPRSSFKAFM
PW1766
(M622I)
ZmPhyC1 EVVKWRSVPWEDVEMDAIHSLQLILRGSLPDEDANRNN-VRSIVKAPSDDMKKIQGLLELRTVTNEMVRLIETATAPVLA
ZmPhyC2 EVVKWRSVPWEDVEMDAIHSLQLILRDSLQGEDANRNN-IRSIVKAPSDDMKKLQGLLELRTVTNEMVRLIETATAPVLA
SbPHYC EVVKWRSVPWEDVEMDAIHSLQLILRGSLQDEDANRNN-VRSIVKAPPDDTKKIQGLLELRTVTNEMVRLIETATAPILA
OsPHYC EVVKWRSVPWEDVEMDAIHSLQLILRGSLQDEDANKNNNAKSIVTAPSDDMKKIQGLLELRTVTNEMVRLIETATAPILA
AtPHYC EIVRWKSVPWDDMEMDAINSLQLIIKGSLQEEHS------KTVVDVPLVDN-RVQKVDELCVIVNEMVRLIDTAAVPIFA
PW11 3961 NW795
(W645*) (T653I) (E690K)
ZmPhyC1 VDIAGNINGWNNKAAELTGLPVMEAIGRPLIDLVVTDSIEVVKQILDSALQGIEEQNMEIKLKTFHEHECNGPVILKVNS
ZmPhyC2 VDIAGNINGWNKKAAELTGLPVMEAIGRPLIDLVVADSVEVVKQILDSALQGIEEQNLEIKLKTFHEQECCGPVILMINS
SbPHYC VDIAGNINGWNNKAAELTGLPVMEAIGRPLIDLVVVDSIEVVKRILDSALQGIEEQNLEIKLKAFHEQECNGPIILMVNS
OsPHYC VDITGSINGWNNKAAELTGLPVMEAIGKPLVDLVIDDSVEVVKQILNSALQGIEEQNLQIKLKTFNHQENNGPVILMVNA
AtPHYC VDASGVINGWNSKAAEVTGLAVEQAIGKPVSDLVEDDSVETVKNMLALALEGSEERGAEIRIRAFGPKRKSSPVELVVNT
PW104 076-C7 4711
(Q738*) (T746I) (W778*)
ZmPhyC1 CCSRDLSEKVIGVCFVAQDLTRQKMIMDKYTRIQGDYVAIVKNPTELIPPIFMINDLGSCLEWNKAMQKITGIKREDAIN
ZmPhyC2 CCSRDLSEKVIGVCFVAQDLTRQKMIMDKYTRIQGDYVAIIKNPSELIPPIFMINDLGSCLEWNKAMQKITGMKREDAIN
SbPHYC CCSRDLSEKVIGVCFVGQDLTTQKMIMDKYTRIQGDYVAIVKNPSELIPPIFMINDLGSCLEWNKAMQKITGIQREDVID
OsPHYC CCSRDLSEKVVGVCFVAQDMTGQNIIMDKYTRIQGDYVAIVKNPSELIPPIFMINDLGSCLEWNEAMQKITGIKREDAVD
AtPHYC CCSRDMTNNVLGVCFIGQDVTGQKTLTENYSRVKGDYARIMWSPSTLIPPIFITNENGVCSEWNNAMQKLSGIKREEVVN
ZmPhyC1 KLLIGEVFTLHDYGCRVKDHATLTKLSILMNAVISGQ-DPEKLFFGFFDTDGKYIESLLTVNKRTDAEGKITGALCFLHV
ZmPhyC2 KLLIGEVFTLHDYGCRVKDHATLTKLSILMNAVISGQ-DPEKLLFGFFGTGGKYIESLLTVNKRTNAEGKITGALCFLHV
SbPHYC KLLIGEVFTLHDYGCRVKDHATLTKLSILMNAVISGQ-DPEKLLFGFFDTDGKYIESLLTVNKRINAEGKITGAICFLHV
OsPHYC KLLIGEVFTHHEYGCRVKDHGTLTKLSILMNTVISGQ-DPEKLLFGFFNTDGKYIESLMTATKRTDAEGKITGALCFLHV
AtPHYC KILLGEVFTTDDYGCCLKDHDTLTKLRIGFNAVISGQKNIEKLLFGFYHRDGSFIEALLSANKRTDIEGKVTGVLCFLQV
ZmPhyC1 ASPELQHALQVQKMSEQAATNSFKELTYIRQELRNPLNGMQFTCNLLKPSELTEEQRQLLSSNVLCQDQLKKILHDTDLE
ZmPhyC2 ASPELQHALEVQKMSEQAATNSFKELTYIRQELRNPLNGMQFTYNLLKPSELTEDQRQLVSSNVLCQDQLKKILHDTDLE
SbPHYC ASPELQHALQVQKMSEQAATNSFKELTYIHQELRNPLNGMQFTCNLLEPSELTEEQRKLLSSNILCQDQLKKILHDTDLE
OsPHYC ASPELQHALQVQKMSEQAAMNSFKELTYIRQELRNPLNGMQFTRNLLEPSDLTEEQRKLLASNVLCQEQLKKILHDTDLE
AtPHYC PSPELQYALQVQQISEHAIACALNKLAYLRHEVKDPEKAISFLQDLLHSSGLSEDQKRLLRTSVLCREQLAKVISDSDIE

Figure 6.3 (Continued)

```
ZmPhyC1  SIEQCYMEMNTVEFNLEQALNTVLMQGIPLGKEKQISIERNWPVEVSCMYLYGDNLRLQQILADYLACALQFTQTAEGPI
ZmPhyC2  SIEQCYMETNTVEFNLEEALNTVLMQGIPLGKEKRISIERDWPVEVSHMYIYGDNIRLQQVLADYLACALQFTQPAEGHI
SbPHYC   SIEQCYMEMNTVEFNLEEALNTVLMQGIPLGKEKRISIERDWPVEISRMYLYGDNLRLQQVLADYLACALQFTQPAEGPI
OsPHYC   SIEQCYTEMSTVDFNLEEALNTVLMQAMPQSKEKQISIDRDWPAEVSCMHLCGDNLRLQQVLADFLACTLQFTQPAEGPI
AtPHYC   GIEEGYVELDCSEFGLQESLEAVVKQVMELSIERKVQISCDYPQEVSSMRLYGDNLRLQQILSETLLSSIRFTPALRGLC

ZmPhyC1  V-LQVMSKKENIGSGMQIAHLEFRIVHPAPGVPEALIQEMFQHN-PGVSREGLGLYISQKLVKTMS-GTVQYLREADTSS
ZmPhyC2  V-LQVIPKKENIGSGMQIAHLEFRIVHPAPGVPEALIQEMFQHN-PGVSREGLGLYISQKLVKTMS-GTLQYLREADTSS
SbPHYC   V-LQVIPKKENIGSGMQIAHLEFRIVHPAPGVPEALIQEMFRHN-PEVSREGLGLYICQKLVKTMS-GTVQYLREADTSS
OsPHYC   V-LQVIPRMENIGSGMQIAHLEFRLVHPAPGVPEALIQEMFRHS-PGASREGLGLYISQKLVKTMS-GTVQYLREAESSS
AtPHYC   VSFKVIARIEAIGKRMKRVELEFRIIHPAPGLPEDLVREMFQPLRKGTSREGLGLHITQKLVKLMERGTLRYLRESEMSA

ZmPhyC1  FIILMEFPVAQLSSKRSKPSTSKF
ZmPhyC2  FIILIEFPVAQLSSKRSKPSPSKF
SbPHYC   FIVLVEFPVAQLSTKRCKASTSKF
AtPHYC   FVILTEFPLI
```

Since confirmed *Mu* insertions were already available for *PhyA1*, *PhyB1* and *PhyB2*, putative TILLING mutants at these three loci (NW2160, PW1729, PW1145, 3845, and 07534, see Table 6.1) were not further characterized. The *phyA1*::*Mu*4912 allele was used to create a *phyA1 phyA2* mutant series. TILLING mutants PW1721 and PW1067, carrying mutations at the *PhyA2* locus, were both advanced to the field nursery for genotyping as they both had a low SIFT score and were from different inbred backgrounds (Table 6.1). Crosses between *phyA1*::*Mu*4912 and *phyA2*-PW1721 and between *phyA1*::*Mu*4912 and *phyA2*-PW1067 were made during the summer 2008. F_1 plants were selfed during the following winter nursery and F_2 families were planted in the summer of 2009 for genotyping and phenotyping. Homozygous F_2 individuals for the four classes of double mutants were selfed and F_3 were screened under monochromatic lights in growth chambers in fall of 2009. Only the *phyA1*::*Mu*4912 *phyA2*-PW1721 mutant series could be planted in sufficient number to allow a phenotypic characterization of mature plant traits in the field. The *phyA1*::*Mu*4912 *phyA2*-PW1067 mutant series was advanced one more generation without being phenotyped (Appendix One). Results from mature traits phenotyping analysis are summarized in Table 6.2 while results from seedlings grown under monochromatic lights in growth chambers are presented in Figure 6.4.

Table 6.2 Phenotypic measurements of the *phyA1::Mu*4912 *phyA2*-PW1721 mutant series [W22] at maturity. Tukey-Kramer test was set at $P = 0.05$.

Trait	Genotype	Number	Mean	Std.Err.	Tukey-Kramer
Leaf number	*phyA1 phyA2*	9	20.11	0.39	Non significant
	phyA1 PhyA2/(+)	42	20.00	0.17	
	PhyA1/(+) *phyA2*	43	19.74	0.19	
	PhyA1/(+) *PhyA2/*(+)	58	19.72	0.20	
Blade width (cm)	*phyA1 phyA2*	9	10.00	0.44	Non significant
	phyA1 PhyA2/(+)	42	10.86	0.15	
	PhyA1/(+) *phyA2*	41	10.46	0.14	
	PhyA1/(+) *PhyA2/*(+)	57	10.19	0.13	
Anthesis (days)	*phyA1 phyA2*	10	87.90	1.22	Non significant
	phyA1 PhyA2/(+)	53	86.36	0.36	
	PhyA1/(+) *phyA2*	52	85.83	0.42	
	PhyA1/(+) *PhyA2/*(+)	73	86.52	0.30	
Plant height (cm)	*phyA1 phyA2*	10	153.80	5.13	Non significant
	phyA1 PhyA2/(+)	53	161.96	1.85	
	PhyA1/(+) *phyA2*	52	154.48	2.37	
	PhyA1/(+) *PhyA2/*(+)	73	157.55	1.92	
Tassel length (cm)	*phyA1 phyA2*	10	30.50	1.09	Non significant
	phyA1 PhyA2/(+)	53	31.85	0.52	
	PhyA1/(+) *phyA2*	52	31.08	0.63	
	PhyA1/(+) *PhyA2/*(+)	72	31.65	0.46	
Sheath length (cm)	*phyA1 phyA2*	10	15.70	0.40	Non significant
	phyA1	12	16.58	0.26	
	phyA2	15	16.47	0.22	
	+ / +	24	15.92	0.23	
Internode length (cm)	*phyA1 phyA2*	10	13.10	0.38	Non significant
	phyA1	12	13.42	0.36	
	phyA2	15	13.87	0.39	
	+ / +	24	13.50	0.30	
Ear node height (cm)	*phyA1 phyA2*	10	61.20	4.93	Non significant
	phyA1	12	69.75	3.49	
	phyA2	15	65.20	3.02	
	+ / +	24	64.79	3.60	
Stem Diameter (cm)	*phyA1 phyA2*	10	2.28	0.11	Non significant
	phyA1	12	2.27	0.08	
	phyA2	15	2.21	0.08	
	+ / +	24	2.23	0.07	

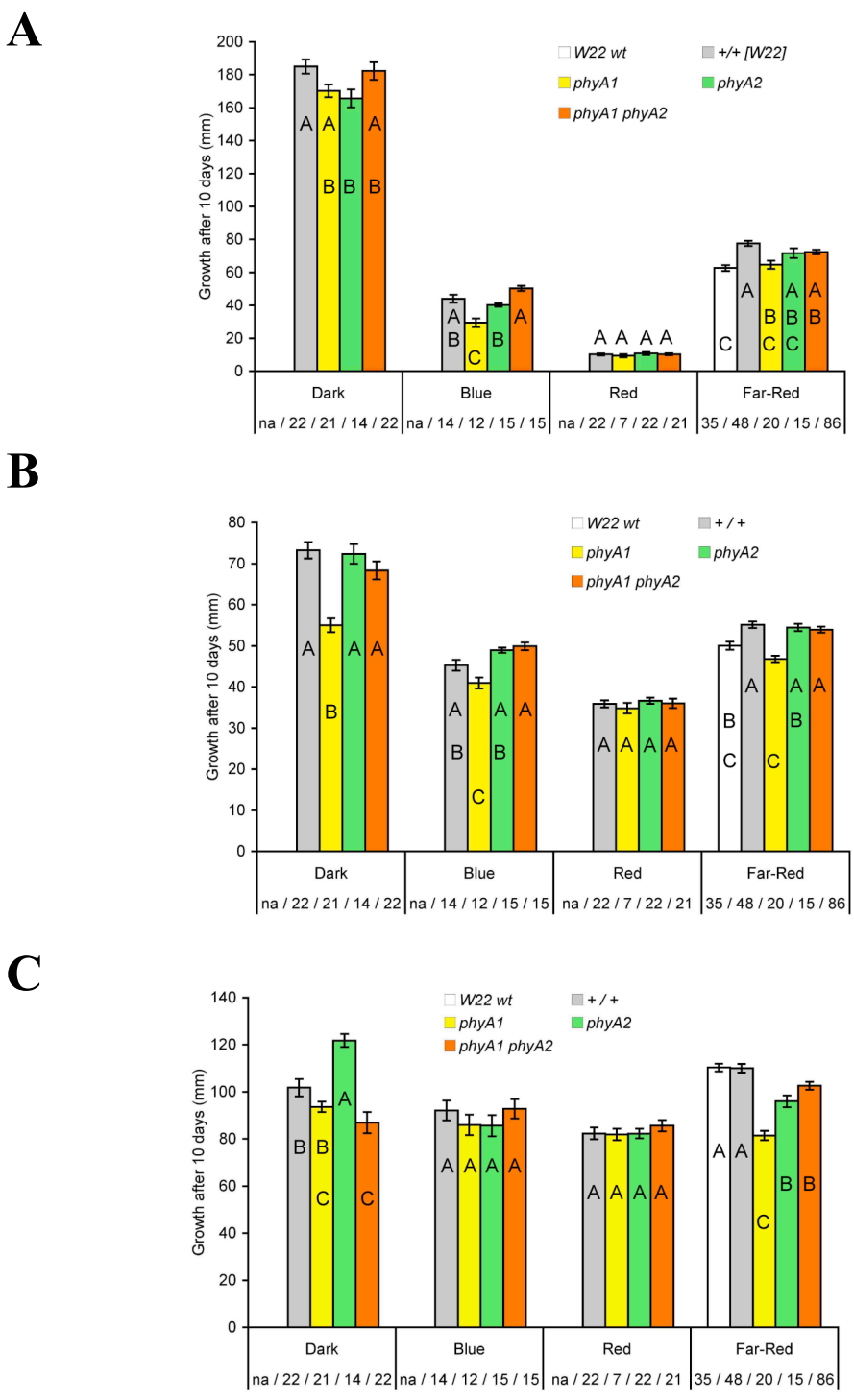

Figure 6.4 Growth chamber screening of the *phyA1*::*Mu*4912 *phyA2*-PW1721 mutant series. Seedlings were grown for 10 d in the dark, Bc, Rc, or FRc. A, mesocotyl length. B, coleoptile length. C, 1st leaf sheath length. Below each bar is the number of seedling measured for each line. na, not available; Wt, wild-type.

Nine traits were measured at maturity: leaf number, blade width, days to anthesis, plant height, tassel length, leaf sheath length, internode length, ear node height, and stem diameter (Table 6.2). A Tukey-Kramer test with a *P*-value set at 0.05 was used to compare means within each member of the mutant series. For all traits measured, no significant difference between the four members of the mutant series was detected. Since *phyA* mutants have never been reported in maize, no specific phenotype could be expected in a field nursery. In rice, the *phyA* mutant does not show any phenotypic difference with a wild-type segregant when grown under natural light conditions (Takano et al., 2001; Takano et al., 2005).

Individual F_2 plants homozygous at both *PhyA* loci were selfed and F_3 were grown under continuous monochromatic light (Fig. 6.4). Seedlings were grown under the following light conditions: darkness, constant blue (Bc), constant red (Rc), and constant far-red (FRc). A Tukey-Kramer test with a *P*-value set at 0.05 was used to compare the four members of the series within each treatment. Under FRc, the W22 wild-type inbred was also used in addition to the wild-type segregant, thus the Tukey-Kramer test compared five lines instead of four.

Significant differences between elongation responses of the four members of the *phyA* mutant series were detected for the three seedling tissues measured. In the case of the mesocotyl tissue, the *phyA1 phyA2* double mutant was not significantly different than the wild-type segregant for all four light treatments (Fig. 6.4A). In the dark, the *phyA2* mutant was significantly shorter than the wild-type segregant, but not different from *phyA1* or *phyA1 phyA2* mutants. Under Bc, the mesocotyl of the *phyA1* mutant is significantly shorter than the remaining of the series. The *phyA2* mutant, while shorter than the double mutant, is not significantly different than the wild-type segregant. Under Rc, all four members of the *phyA1 phyA2* mutant series are not significantly different from each other. In the case of the FRc screen, the W22 wild-

type inbred was added to the screen. Interestingly, the wild-type inbred control and the wild-type segregant have significantly different mesocotyl length. This result can be attributable to the presence of other EMS-induced mutations in the wild-type segregant or differences that segregate within W22 populations. For *phyA* TILLING mutants, no introgressions into the W22 background have yet been made which can remove unlinked mutations. The *phyA1 phyA2* double mutant is not significantly different than the wild-type segregant or the two *phyA* single mutants. In Arabidopsis and rice, PhyA is the photoreceptor responsible for de-etiolation under FRc and *phyA* mutants show significantly more elongation of their hypocotyl when grown under FRc (Nagatani et al., 1993; Whitelam et al., 1993; Takano et al., 2001). A similar response (alleviation of de-etiolation) was expected for the homozygous *phyA1 phyA2* maize double mutant.

Results for the coleoptile tissues are presented in Figure 6.4B. Like the mesocotyl, no significant difference was observed between the *phyA1 phyA2* double mutant and the wild-type segregant under the four light treatments. In the dark and under Bc, only the *phyA1* mutant coleoptile is significantly shorter than the wild-type segregant. Under Rc, all four members of the mutant series are not significantly different from each other. Under FRc, the W22 inbred control coleoptile is significantly shorter than the wild-type segregant. The *phyA1* mutant is equivalent to the wild-type inbred but shorter than the wild-type segregant. Both the *phyA2* and *phyA1 phyA2* mutants are not significantly different than the wild-type segregant.

The 1st leaf sheath tissue lengths are presented in Figure 6.4C. In the dark, the *phyA1 phyA2* double mutant is significantly shorter than the wild-type segregant while the *phyA2* mutant is significantly longer. Under both Bc and Rc, the four members of the *phyA* mutant series are not significantly different. Under FRc, unlike the mesocotyl and coleoptile, the 1st leaf sheath of the inbred and the wild-type segregant are not

significantly different from each other. The *phyA2* and *phyA1 phyA2* mutants are both equivalent and shorter than the controls, while the *phyA1* mutant is significantly shorter than the four other lines. Taken together, this survey of the *phyA1 phyA2* mutant series under monochromatic light and in the dark did not produced any obvious phenotypes when the seedlings were visually compared. Only precise measurements performed on several seedlings revealed significant differences in the length of the three tissues measured. The largest difference identified was between the mesocotyl length of the *phyA1* mutant and the wild-type segregant (~33%), while most of the remaining differences are within 10%. Such small variations, despite their statistical significance, appear to be attributable to other mutations present in the background. Only several round of introgressions into the wild-type inbred could clarify the interpretation of these results. Moreover, the *phyA1 phyA2* double mutant was expected to produce the most severe phenotype but remain non-differentiable from the wild-type segregant in all cases except for the 1st leaf sheath grown in the dark and under FRc.

A maize *phyC* mutant series was examined using *phyC1*-3916 and *phyC2*-PW104 introgressed once into the W22 inbred and *phyC1*-NW1036 and *phyC2*-NW795 (B73, no recurrent introgression made). Only the *phyC1*-3916 *phyC2*-PW104 mutant series was phenotyped at maturity in the summer of 2009 and at the seedling stage using monochromatic light screens. In the field, only plants homozygous at either one or both *phyC* loci were phenotyped and selfed. As shown in Table 6.3, no significant difference was identified for the nine traits measured at maturity.

Table 6.3 Phenotypic measurements of the *phyC1*-3916 *phyC2*-PW104 mutant series [W22^1] at maturity. Tukey-Kramer $P = 0.05$.

Trait	Genotype	Number	Mean	Std. Err.	Tukey-Kramer
Leaf number	*phyC1 phyC2*	5	20.60	0.24	Non significant
	phyC1	16	20.06	0.19	
	phyC2	18	19.83	0.20	
	+ / +	20	19.95	0.22	
Blade width (cm)	*phyC1 phyC2*	12	8.92	0.34	Non significant
	phyC1	38	8.50	0.18	
	phyC2	43	8.42	0.19	
	+ / +	49	8.47	0.14	
Anthesis (days)	*phyC1 phyC2*	11	89.45	0.78	Non significant
	phyC1	37	88.89	0.41	
	phyC2	40	89.60	0.36	
	+ / +	50	89.36	0.43	
Plant height (cm)	*phyC1 phyC2*	12	121.83	3.24	Non significant
	phyC1	36	123.75	2.15	
	phyC2	44	119.55	2.52	
	+ / +	49	119.49	2.87	
Tassel length (cm)	*phyC1 phyC2*	12	27.00	1.01	Non significant
	phyC1	36	26.42	0.64	
	phyC2	44	26.20	0.60	
	+ / +	49	25.59	0.52	
Sheath length (cm)	*phyC1 phyC2*	12	15.83	0.47	Non significant
	phyC1	17	15.59	0.26	
	phyC2	12	14.42	0.57	
	+ / +	5	16.00	0.55	
Internode length (cm)	*phyC1 phyC2*	12	10.92	0.42	Non significant
	phyC1	17	10.82	0.30	
	phyC2	12	10.25	0.43	
	+ / +	5	10.80	0.49	
Ear node height (cm)	*phyC1 phyC2*	12	45.75	2.45	Non significant
	phyC1	17	47.24	2.04	
	phyC2	12	42.83	2.63	
	+ / +	5	48.60	4.46	
Stem Diameter (cm)	*phyC1 phyC2*	12	2.00	0.07	Non significant
	phyC1	17	2.05	0.08	
	phyC2	12	2.02	0.11	
	+ / +	5	2.04	0.06	

This *phyC1 phyC2* mutant series was also grown under monochromatic Bc, Rc and FRc and in darkness and the results are presented in Figure 6.5. No significant difference was detected between the wild-type segregant and the *phyC1 phyC2* double mutant for mesocotyl elongation in each of the four light treatments (Fig. 6.5A). The two single mutants *phyC1* and *phyC2* were both not significantly different from the wild-type segregant, with the exception of the Rc screen. The coleoptile of the double mutant was significantly longer than the wild-type segregant in the dark and under Rc (Fig. 6.5B). No significant difference was detected under Bc and FRc. The *phyC2* single mutant had a significantly longer coleoptile than the wild-type control in all four treatments. The length of the *phyC1 phyC2* double mutant 1st leaf sheath was longer than wild-type segregant under Bc and Rc (Fig. 6.4C). The 1st leaf sheath of the *phyC2* single mutant was significantly longer than the three other members of the mutant series, but unlike the coleoptile of *phyC2*, under Bc and Rc treatments. As observed for the screens of *phyA* TILLING mutants presented in Table 6.2 and Figure 6.4, these similar results can possibly be due to the presence of other EMS-induced mutations linked (or unlinked, as only one backcross into the W22 background was performed) to one of the *PhyC* loci and for which the recurrent introgression into the W22 background was unable to segregate away.

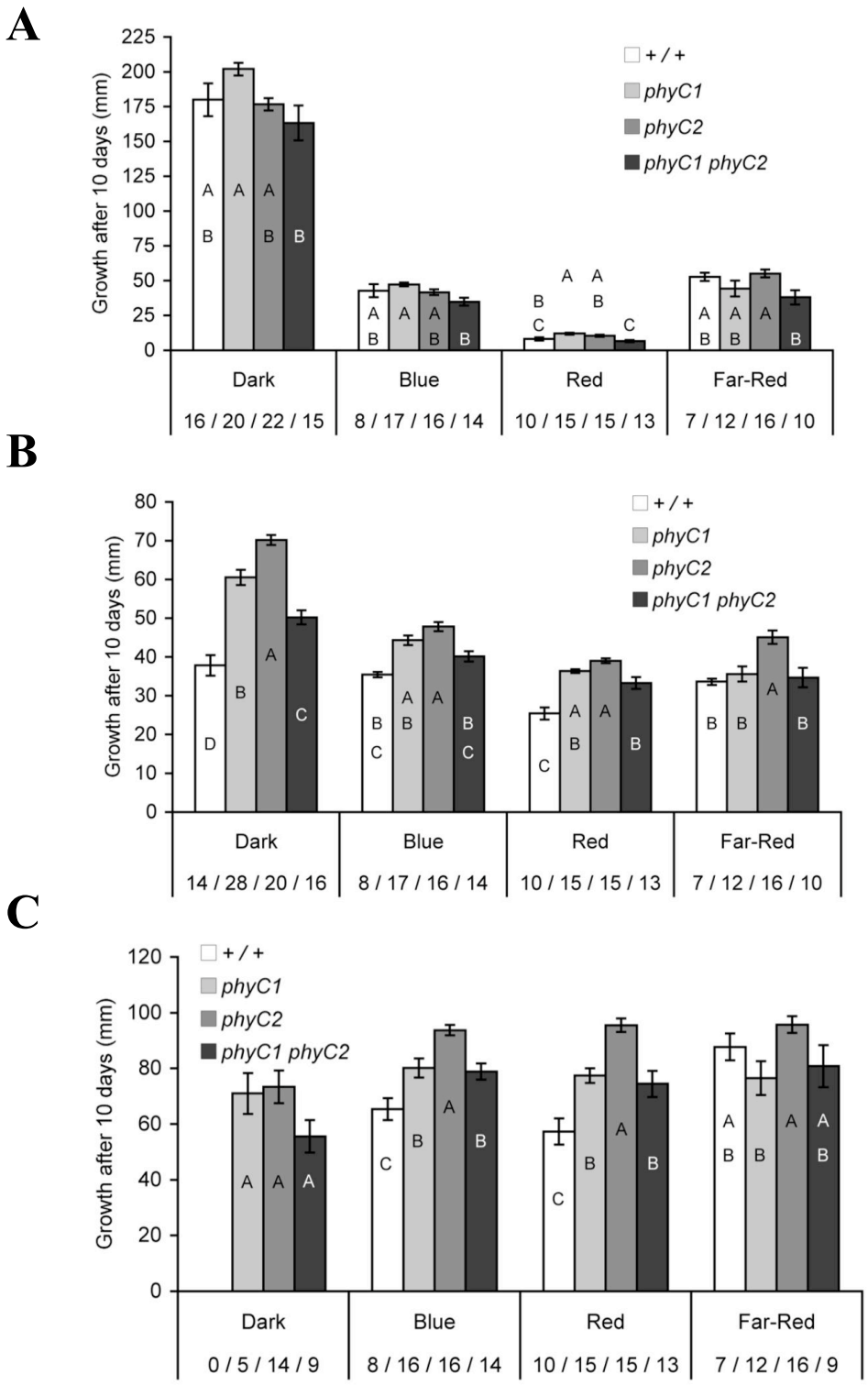

Figure 6.5 Growth chamber screening of the *phyC1*-3916 *phyC*-PW104 mutant series. Seedlings were grown for 10 d in the dark, Bc, Rc, or FRc. A, mesocotyl length. B, coleoptile length. C, 1st leaf sheath length.

Because similar subfunctionalization patterns can be observed in more than one light treatment, the relatively low number of individuals used in some screens should not be a major issue with the results observed. In Arabidopsis, PHYC has been shown to mediate variation in flowering and growth responses (Balasubramanian et al., 2006). If maize PHYC1 and PHYC2 function similar to Arabidopsis PHYC, then the *phyC1 phyC2* double mutant would be expected to flower earlier than the wild-type segregant. In rice, under Rc, the elongation of the coleoptile is severely inhibited in the wild-type, *phyA* and *phyC* mutants. The coleoptiles of *phyA* mutants are longer than those of the wild-type under FRc but still shorter than those of dark-grown seedlings (Takano et al., 2005).

Taken together, the phenotypic characterization of the phytochrome mutant series *phyA1*::*Mu*4912 *phyA2*-PW1721 and *phyC1*-3916 *phyC2*-PW104 in the field at maturity and at the seedling stage under monochromatic light treatments did not result in any dramatic phenotype (visually identifiable) nor in any expected phenotypes based on the similar characterizations of phytochrome family members in Arabidopsis and rice. In particular, the absence of an elongation phenotype in the *phyA1 phyA2* double mutant grown under FRc suggests that one or two *phyA* mutant alleles are still functional. In this case, it is highly improbable the *phyA1*::*Mu*4912 allele produce a functional transcript, considering the large size (1.4 kb) of the *Mu* insertion. But it is possible that the *phyA2*-PW1721 allele does not carry a loss-of-function mutation and encodes a functional protein. In this case, it would also suggest that a high degree of redundancy exist between PHYA1 and PHYA2, and one can complement the absence of the second. Another explanation would be the existence of heterodimer between PHYA and PHYB or between PHYA and PHYC. The presence of phytochrome heterodimers was recently demonstrated in Arabidopsis, where obligate heterodimerization take place between PhyC and PhyE in an interaction with PIF3

(Clack et al., 2009). If similar heterodimerizations take place in maize, it can be expected to be more complex due to the allopolyploidization of the gene family. In such scenario, each phytochrome paralog can not only homodimerize but also form heterodimers, not only with its paralog but also with paralogs of other phytochrome family members. This would mean that only the creation of quadruple phytochrome mutants such as *phyB1 phyB2 phyC1 phyC2* could help identify a phenotypic response. The formation of heterodimers between PHYB and PHYC paralogs in maize is more likely to take place than between either PHYB or PHYC with PHYA due to the mutual antagonistic roles PHYA and PHYB have in mediating several developmental responses in plants (Quail et al., 1995; Smith et al., 1997).

6.3 Material and Methods

EMS-generated mutant lines used in these experiments were identified by the Purdue University Tilling Service and are listed in Table 6.1. For all growth chamber experiments, seeds were uniformly sown at a depth of 2 cm in germination trays containing internal plastic cell dividers (6 cm x 6 cm) filled to the top with a soil mixture composed of 35% peat moss, 10% vermiculite, 35% baked clay, 10% sand, and 10% topsoil. The same planting density of 4 kernels per cell divider was used for all experiments. All kernel pedicels were oriented toward the bottom of the tray to improve emergence uniformity. After 10 d, phenotypic data were collected using an electronic caliper (Fowler) with direct data entry to a computer. Plants were grown under a constant photoperiod of the following light treatments: constant red (Rc, 2540 nE m^{-2} sec^{-1}), constant far-red (FRc, 0.11 nE m^{-2} sec^{-1}), constant blue (Bc, 120.3 μE m^{-2} sec^{-1}) or constant darkness. All experiments were conducted at a temperature of 28°C and relative humidity of 40%. Spectral irradiances of each light treatment were

measured using a spectroradiometer (Apogee Instruments). Maize lines were also grown in a field nursery in Aurora (N.Y.) during the summer of 2009 and all phenotypic traits were measured at maturity.

All introgressions of the *phyA1*::Mu4912 transposon insertion, which is located in the GAF domain of the *PhyA1* sequence, and its corresponding wild-type allele were confirmed by PCR-based genotyping and resolved on agarose gel. A 1.2 kb fragment specific to the *phyA1*::*Mu*4912 allele was amplified using the *Mu*-specific primer MuMTM (5'-GCCTCCATTTCGTCGAATC-3') located in the inverted terminal repeat of the transposon and the *PhyA1*-specific primer phyA1-d (5'-CGTTTCTTTTTTCTGAAGGTTGAC-3'). A 1.6 kb *PhyA1* wild-type allele DNA fragment was amplified using *PhyA1*-specific primers a-MuphyA1F1 (5'-ATTCTGTTTTTGCATCATACTGGGG-3') and g-MuphyA-R1 (5'-TATCCAGCATCCTGGAGGCTATCAG-3'). The *phyA1*::*Mu*4912 DNA fragment allele was amplified using the following PCR conditions: 95°C for 3 min followed by 35 cycles of 95°C for 30 sec, 55°C for 30 sec and 72°C for 2:30 min. The *PhyA1* DNA fragment allele was amplified using the following PCR conditions: 95°C for 3 min followed by 35 cycles of 95°C for 30 sec, 59°C for 30 sec and 72°C for 3 min.

All the tilling mutants were genotyped by sequencing following the PCR amplification of a paralog-specific DNA fragment containing a base substitution. The *phyA1*-PW1729 allele was detected as a PCR product of 396 bp amplified using primers 1phyA-4227F (5'- GCTTGTGTGGTTCAACTCTTAGAGC-3') and 4phyA1-4623R (5'-GTCCATGATATTTGGACTCCCGGAT-3'). The sequencing primer was 1phyA-4227F. Both *phyA2*-PW1721 and *phyA2*-PW1067 alleles were detected as a single PCR product of 394 bp amplified using primers zmphya2-F (5'-CATCTCCCTTGAGTATCGTGTCT-3') and zmphya2-R (5'-TCAAGGAA-

AGCCTTAAAGGATAAC-3'). Sequencing primers were zmphya2-R for *phyA2*-PW1721 and zmphya2-F for *phyA2*-PW1067. The *phyC1*-1036 allele was a PCR product of 349 bp amplified using primers 1-phyC1-F1 (5'-GAGGAGG-AAGATGGGGATACCGGG-3') and 3-phyC1-R1 (5'-GGGTGTTGATCCAA-GCACCAAAAG-3'). The sequencing primer was 3-phyC1-R1. The *phyC1*-3916 allele was detected as a PCR fragment of 312 bp amplified using primers 9-phyC1-F5 (5'-GAAGATGCCAACAGAAACAATGTA-3') and 11-phyC-R7 (5'-GTGACAAACCTTGTAAAGCTGAGTC-3'). The sequencing primer was 11-phyC-R7. The *phyC2*-PW104 allele was detected as a PCR product of 412 bp using primers 13-phyC2-F8 (5'-GGTTCCCAGCTTAATCTGAA-CGTG-3') and 14-phyC-R8 (5'-AGCGTGAAGACCTCCCCAAT-TAAC-3'). The sequencing primer was 14-phyC-R8. The *phyC2*-NW795 tilling mutant allele was using a PCR product of 421 bp using primers 13-phyC2-F8 (5'-GGTTCCCAGCT-TAATCTGAACGTG-3') and 14-phyC-R8 (5'-AGCGTGAAGACCTCCCCAAT-TAAC-3'). The sequencing primer was 14-phyC-R8. Amplification conditions were: 95°C for 3 min followed by 12 cycles of 95°C for 30 sec, 65°C for 30 sec (decreasing by 1°C at each subsequent cycle) and 72°C for 1:30 min, followed by 25 cycles of 95°C for 30 sec, 53°C for 30 sec and 72°C for 1:30 min. Genomic DNA was isolated from leaf tissue (Ahern et al., 2009) and DNA fragments were amplified using GoTaq DNA polymerase according to the manufacturer's recommendations (Promega).

From a PCR reaction of 20 μL, an aliquot of 5 μL was used for an agarose gel validation of the amplification. The PCR reaction was then simultaneously treated with an *Exo*I and shrimp alkaline phosphatase (SAP). The SAP removes phosphate groups from the excess of dNTPs while the *ExoI* degrades single-stranded DNA in a 3' to 5' direction, releasing deoxyribonucleoside 5'-monophosphates in a stepwise manner and leaving 5'-terminal dinucleotides intact. A volume of 6 μL of the PCR

reaction was added to 0.6 μL of SAP (Fermentas), 0.15 μL of *Exo*1 (Fermentas), 0.3 μL of 10X SAP buffer (Fermentas), 0.1 μL of 10X *Exo1* buffer (Fermentas), and 2.85 μL of distilled water, and incubated 30 min at 37°C followed by 10 min at 80°C. The sequencing reaction was performed using 3 μL of *Exo1* / SAP-treated PCR product combined to 1 μL of sequencing primer, 0.5 μL of Big Dye sequencing cocktail (Cornell Sequencing Center), 0.5 μL of betaine, 2.5 μL of 5X sequencing buffer (Applied Biosystem), and 4.5 μL of distilled water. The sequencing were conditions: 95°C for 4 min followed by 25 cycles of 96°C for 10 sec, 50°C for 5 sec and 60°C for 3 min. Reactions were purified by ethanol precipitation, resuspended in 10 μL of Hi-Di formamide (Applied Biosystem) and denatured 3 min at 94°C. Sequencing-by-capillaries was performed by the Cornell Sequencing Center and analysis was performed using the DNAstar software package (Lasergene).

REFERENCE

Ahern KR, Deewatthanawong P, Schares J, Muszynski M, Weeks R, Vollbrecht E, Duvick J, Brendel VP, Brutnell TP (2009) Regional mutagenesis using *Dissociation* in maize. Methods **49:** 248-254

Aukerman MJ, Hirschfeld M, Wester L, Weaver M, Clack T, Amasino RM, Sharrock RA (1997) A deletion in the PHYD gene of the Arabidopsis Wassilewskija ecotype defines a role for phytochrome D in red/far-red light sensing. Plant Cell **9:** 1317-1326

Balasubramanian S, Sureshkumar S, Agrawal M, Michael TP, Wessinger C, Maloof JN, Clark R, Warthmann N, Chory J, Weigel D (2006) The PHYTOCHROME C photoreceptor gene mediates natural variation in flowering and growth responses of *Arabidopsis thaliana*. Nat Genet **38:** 711-715

Bennetzen JL (1984) Transposable element *Mu1* is found in multiple copies only in Robertson's Mutator maize lines. J Mol Appl Genet **2:** 519-524

Clack T, Shokry A, Moffet M, Liu P, Faul M, Sharrock RA (2009) Obligate Heterodimerization of Arabidopsis Phytochromes C and E and Interaction with the PIF3 Basic Helix-Loop-Helix Transcription Factor. Plant Cell

Colbert T, Till BJ, Tompa R, Reynolds S, Steine MN, Yeung AT, McCallum CM, Comai L, Henikoff S (2001) High-throughput screening for induced point mutations. Plant Physiol **126:** 480-484

Cooper JL, Till BJ, Laport RG, Darlow MC, Kleffner JM, Jamai A, El-Mellouki T, Liu S, Ritchie R, Nielsen N, Bilyeu KD, Meksem K, Comai L, Henikoff S (2008) TILLING to detect induced mutations in soybean. BMC Plant Biol **8:** 9

Dalmais M, Schmidt J, Le Signor C, Moussy F, Burstin J, Savois V, Aubert G, Brunaud V, de Oliveira Y, Guichard C, Thompson R, Bendahmane A (2008) UTILLdb, a *Pisum sativum* in silico forward and reverse genetics tool. Genome Biol **9:** R43

Devlin PF, Patel SR, Whitelam GC (1998) Phytochrome E influences internode elongation and flowering time in Arabidopsis. Plant Cell **10:** 1479-1487

Franklin KA, Davis SJ, Stoddart WM, Vierstra RD, Whitelam GC (2003) Mutant analyses define multiple roles for phytochrome C in Arabidopsis photomorphogenesis. Plant Cell **15:** 1981-1989

Franklin KA, Praekelt U, Stoddart WM, Billingham OE, Halliday KJ, Whitelam GC (2003) Phytochromes B, D, and E act redundantly to control multiple physiological responses in Arabidopsis. Plant Physiol **131:** 1340-1346

Hofer J, Turner L, Moreau C, Ambrose M, Isaac P, Butcher S, Weller J, Dupin A, Dalmais M, Le Signor C, Bendahmane A, Ellis N (2009) Tendril-less regulates tendril formation in pea leaves. Plant Cell **21:** 420-428

May BP, Liu H, Vollbrecht E, Senior L, Rabinowicz PD, Roh D, Pan X, Stein L, Freeling M, Alexander D, Martienssen R (2003) Maize-targeted mutagenesis: A knockout resource for maize. Proc Natl Acad Sci U S A **100:** 11541-11546

McCallum CM, Comai L, Greene EA, Henikoff S (2000) Targeting induced local lesions IN genomes (TILLING) for plant functional genomics. Plant Physiol **123:** 439-442

Minoia S, Petrozza A, D'Onofrio O, Piron F, Mosca G, Sozio G, Cellini F, Bendahmane A, Carriero F (2010) A new mutant genetic resource for tomato crop improvement by TILLING technology. BMC Res Notes **3:** 69

Nagatani A, Reed JW, Chory J (1993) Isolation and initial characterization of Arabidopsis mutants that are deficient in phytochrome A. Plant Physiol **102:** 269-277

Quail PH, Boylan MT, Parks BM, Short TW, Xu Y, Wagner D (1995) Phytochromes: photosensory perception and signal transduction. Science **268:** 675-680

Reed JW, Nagatani A, Elich TD, Fagan M, Chory J (1994) Phytochrome A and phytochrome B have overlapping but distinct functions in *Arabidopsis* development. Plant Physiol **104:** 1139-1149

Sawers RJ, Linley PJ, Farmer PR, Hanley NP, Costich DE, Terry MJ, Brutnell TP (2002) *elongated mesocotyl1*, a phytochrome-deficient mutant of maize. Plant Physiol **130:** 155-163

Sawers RJ, Linley PJ, Gutierrez-Marcos JF, Delli-Bovi T, Farmer PR, Kohchi T, Terry MJ, Brutnell TP (2004) The *Elm1* (Zm*Hy2*) gene of maize encodes a phytochromobilin synthase. Plant Physiol **136:** 2771-2781

Sheehan MJ, Farmer PR, Brutnell TP (2004) Structure and expression of maize phytochrome family homeologs. Genetics **167:** 1395-1405

Sheehan MJ, Kennedy LM, Costich DE, Brutnell TP (2007) Subfunctionalization of *PhyB1* and *PhyB2* in the control of seedling and mature plant traits in maize. Plant J **49:** 338-353

Slade AJ, Fuerstenberg SI, Loeffler D, Steine MN, Facciotti D (2005) A reverse genetic, nontransgenic approach to wheat crop improvement by TILLING. Nat Biotechnol **23:** 75-81

Smith H, Xu Y, Quail PH (1997) Antagonistic but complementary actions of phytochromes A and B allow seedling de-etiolation. Plant Physiol **114:** 637-641

Somers DE, Sharrock RA, Tepperman JM, Quail PH (1991) The *hy3* long hypocotyl mutant of Arabidopsis is deficient in phytochrome B. Plant Cell **3:** 1263-1274

Strasser B, Sanchez-Lamas M, Yanovsky MJ, Casal JJ, Cerdan PD (2010) *Arabidopsis thaliana* life without phytochromes. Proc Natl Acad Sci U S A

Takano M, Inagaki N, Xie X, Yuzurihara N, Hihara F, Ishizuka T, Yano M, Nishimura M, Miyao A, Hirochika H, Shinomura T (2005) Distinct and cooperative functions of phytochromes A, B, and C in the control of deetiolation and flowering in rice. Plant Cell **17:** 3311-3325

Takano M, Kanegae H, Shinomura T, Miyao A, Hirochika H, Furuya M (2001) Isolation and characterization of rice phytochrome A mutants. Plant Cell **13:** 521-534

Till BJ, Cooper J, Tai TH, Colowit P, Greene EA, Henikoff S, Comai L (2007) Discovery of chemically induced mutations in rice by TILLING. BMC Plant Biol **7:** 19

Till BJ, Reynolds SH, Weil C, Springer N, Burtner C, Young K, Bowers E, Codomo CA, Enns LC, Odden AR, Greene EA, Comai L, Henikoff S (2004) Discovery of induced point mutations in maize genes by TILLING. BMC Plant Biol **4:** 12

Weil CF (2009) TILLING in grass species. Plant Physiol **149:** 158-164

Weller JL, Schreuder ME, Smith H, Koornneef M, Kendrick RE (2000) Physiological interactions of phytochromes A, B1 and B2 in the control of development in tomato. Plant J **24:** 345-356

Whitelam GC, Johnson E, Peng JR, Carol P, Anderson ML, Cowl JS, Harberd NP (1993) Phytochrome A null mutants of Arabidopsis display a wild-type phenotype in white-light. Plant Cell **5:** 757-768

CHAPTER SEVEN

FUTURE DIRECTIONS

7.1 Future Directions in the Investigations of the Shade Avoidance Syndrome In Maize

Tremendous progress has been made in the last twenty years in the comprehension of light signaling in plants, the central role of the phytochromes in mediating them and on transduced developmental responses such as the shade avoidance syndrome (SAS). With the sequencing of the model plant *Arabidopsis thaliana*, the availability of genetic tools such as indexed knock-out lines and the ability to create over-expression lines, a wealth of discoveries on phytochrome functions has been achieved in this species (Chory, 2010). While the use of model organisms is fundamental to our understanding of biological processes, these findings can only partially be mirrored in a crop such as maize (*Zea mays* ssp. *mays*). Unlike the small weed Arabidopsis, maize has been domesticated from teosinte (*Zea mays* ssp. *parviglumis*) (Doebley et al., 2006) and under tremendous selection by modern breeding (Lee and Tollenaar, 2007). The hybrid maize plant grown today bears little resemblance with its ancestor teosinte. A better understanding of the SAS in maize should lead to novel breeding and transgenic strategies aiming at further yield increases.

In Arabidopsis, the availability of loss-of-function alleles for all five phytochrome gene members was paramount in their characterization. A similar series of mutants of all the phytochrome genes has yet to be achieved in maize. To date,

only *Mutator* (*Mu*) insertions at the *PhyB1* loci and a natural deletion at the *PhyB2* loci have been reported (Sheehan et al., 2007). Two other *Mu* insertions were identified in *PhyA1* and *PhyB2* (see Chapters Two and Six). The identification of EMS-induced mutants through TILLING screens failed to generate any expected or striking phenotypes for *phyA1 phyA2* and *phyC1 phyC2* mutant series based on similar screens in Arabidopsis and rice (*Oryza sativa*) (see Chapter Six). The best alternative to obtain at six maize loss-of-function phytochrome mutants would be to pursue a *Dissociation* transposon mutagenesis strategy (Vollbrecht et al., 2010).

Research derived from this thesis work on the SAS in maize will be pursued at the University of Buenos Aires. This project will investigate the role of phytochromes in the early establishment of variability between plants of the same genotype and follow the progression of the variability through the season (Maddonni and Otegui, 2004; Pagano and Maddonni, 2007). Variability at the population level for biomass production and partitioning (stem versus root) in relation to variations in the red to far-red light ratio (R:FR) of two maize hybrids has recently been characterized (Pagano and Maddonni, 2008). These results suggest a different sensitivity to R:FR between genotypes and also between individuals of the same genotype. A similar experiment using the *phyB* mutant series (introgressed in the France 2 inbred background) is currently underway. The *phyB* mutant series has since been introgressed into the B73 and W22 backgrounds and these introgression series will also be added to these experiments. Maize plants will be grown at low and high densities and in both uniform stands (a single genotype per row) and in mixed stands (random genotype mixture in each row). As previously described (see Chapter Three; Sheehan et al., 2007), the subfunctionalization between *PhyB1* and *PhyB2* is background-specific, and the influence of genetic modifiers is significant.

Another aspect of the SAS that will be investigated is its interaction with herbivore defense responses (Ballare, 2009). As plants reallocate resources to allow the SAS to take place, a hierarchal down regulation of defense mechanisms takes place. Application of *Spodoptera frugiperda* oral secretions or jasmonate (JA) to mechanically made Arabidopsis woundings was demonstrated to induce defense mechanisms (Moreno et al., 2009). In the same study, R/FR sensing was shown to modulate the sensitivity of plant tissues to JA, the principal hormones involved in defense against chewing insects and necrotrophic pathogens. Investigation of this relation between R/FR sensing and defense mechanisms is relevant for crops such as maize where the high planting density reduce the R:FR under the canopy and for which new insect resistance traits are constantly needed.

A bioassay using *Spodoptera exigua* on maize seedlings was recently developed (Dubois, unpublished). The *phyB1 phyB2* mutant series will be used to investigate the role of PHYB on maize herbivore defenses. In controlled conditions of growth chambers, the different inbreds and mutants can in integrated to a factorial analysis combining maize wild-type and *phyB* mutants, light treatments (high and low R:FR), insect feeding, JA and oral secretions treatments. Seedling tissues derived from the most insightful experiments can then be used for transcription profiling (Wang et al., 2010). This approach should generate a wealth of information about the light regulation of crop defense mechanisms and allow the identification of yield and insect protection leads for crop improvement.

Identification of quantitative trait loci (QTL) controlling SAS-related traits at maturity should also help characterize its genetic architecture and also help to identify the underlying genes controlling it. A survey of the Intermated B73 x Mo17 (IBM) population (Lee et al., 2002), submitted to an end-of-day FR daily treatment at seedling stage, revealed distinct QTLs for the mesocotyl and 1st leaf sheath (see

Chapter Two). If a number of QTLs responsible for mediating shade signals are assumed to be operational throughout the life span, others will likely be present only at specific developmental stages. For this reason, it is also important to explore the genetic architecture of SAS past the seedling developmental stage.

The recent sequencing of its two inbred parents, B73 and Mo17, and also of 275 of its RIL (Glaubitz et al., 2010) makes IBM a population of choice to conduct a QTL on SAS in a field nursery. Other mapping population such as the 5000 lines of the Nested Association Mapping (NAM) population may be too large to handle without a significant investment of labor (McMullen et al., 2009). Based on pilot experiments (see Chapter Five), the IBM population can be planted at two or three different planting densities in a nursery field and phenotyped for a series of phenotypic traits. Using planting densities of 10 and 40 kernels per row, significant differences in days-to-anthesis and azimuthal leaf orientation could be detected. A more rigorous approach would be to not only vary the within row plant number but also the distance between rows. The combination of both within and between row densities would likely be optimal in the creation of contrasting plant densities.

The power of isogenic introgression lines (IL) for QTL mapping have recently demonstrated in tomato (*Solanum* sp.) (Semel et al., 2006; Lippman et al., 2007) and can represent an alternative approach can be adopted for the identification of genetic variation that contributes to the SAS in maize. In contrast to recombinant inbred lines (RIL) where each line consists of numerous recombinaitions between the parental genotypes, ILs possess one genomic fragment of the introgressed parent into a common genetic background. A collection of interspecific tomato ILs was created from a cross between the wild small green-fruited desert species *S. pennellii* and *S. lycopersicum* (domesticated tomato acting as the recurrent parent). Hybridizing the collection of 76 ILs to the recurrent parent has allowed the discovery of several loci

governing heterosis. Several small over-dominant genomic regions associated with reproductive fitness traits such as seed number per plant, fruit number, total yield and biomass were identified (Semel et al., 2006). Furthermore, three independent yield-promoting introgressions identified from *S. pennellii* were later successfully introduced into commercial lines of processing tomato. These *S. pennellii* alleles increased yields by 50% compared to leading commercial varieties (Gur and Zamir, 2004), illustrating the tangible contribution of wild alleles to commercial breeding programs. ILs mapping populations represent an attractive alternative to recombinant inbred lines (RIL) for QTL discovery and as a source of novel allelic variation. A collection of near isogenic ILs (NIL) derived from the introgression of 10 different teosinte accessions with the modern inbred B73 recurrent parent was recently created (Flint-Garcia et al., 2009). The capacity of using the teosinte gene pool to re-introduce wild alleles into elite maize germplasms can improve stress-related traits such as water deficit, disease resistance and the SAS.

REFERENCES

Ballare CL (2009) Illuminated behaviour: phytochrome as a key regulator of light foraging and plant anti-herbivore defence. Plant Cell Environ **32:** 713-725

Chory J (2010) Light signal transduction: an infinite spectrum of possibilities. Plant J **61:** 982-991

Doebley JF, Gaut BS, Smith BD (2006) The molecular genetics of crop domestication. Cell **127:** 1309-1321

Flint-Garcia SA, Bottoms C, McMullen M (2009) Development and marker characterization of maize-teosinte introgression libraries. *In* 51st Maize Genetics Conference, St-Chales, IL.

Glaubitz JC, Elshire RJ, Sun Q, Guill K, McMullen M, Buckler ES (2010) Genotyping by sequencing in maize *In* Maize Genetics, Riva del Garda

Gur A, Zamir D (2004) Unused natural variation can lift yield barriers in plant breeding. PLoS Biol **2:** e245

Lee EA, Tollenaar M (2007) Physiological basis of successful breeding strategies for maize grain yield. Crop Sci **47(S3):** S202-S215

Lee M, Sharopova N, Beavis WD, Grant D, Katt M, Blair D, Hallauer A (2002) Expanding the genetic map of maize with the intermated B73 x Mo17 (IBM) population. Plant Mol Biol **48:** 453-461

Lippman ZB, Semel Y, Zamir D (2007) An integrated view of quantitative trait variation using tomato interspecific introgression lines. Curr Opin Genet Dev **17:** 545-552

Maddonni GA, Otegui ME (2004) Intra-specific competition in maize: early establishment of hierarchies among plants affects final kernel set. Field Crops Res **85:** 1-13

McMullen MD, Kresovich S, Villeda HS, Bradbury P, Li H, Sun Q, Flint-Garcia S, Thornsberry J, Acharya C, Bottoms C, Brown P, Browne C, Eller M, Guill K, Harjes C, Kroon D, Lepak N, Mitchell SE, Peterson B, Pressoir G, Romero S, Oropeza Rosas M, Salvo S, Yates H, Hanson M, Jones E, Smith S, Glaubitz JC, Goodman M, Ware D, Holland JB, Buckler ES (2009) Genetic properties of the maize nested association mapping population. Science **325:** 737-740

Moreno JE, Tao Y, Chory J, Ballare CL (2009) Ecological modulation of plant defense via phytochrome control of jasmonate sensitivity. Proc Natl Acad Sci U S A **106:** 4935-4940

Pagano E, Maddonni GA (2007) Intra-specific competition in maize: Early established hierarchies differ in plant growth and biomass partitioning to the ear around silking. Field Crops Res **101:** 306-320

Semel Y, Nissenbaum J, Menda N, Zinder M, Krieger U, Issman N, Pleban T, Lippman Z, Gur A, Zamir D (2006) Overdominant quantitative trait loci for yield and fitness in tomato. Proc Natl Acad Sci U S A **103:** 12981-12986

Sheehan MJ, Kennedy LM, Costich DE, Brutnell TP (2007) Subfunctionalization of *PhyB1* and *PhyB2* in the control of seedling and mature plant traits in maize. Plant J **49:** 338-353

Vollbrecht E, Duvick J, Schares JP, Ahern KR, Deewatthanawong P, Xu L, Conrad LJ, Kikuchi K, Kubinec TA, Hall BD, Weeks R, Unger-Wallace E, Muszynski M, Brendel VP, Brutnell TP (2010) Genome-wide distribution of transposed *Dissociation* elements in maize. Plant Cell **In Press**

Wang L, Li P, Brutnell TP (2010) Exploring plant transcriptomes using ultra high-throughput sequencing Brief Funct Genomic Proteomic **9:** 118-128

APPENDIX

MAIZE SEED STOCKS

Genotype	**Inbred**	**PGD- Seed Stocks**
elm1 R-sc:m3	W22	08-88, 89, 09-150
elm1 r-sc:m3	B73^5	09-148, 149
PhyB1 PhyB2	B73^4	09-213.2, 213.6, 214.9, 216.6, 238.3, 238.4, 238.8, 240.5, 241.1,
phyB1-563	B73^4	09-214.2, 214.12, 216.1, 216.5, 218.6, 218.10, 234.1, 234.6, 234.9, 237.6, 240.7, 244, 245
phyB2-12058	B73^4	09-220.9, 220.12
phyB1-563 phyB2-12058	B73^4	09-219.11, 220.5, 220.14, 235.8, 236.1
phyB1-563/+ phyB2-12058/+	B73^5	B73 x09-233.2, x 235.8
(phyB1-563)/(+) (phyB2-12058)/(+)	B73^5	10-23
PhyB1 PhyB2	W22^4	09-184, 188, 192, 196, 338,
phyB1-563	W22^4	09-30, 185, 189, 193, 197, 339,
phyB2-12058	W22^4	09-28, 29, 186, 190, 194, 198,
phyB1-563 phyB2-12058	W22^4	07-93.7, 09-27, 183, 187, 199, 341, 355
(phyB1-563)/(+) (phyB2-12058)/(+)	W22^5	09-53, 74
Z033E0026/+ (B73 BC1)	B73^1	B73 x10-55
phyC1-NW1036	B73^1	09-228.2
phyC2-NW795	B73^1	09-224, 226.6, 229.1, 229.12
phyC1-NW1036 phyC2-NW795	B73^1	09-226.12, 228.3, 228.4
PhyC1 PhyC2	B73^1	09-226.3
phyC1-3916	W22^1	09-247, 249, 251, 264.1, 265.2, 265.5, 267.10, 268.5, 271.7
phyC2-PW104	W22^1	09-253, 254, 255, 258, 259, 260, 261.2, 263.6, 272.9 277.12, 278.5
phyC1-3916 phyC2-PW104	W22	09-246, 248, 250, 252

Genotype	Inbred	PGD Seed Stocks
phyC1-3916 phyC2-PW104	W22^1	09-263.7, 264.8, 268.3, 268.10
PhyC1 PhyC2	W22^1	09-267.4, 269.7, 271.10, 278.6
phyA1-PW1729	W22^2	09-129.7
phyA1-Mu4912	W22^5	09-119, 121
phyA1-Mu4912	B73^1	09-142.2
phyA1-Mu4912/+	B73^2	B73 x 09-142.2
phyA2-PW1067	W22	09-111.8
phyA2-PW1067	W22^1	09-134.10, 135.1, 135.7
phyA1-Mu4912	W22	09-95.12, 96.5, 96.11, 98.6, 104.10, 106.12, 107.9, 111.5
phyA2-PW1721	W22	09-84.3, 94.5, 94.9, 94.11, 96.4, 97.4, 97.6, 98.1, 100.5, 103.10, 104.3
phyA2-PW1721	W22^1	09-136.2, 137.10 137.12
PhyA1 PhyA2	W22	09-84.2, 85.3, 86.5, 86.11, 86.12, 90.9, 91.7, 92.1, 92.4, 93.2, 93.6, 94.6, 95.8, 95.11, 96.1, 97.1, 99.8 101.1 101.4 103.9 105.3
phyA1-Mu4912 phyA2-PW1721	W22	09-85.11, 90.1, 93.8, 95.1, 95.2, 98.9, 98.10, 100.3, 106.3
phyA1-Mu4912/+ (phyA2-PW1067)/+	W22^1	W22 x09-111.4
(phyA1-Mu4912)/(+) phyA2PW1067	W22	09-111.7
d1	Mixed	08-193.1
d1/+	B73^1	B73 x08-193.1
(d1)/(+)	B73^1	09-40, 69
d1/+	B73^1	09-160.1, 160.2, 161.2, 161.5
d1	B73^1	09-160.5, 160.6, 161.6
d1/+	B73^2	B73 x09-160.5, x161.6
d1/+	Mo17^1	Mo17 x09-161.6
d1	W22^5	08-98.8
(d1)/(+)	W22^1	09-42

Genotype	Inbred	PGD Seed Stocks
(d1)/+ elm1/+	W22^5	08-88 x98.1, x98.2, x98.3
(d1)/(+) elm1	W22*	09-162.1 162.3 163.2 163.3
(d1)/(+) elm1	W22*	10-52, 53
d1/+ elm1/+	B73^1	08-87 x193.1
(d1)/(+) (elm1)/(+)	B73^1	09-41
d1/+ phyB1-563/+ phyB2-12058/+	B73*	08-199 x193.1
(d1)/(+) (phyB1-563)/(+) (phyB2-12058)/(+)	B73*	09-43
(d1)/+ (phyB1-563)/+ phyB2-12058/+	B73^1	B73 x09-168.2
(d1)/+ phyB1-563/+ (phyB2-12058)/+	B73^1	B73 x09-165.1, x169.3, x171.1
(d1)/+ (phyB1-563)/(+) (phyB2-12058)/(+)	B73^1	B73 x09-164.4
d1/+ phyB1-563/+ phyB2-12058/+	W22^1	08-203 x193.1
(d1)/+ (phyB1-563)/(+) (phyB2-12058)/(+)	W22^2	W22 x09-164.4
(d1)/+ phyB1-563 (phyB2-12058)/(+)	W22^1	09-165.1, 166.5, 169.3, 170.10
(d1)/+ phyB1-563/+ (phyB2-12058)/+	W22^2	W22 x09-165.1, x166.5, x169.3
(d1)/+ (phyB1-563)/(+) phyB2-12058	W22^1	09-168.2, 170.4
(d1)/+ (phyB1-563)/+ phyB2-12058/+	W22^2	W22 x09-168.2, x170.4
(d1)/+ (phyB1-563)/(+) (phyB2-12058)/(+)	W22^1	09-168.4
(d1)/(+) (phyB1-563)/(+) phyB2-12058	W22^1	10-41, 44
(d1)/(+) phyB1-563 (phyB2-12058)/(+)	W22^1	10-42, 46, 47
D8-1/+	Mixed	08-197.3
(D8-1)/+	B73^1	B73 x08-197.3
D9/+	Mixed	08-198.1
(D9)/+ phyB1-563/+ phyB2-12058/+	W22^1	08-203 x198.1
D8-Mpl	Mixed	08-196.1
(D8-Mpl)/+	B73^1	B73 x09-174.4
D8-Mpl/+	W22^1	W22 x08-196.1
(D8-Mpl)/(+)	W22^1	09-26, 174.3, 174.4, 10-48.3
(D8-Mpl)/+	W22^2	W22 x09-174.4, x10-48.1

Genotype	Inbred	PGD Seed Stocks
(D8-Mpl)/(+) (phyB1-563)/(+) (phyB2-12058)/(+)	W22^1	09-47
D8-Mpl phyB1-563	W22^1	09-175.1
D8-Mpl (phyB1-563)/(+) (phyB2-12058)/(+)	W22^1	09-175.9
D8-Mpl phyB1-563 (phyB2-12058)/(+)	W22^1	09-176.4, 176.7, 10-49.1
D8-Mpl/+ phyB1-563/+ (phyB2-12058)/+	W22^2	W22 x09-176.4, x176.7
br2	Mixed	08-192
br2/+ phyB1-563/+ phyB2-12058/+	B73*	08-199 x192
br2/+ phyB1-563/+ phyB2-12058/+	B73*	08-200 x192
(br2)/(+) (phyB1-563)/(+) (phyB2-12058)/(+)	B73*	09-50
br2 elm1	W22^2	08-96.8, 97.2
br2/+ elm1/+	W22^3	W22 x08-96.8, x97.2
(br2)/(+) (elm1)/(+)	W22^3	09-49
br2 (elm1)/(+)	W22^3	09-172.4, 172.13, 173.1,173.3
br2/+ (elm1)/+	W22^4	W22 x09-172.4, x172.13, x173.1
br2/+ phyB1-563/+ phyB2-12058/+	W22^1	08-201 x192
(br2)/(+) (phyB1-563)/(+) (phyB2-12058)/(+)	W22^1	09-51
br2/+ elm1/+ phyB1-563/+ phyB2-12058/+	W22^1	08-203 x96.8
br2/+ elm1/+ phyB1-563/+ phyB2-12058/+	W22^1	08-133 x96.8, x97.2, 132 x 97.2
(br2)/(+) (elm1)/(+) (phyB1-563)/(+) (phyB2-12058)/(+)	W22^1	09-48

*Unresolved introgression. ^, Number of introgressions in a maize inbred background. To make the table more legible, the following names are substituted; *phyA1-4912* is synonymous of *phyA1*::*Mu4912, phyB1-563* is synonymous of *phyB1*::*Mu*563*,* and *phyB2-12058* is synonymous of *phyB2*::*Mu*12058.